JIMMA UNIVERSITY

JIMMA INSTITUTE OF TECHNOLOGY

SCHOOL OF GRADUATE STUDIES

HYDROLOGY AND HYDRAULIC ENGINEERING CHAIR

MASTERS OF SCIENCE IN HYDRAULIC ENGINEERING

Dam Break Analysis: Case Study of Dire Embankment Dam, Oromia Region

A thesis submitted to the School of Graduate Studies of Jimma University in Partial fulfillment of the requirements for the Degree of Masters of Science in Hydraulic Engineering

By:

Segni Wandimu Gudeta

March, 2021

Jimma, Ethiopia

JIMMA UNIVERSITY

JIMMA INSTITUTE OF TECHNOLOGY

SCHOOL OF GRADUATE STUDIES

HYDROLOGY AND HYDRAULIC ENGINEERING CHAIR

MASTERS OF SCIENCE IN HYDRAULIC ENGINEERING

Dam Break Analysis: Case Study of Dire Embankment Dam, Oromia Region

A thesis submitted to the School of Graduate Studies of Jimma University in Partial fulfillment of the requirements for the Degree of Masters of Science in Hydraulic Engineering

By:

Segni Wandimu Gudeta

Advisor: Zeinu Ahmed (PhD.)

Co-Advisor: Wondmagegn Taye (MSc.)

March, 2021

Jimma, Ethiopia

Declaration

I hereby declare that this thesis entitled “Dam Break Analysis: Case Study of Dire Embankment Dam” has been done by myself under the guidance of my advisors Zeinu Ahmed (PhD) and Wondmagegn Taye (MSc). I further declare that this work has not been submitted to any other University or Institution for the award of any degree or professional qualification.

Segni Wandimu	……	……
Name	Signature	Date

Approval Sheet

The undersigned certify that the thesis entitled: **"Dam Break Analysis: Case Study of Dire Embankment Dam Oromia Region"** is the work of Segni Wandimu and we hereby recommend for the acceptance by school of Post Graduate Studies of Jimma University in partial fulfillment of the requirements for Degree of Master of Science in Hydraulic Engineering.

Dr. Zeinu Ahmed (PhD.)	……	……
Main Advisor	Signature	Date
Mr. Wondmagegn Taye (MSc.)	……	……..
Co-Advisor	Signature	Date

As member of Board of Examiners of the MSc. Thesis Open Defense Examination, we certify that we have read, evaluated the thesis prepared by Segni Wandimu and examined the candidate. We recommended that the thesis could be accepted as fulfilling the thesis requirement for the Degree of Master of Science in Hydraulic Engineering.

Dr. Eng. Adane Abebe (PhD)	……	……
External Examiner	Signature	Date
Mr. Wana Geyisa (MSc.)	……..	…….
Internal Examiner	Signature	Date
Mr. Nasir Gebi	……	……
Chairman	Signature	Date

Abstract

When dam breach occurs, the resulting flood can cause enormous damages to infrastructures and loss of life. The study was conducted on the Dire dam located at 30 km to the east of Addis Ababa city within the boundary of the Oromia region. The failure modes assumed for dam breach analysis in this study were overtopping and piping through the dam body. The dam breach analysis was carried out through HEC-RAS model incorporates with GIS and HEC-GeoRAS. The HEC-RAS model performs unsteady flow simulation using Dire dam breach parameters, Dire dam geometric data, Dire reservoir elevation-volume data, unsteady flow data, and geometric data of Legadadi River as an input data. The GIS develops flood inundation map after water surface elevation, maximum flood depth, and velocity were exported from HEC-RAS to GIS. Dire dam breach parameters of input data for HEC-RAS model were computed through the empirical method of Froehlich 2008. The computation was done utilizing the Dire dam and reservoir geometrical data. The breach parameters value of breach bottom width (B), breach formation time (tf), and breach side slopes (bss) for overtopping failure mode were 51.3m, 0.65hr, and 1. The breach parameters value of breach bottom width (B), breach formation time (tf), and breach side slopes (bss) for piping failure mode were 45.98m, 0.75hr, and 0.7. The peak breach outflow discharges at the dam location due to overtopping and piping failure simulated in HEC-RAS model were 9285.30m^3/s and 7712.10m^3/s respectively. The maximum flood depth and maximum flood velocity occurred due to dam overtopping failure were 16.41m and 22.74m/s respectively. The maximum flood depth and maximum flood velocity occurred due to dam piping failure were 14.43m and 19.56m/s respectively. The simulation outcomes presented that in the event of Dire dam breach due to the assumed dam break modes, some Dire dam downstream areas were observed as having high flood hazard due to the significant flood water depth and velocity values.

Key words: Dam breach, Flood Mapping, HEC-RAS

Acknowledgement

First of all, I would like to thank the almighty God for his unspeakable gift, help, and protection during my work. I gratefully acknowledge my Advisor, Zeinu Ahmed (PhD.) and co-advisor wondmagegn Taye (MSc.) for their extending support and guiding me on the right direction to this thesis work.

I would like to acknowledge my sponsor, Ministry of Education for its financial support and providing me higher education opportunity. Also, my thank goes to Jimma University, Jimma Institute of Technology for accepting and providing me the Master's Program.

Last but not least I would like to acknowledge my best friend Ibsa Fedesa (MSc.) who encouraged me during the thesis work and my family who always encouraged me in all situations including academic issues and also I would like to acknowledge all my friends for their moral supporting during this thesis work.

Table of Contents

List of Tables

List of Figures

Acronyms and Abbreviations

A	Cross-sectional area of flow
AAWSA	Addis Ababa Water and Sewage Authority
Bavg	average breach width
B	Breach bottom width
Bss	Breach side slope
Btop	breach top width
C	Dam crest width
Cb	coefficient which is a function of a reservoir size
CWC	Central Water Commission
DEM	Digital Elevation Model
FEMA	Federal Emergency Management Agency
G	gravitational acceleration
GIS	Geographical information system
GUI	Graphical User Interface
Hb	height from the top of the dam to bottom of breach
Hd	dam height
HEC-GeoRAS	Hydrologic Engineering Centers- geographic River Analysis System
HEC-RAS	Hydrologic Engineering Center's River Analysis System
Hr	Hour
Hw	depth of water above the bottom of the breach
Km	Kilometer
M	Meter
m^3	Cubic meter
m^3/s	Cubic meter per second
PMF	Probable maximum flood
Q	Discharge
Qp	peak discharge
RS	River station
So	expansion contraction slope
Sf	friction slope

1. INTRODUCTION

1.1. Background

Through worldwide, water is collected and stored by means of constructing dam. Dam is essential hydraulic structure constructed across river for the purpose of creating reservoir to store water. The stored water as public needs may give function for irrigation, hydropower, water supply, recreational, flood control, and fishing purposes. On the other hand, in the unforeseen and unusual event of dam break, this may cause disastrous flooding in a downstream area. The flood disastrous resulting from dam break may cause severe loss to human life, massive destruction to infrastructure and loss to economic stability. Prior to the occurrences of flood catastrophic from dam break, knowing the flood extent and depth using dam break analysis technique is the important issue. Dam break analysis performs the major tasks comprising estimating breach outflow hydrograph and mapping the downstream flooded area. It is carried out through unsteady flow simulation (Saleh and Kareem, 2011).

The breaking of a dam is an event that can take place due to different causes. The assessment of potential impacts is a precautionary procedure that is part of the responsibility of the owner. This analysis must define the possible consequences of the breaking of the dam and preventative measures to alleviate the potential consequences. The possibility of break of a dam is a basis for risk to the potentials of the area downstream (Maria, 2016).

In the year 1979, the Central Water Commission (CWC) of India establishes Dam safety organization taken up measures for ensuring dam safety in their respective jurisdiction. Dam provides many benefits for our society, but floods resulting from the failure of constructed dams also produced some of the most devastating disasters. Simulation of such dam break events and the resulting floods can reduce threats due to potential dam failures. Predicting the dam break floods using observations of natural floods is not possible as well while a breached dam releases large volumes of water very rapidly. Most of the dam-break models were complex, tricky and time consuming. Dam break is modeled and analyzed using one dimensional HEC-RAS model based on available geometry data (Razack, 2014).

In Embankment dam, the principal cause of the breaks is related to soil materials that are the most vulnerable in relation to the overtopping. Internal erosion and flow concentration in the

body of the dam and in contact with rigid structures or the foundation is another significant factor in the deterioration. Other aspects to expect are the excessive settlements of dam crest, due to insufficient depiction of deformation of materials and landslides of the slopes, particularly to neutral tensions for faulty drainage system. Another imperative point of cause of breaking is the use of poor quality landfill materials like soil-mixes rock and liquefaction problems on foundations of sand or silt soil in the event of earthquakes (Maria, 2016). As stated by studies carried out universal (Balaji and Kumar, 2018) until the year 1980, about 200 dams went into break with catastrophic consequences, having occurred more than 8,000 deaths in such disasters.

Particularly in Ethiopia, dam offers many benefits for societies including water supply, irrigation, hydropower, flood control and fishing. Even though the dam provides the benefits for the societies, unusual event of the dam break may cause catastrophic disasters in the downstream civilian population and infrastructures. The dam under the case study Dire dam was an embankment dam constructed on Legadadi River in the year 1999 for water supply purpose and was located 30 km to the east of the Addis Ababa city within the boundary of the Oromia region. The overall objective of this study is analyzing Dire dam breach using one dimensional HEC-RAS hydraulic model. The dam failure mode for this dam was assumed as overtopping and piping (through the dam body).

1.2. Statement of the Problem

In recent years, dam safety has drawn increasing attention from the community. This is for the reason that floods resulting from breaking of dams can cause to highly destructive disasters with massive loss of life and property, mainly in downstream populated areas. Historical dam breach disasters indicated that the loss of life in the event of a dam failure is widely occurred at downstream area of the dam. Embankment dams are widely used all over the world, and most of the dam failures encompass such dams. In order to speak out about breaches of dams without a brief description of these happenings in the dam world is not possible. Hence, it is indispensable to go through the case histories of such dam breaches to recognize the causes of breaches of the dams failed in the past. The main causes of breaches of such dams are attributed to overtopping and piping (Sharma and Kumar, 2013).

As observed from the previous study of dam failures, the Belci earth fill dam of a clay core and upstream concrete facing built in 1962 on Tazlaur River, near Slobozia in Romania was failed

after 29 years of operation by overtopping. Because of the flood wave occurred by the dam break, twenty five people were killed and 119 houses were destroyed. The Tous rock fill dam with a central clay core located near Valencia, Spain was failed also due to overtopping. Because of the unexpected flood, in the downstream area 8 people lost their lives and about 100,000 people had to be evacuated. The Teton earth fill dam constructed across the Teton River in Madison County, United States was failed by piping and causing the loss of 11 lives and extensive flooding in the farmland and towns downstream of the dam (Afsal *et al.*, 2016).

In the event of a dam failure, the possible loss of lives and destruction of infrastructures can be occurring at the downstream areas. Since the flood resulting from the breaching of a dam can cause massive destruction to the downstream civilian population and infrastructures, observing and analyzing embankment dams breaking condition is important to protect the dam from irreversible failure and to reduce catastrophic disasters on the downstream of the dam due to unusual flood (Duressa and Jubir, 2018).

Dire Embankment dam under this case study is a rock fill dam constructed of impervious clay core. The dam was located at the upper side of the downstream areas of small house housing wires from piezometers, Legadadi town of different infrastructures such as Residential areas, Religious areas, and High way road serving for transportation from Addis Ababa to Debre Birhan and to Dessie. Since the flood resulting from this dam in the event of its breach would cause catastrophic disasters to these downstream areas, analyzing dire dam breach by assuming the overtopping and piping failure mode is very essential.

1.3. Objective of the Study

1.3.1. General Objective

The primary objective of the study is to analyze the dire dam break using HEC-RAS hydraulic model.

1.3.2. Specific Objectives

The specific objectives of the study are:

1) To estimate dimension of dam break parameters of Dire dam
2) To predict peak outflow hydrograph for overtopping and piping failure modes
3) To Map the downstream of Dire dam flood inundation area

1.4. Research Questions

This study was aimed to answer the following issues:

1) How much is the dimension of Dire Dam break parameters?
2) How much flow would be released to downstream area for overtopping and piping failure modes if the dire dam may breach?
3) Which downstream areas are prone to flood if Dire Dam breaks?

1.5. Significance of the Study

This study is looking forward to analyzing the Dire dam breach condition due to the assumed failure scenarios including of predicting the breach parameters, predicting the maximum breach discharge and predicting the flood extent and mapping the flooded area. The results of the study found can be used by dam owner, and downstream civilian population to perform effective and urgent action plan for flood resulting in the event of the dam failure. The study can be used for other researchers for doing their study on dam breach analysis of embankment dam in the world wide.

1.6. Scope of the Study

The scope of the study was bounded to dam break analysis due to overtopping and piping failure mode using one dimensional HEC-RAS hydraulic model. The analysis through the model is limited to about 12km at the downstream end distance in which the Legadadi River downstream of Dire dam joins with Sendafa River and forms combined stream to join Akaki River.

1.7. Limitation of the study

Since the study was conducted based on utilizing secondary data, lack of primary data is a problem during the study. For the duration of collecting secondary data that can be obtained from concerned organizations, there is no immediate response to the requested data; it delays certain time which has influence on the time for doing study findings. In addition the study limited to overtopping and piping failure scenario since the HEC-RAS hydraulic model allows only overtopping and piping dam breach modeling. Therefore it is better if other failure scenario including slope stability analysis is done by other researchers.

1.8. Structures of the Study

The Study was structured into five chapters. Figure 1-1 showed the overall structures of the study

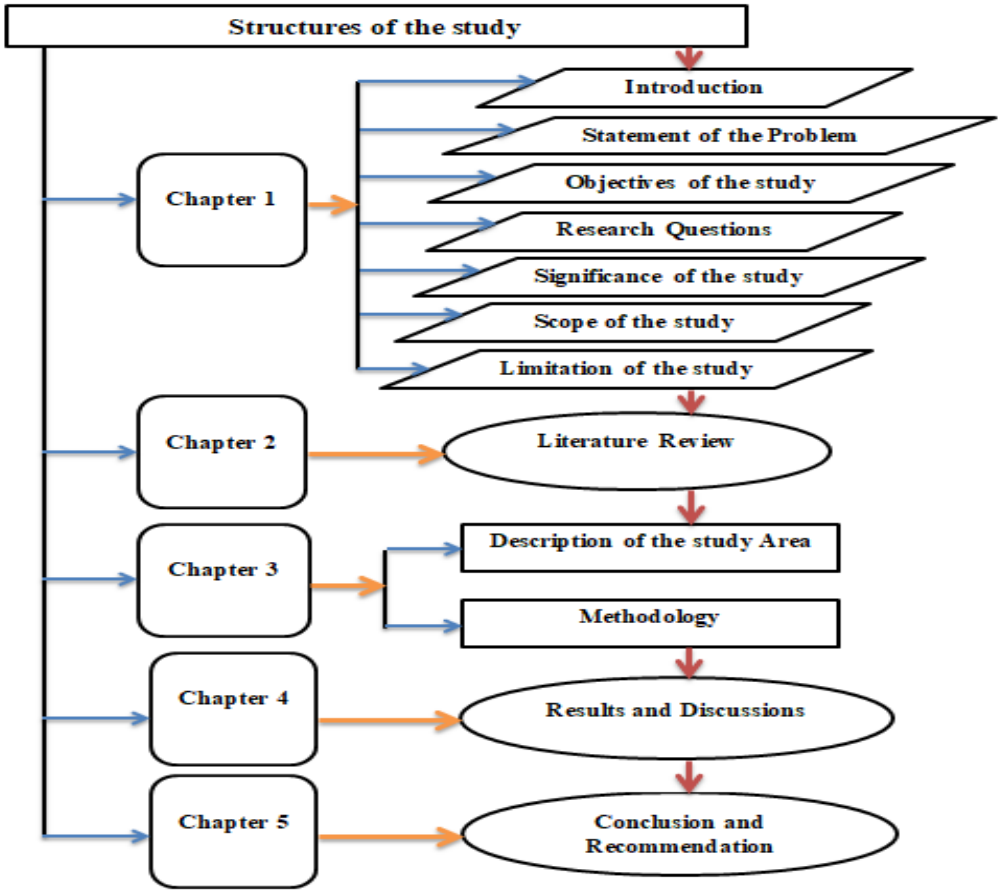

Figure 1-1: The overall structure of the study

2. LITERATURE REVIEW

2.1. General

Dam break analysis is the indispensable theme in which stability of dam is checked against failures due to various factors. Also dam break analysis is important to protect the downstream civilian population and infrastructures located on the downstream of the dam from risk due to its break. Then some literatures are reviewed to encourage the study of dam break analysis for the dam under the case study.

2.2. Dam Break History

The historic dam break data sets over the worldwide from 1900 until 1975 depicted that, dams of height more than 15 meters experienced break commonly caused by overtopping failure mode followed by wearing down of the dam crest and several of the dam failures were triggered by seepage, piping and other failure due to earthquake events (Ekaningtyas, 2017).

Table 2-1: Causes of the dam break in the world 1900-1975

Cause	Concrete dam	Rock fill dam	Others
Overtopping	29%	35%	34%
Piping	53%	21%	30%
Seepage	0%	6%	8%
Others	18%	6%	8%
Total	100%	100%	100%

Source: (Ekaningtyas, 2017).

The major two consequences of a dam failure are Life loss, because of heavy flood resulting from dam break this loss may occurs if the villages and the residing families are washed away and also Economic loss, calculated in terms of revenue which is required to rebuild the washed away villages in terms of infrastructure, and other allied facilities. The dam break analysis will make possible to predict the flood and areas affected by flood at downstream due to breach. The study predicts the potential of precautionary measures which can be taken to completely avoid the dam break which avoid or minimize damage (Kulkarni and Jagtap, 2017).

Even if the latest technologies in design methodologies and construction techniques are advanced, failure of dams still occurs. Numerous failures of dams happened in India as well as over worldwide point out the hazard according to conducted study. Consequently in order to reduce the hazards, attention to be paid on improving management of the flood by formulating emergency action plan in the floodplain. Analyzing the behavior of flood before proposing flood

management measures is important and can be done through analyzing the flood based on the observed floods (Kumar *et al.*, 2017).

Dam break may be summarized as the partial or catastrophic failure of a dam which results in quick release of water from the reservoir. In the event of dam break, the energy stored behind the dam is capable of causing rapid and unexpected flooding on the downstream areas, causing in loss of life and damages infrastructures. Analysis of dam failures aids in providing adequate warnings to the public in the downstream areas. For that reason, dam break analysis and preparation of inundation map is very important (Sharma, 2016).

2.3. Dam Break Analysis

Dam break analysis is performed as part of a dam safety assessment in order to evaluate downstream hazard potential for a dam failure which will assist the decision making authorities in land use planning and in developing emergency action plans to help mitigate catastrophic loss to human life and property. Accurate simulation of the dam break flood wave and its propagation along the downstream valley resulting from a potential dam failure are typically undertaken by hydraulic models (Derdous *et al.*, 2015).

The study of dam break is vital for disaster management in the vicinity of the dam. Dam break modeling helps in making awareness plans, issue of emergency warnings and planning downstream development. Dam break modeling entails determining the outflow hydrograph and the peak discharge, Routing the peak discharge and prediction of hydrograph at different sections downstream up to the point of consideration on the river and mapping of inundation levels (Nema and Desmukh, 2016).

2.4. Dam Break Analysis Study Approaches

The two primary study approaches for dam breach analysis are an event-based approach and a risk-based approach (FEMA, 2013).

2.4.1. Event-based approach for Dam Break Analysis

The event-based approach is the most extensively used for dam breach analysis. An event-based approach is a method that requires the use of series of particular precipitation and non-precipitation events for the analysis of dam failure and downstream flood mapping. For an event-based approach, a non-hydrologic “fair weather failure,” also referred to as a “sunny day failure,” and a specific hydrologic failure event, such as the Probable Maximum Flood are

usually established for dam breach analysis. This approach is more preferable to a risk-based approach since the approach is a direct, is less complex to execute, order, and produces more conservative breach flood zone mapping.

Hydrologic breaches that occur with extreme precipitation and runoff are termed “rainy day” or hydrologic failures. Hydrologic failures that cause dam breach events are generally analyzed based on the Probable maximum flood. A fair weather breach is a dam failure that happens during non-hydrologic or non-precipitation conditions.

2.4.2. Risk-based Approach for Dam Break Analysis

The Risk-based approaches to dam breach analysis have become more suitable for dam safety and dam design purposes. This approach is usually used for dam design purposes to establish the Inflow Design Flood for a dam. A risk-based method to dam design and dam safety assessments has been established to account for the downstream consequences of a potential dam failure. The consequences evaluation is not based on the probability of failure, but instead on the potential loss of life or increase in economic losses caused by a potential dam failure.

2.5. Causes of Dam Failures

Dam failure initiates when appreciable amounts of water begin flowing over or around the dam face and begin to erode the face of the dam. Dam break failures are often caused by overtopping of the dam due to inadequate spillway capacity during large inflows into the reservoir from heavy rainfall-generated runoff and may also be caused by seepage or piping through the dam, earthquake and landslide generated waves in the reservoir (Afsal *et al.*, 2016). Flood or overtopping is the most common cause of dam failure, followed by piping or seepage (FEMA, 2013). The most common causes of dam failure between 1975 and 2011 are summarized in Table 2-2

Table 2-2: Causes of dam failure during the period of 1975–2011

Cause of failure	Number of dam failures	Percentage of dam failure
Flood or overtopping	465	70.9%
Piping or seepage	94	14.3%
Structural	12	1.8%
Human related	4	0.6%
Animal activities	7	1.1%
Spillway	11	1.7%
Erosion/slide/Instability	13	2.0%
Unknown	32	4.9%
Other	18	2.7%
Total number of dam failure	656	100%

Source: (FEMA, 2013).

2.6. Dam Break Mechanisms

2.6.1. Break Mechanism for Embankment Dam

The breach is the opening which develops during the occurrence of dam failure. Dam break mechanism actually described in part for the embankment dams and smaller for the concrete dams. In order to predict downstream flooding which occurs from dam break, numerous researchers approved comprehensive and instantaneous dam break mechanism before the year 1970. A number of factors for instance embankment dimensions, construction material, method of construction, slope protection cover, reservoir geometry and flow entering the reservoir during break and failure mode can affect the shape of break in the embankment dam (Sammen *et al.*, 2017).

For embankment dams, the failure typically begins at a point on the top of the dam and expands in a generally trapezoidal shape. The water flow through the expanding breach acts as a weir; however, depending on conditions such as head water and tail water, various flow characteristics can be observed during a breach development including weir flow, converging flow, and channel flow (Xoing, 2011). Even though breaking in embankment dams may take place for a variety of causes, breaks in embankment dams are regularly modeled as overtopping or piping breaks (FEMA, 2013).

2.6.2. Overtopping Failure of Embankment Dam

Overtopping is the most cause of embankment dams to fail and is happening when the water level exceeds the dam crest elevation, causing it to spill over the dam. After water begins to

overtop the dam, erosion of the dam crest occurs and removes massive amounts of material starting from the downstream face of the dam and head cut will develop towards the upstream face of the dam. While water is flowing over the crest of dam, the dam crest performances like a broad crested weir and the appropriate weir coefficient value is more in the range of a broad crested weir, as the downward cut reaches the natural river bed elevation and the break is more in a widening phase (Joshi, 2017).

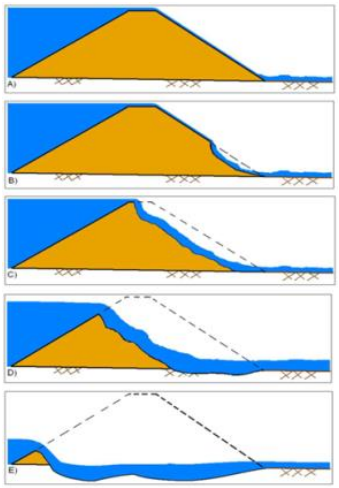

Figure 2-1: Breach process for an overtopping failure, Source: (Hong and Changzhi, 2014).

2.6.3. Piping Failure of Embankment Dam

Piping is also major causes of embankment dam failures which causes erosion and saturation in the dam body or foundation material and causes it to lose strength. Erosion generally begins in the downstream portion of the dam, and works backwards toward the upstream end. While Water is leaking through the dam at a substantial enough rates, it is firstly eroding material and moving it out of the dam. The eroded material results formation of large hole which have a capable of carrying more water and erode extra material. The movement of water via the dam body is modeled in terms of a pressurized orifice type flow. As the piping hole continues to grow concurrently, the head cutting and sloughing processes will continue to move back towards the upstream face of the dam. As the head cutting and erosion process continues back via the dam and downward, the break will be widening. The break may continue to cut down and widen until the natural river bed is developed based on the volume of water in the dam reservoir (Joy, 2016).

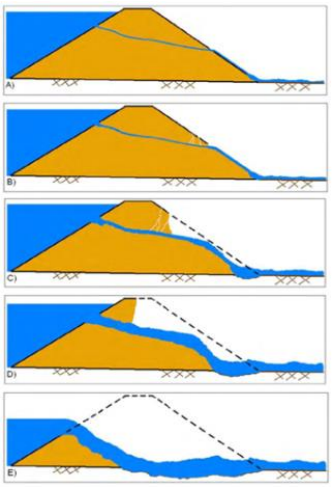

Figure 2-2: Breach process for a piping failure, Source: (Hong and Changzhi, 2014).

2.7. Dam Break Parameters

Parameters which are required to characterize the breach are known as breach parameters. Breach parameters can be divided into two categories: Geometric parameters (The geometric parameters define the shape and size of the breach) and Hydrographic parameters (The hydrographic parameters include peak outflow rate and time of failure). After the commencement of breaching, the outflow through the breach increases until it reaches a peak discharge, and then decreases until there is no longer any water in the reservoir or the breaching process ceases to develop (Nema and Desmukh, 2016).

The most important breach parameters used for dam breach are: breach formation time (also time to failure); Break height, The break height is defined as the vertical extent of the break measured from dam crest elevation or from a particular elevation to the bottom elevation of the dam break; Break width, The break width is demarcated as the average of the final break width normally measured at the vertical center of the break; Break side slope, The break side slope is expressed a measure of the angle of the break sides denoted as X horizontal to 1 vertical (XH: 1V) and break location, The break location is expressed in terms of center line stationing of the break in the dam (FEMA, 2013).

The assessment of a dam's potential risk is greatly related with the prediction of dam break location, dimensions and break development time. This is mainly true in a risk assessment where dams will be ordered based on the potential for destruction of life and property damage. The break parameters like the break location, break size, and break formation time will directly affect

the prediction of the peak breach outflow coming out of the dam, in addition to any possible warning time available to downstream sites (Brunner, 2014).

2.8. Estimating Dam Break Parameters

Dam break study depends on two primary tasks of estimating the breach flood hydrograph and routing this hydrograph downstream of dam. Essentially the breach flood hydrograph depends on the prediction of Dam break parameters (breach geometry and breach formation time). Empirical approaches used for predicting breach parameters rely on data obtained from historical dam failures (Basheer *et al.*, 2017).

The basic approach for dam failure modeling in some models is to ask the user to specify geometric parameters (that describe the final break size and shape of the break opening which guides the reservoir outflow) and the break formation time. The reservoir outflow is calculated by supposing that the break opening functions as broad crested weir. Most advanced models assume that the break can be demarcated geometrically by a simple trapezoidal shape, as revealed in figure 2-3. The significant parameters which defines a break are the bottom break width (B), average break width (Bavg), break height (Hb), break side slope ratio (Z:1 (H:V)), and the water depth above the final break bottom at the time of break (Hw). Besides the geometric break parameters, the user is requested to describe the time required for the break formation and this time parameter is used to enlarge the break from zero size to the final size at the specified time (Wahl, 2014).

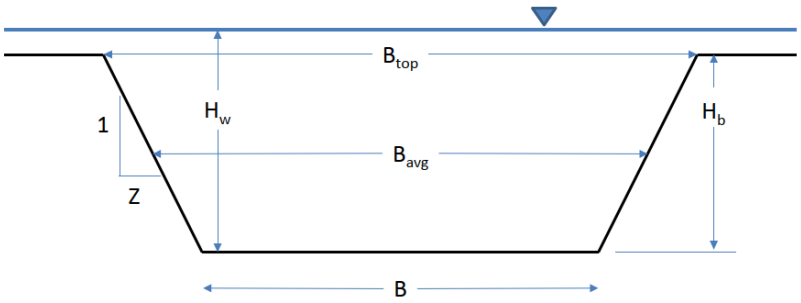

Figure 2-3: Idealized dam breach geometry, Source: (Wahl, 2014)

2.9. Methods for Estimating Dam Break Parameters

The numerous methods for predicting a break parameters that serve as input to different models for analysis purpose are: Comparative analysis (comparing study dam to historical failures of dams of similar size, materials and water volume), Regression approaches (developed from

historical dam failures in order to estimate break size (width, height and side slope), break development time and peak outflow), and physically based computer models (software that attempts to model the physical breaking process by using sediment transport or erosion equations, soil mechanics and principles of hydraulics) (Davide and Canale, 2016).

(Davide and Canale, 2016) presented Equations to predict break parameters and peak outflows through regression analysis of data obtained from real dam failure case studies. The regression analysis relates input parameters such as height of dam and volume of water stored to the observed break parameters from real failures.

2.10. Parametric Regression Approaches for Estimating Dam Break Parameters

The parameters of a dam break can be estimated by parametric models which offer simple and accessible methods. The data sets are collected from historic dam failure data and its analysis is statistically done through regression methods. The outcome is a set of parametric equations relating breaking parameters such as break depth, break width, break side slope, break formation time and peak outflow in terms of a function of simple dam or reservoir properties. This approach has preferable advantages like the speed, ease of use and the lessening of costs to the more advanced physically based models. The fewer input parameters to determine dam break parameters by simple equations normally comprise; total reservoir volume (V_r), dam height (h_d), water volume above final break bottom (V_w), break height (h_b) and height of water above final break bottom (h_w) (Morris and Hassan, 2018).

Parametric regression approaches are empirically derived using historic dam break case study data to estimate the time to failure and ultimate breach geometry. Several equations to calculate break parameters have been developed based on analyses of historic dam break case studies and the most common parametric regression equations developed are: MacDonald & Langridge-Monopolis 1984, Von Thun and Gillette 1990, Froehlich 1995, and Froehlich 2008. These methods have reasonably good correlation when comparing predicted values to actual observed values (Davide and Canale, 2016). Therefore, the empirical equations developed through these parametric regression approaches are described as the following:

2.10.1. MacDonald & Langridge-Monopolis 1984 Regression Approach

MacDonald & Langridge-Monopolis utilized 42 historic dam failures data sets (predominantly earth fill dams, earth fill dams with a clay core, rock fill dams). MacDonald & Langridge-

Monopolis then related the breach formation time to the volume of material eroded from the dam's embankment. MacDonald & Langridge-Monopolis stated that the equation for the breach formation time is an envelope of the data from the earthen dams and the breach should be trapezoidal with breach side slopes of 0.5H: 1V (for overtopping and piping) and then the break size is calculated by considering the break wear away vertically to the bottom of the dam and it wear away horizontally up to the maximum quantity of material has been eroded. Then MacDonald & Langridge-Monopolis 1984 develops regression equation to predict volume of material eroded, breach formation time, breach bottom width and peak breach outflow discharge as follows:

For earth fill dams

$$\text{Veroded} = 0.0261\ (\text{Vout} \times \text{hw})^{0.769} \quad \text{..(2-1)}$$

$$\text{tf} = 0.0179\ (\text{Veroded})^{0.364} \quad \text{..(2-2)}$$

For earth fill with clay core or rock fill dams

$$\text{Veroded} = 0.00348\ (\text{Vout} \times \text{hw})^{0.852} \quad \text{.(2-3)}$$

$$\text{B} = \frac{\text{Veroded} - \text{hb}^2\left(\text{CZb} + \frac{\text{hbZbZ3}}{3}\right)}{\text{hb}\left(\text{C} + \frac{\text{hbZ3}}{2}\right)} \quad \text{.....(2-4)}$$

$$\text{Qp} = 1.153\ (\text{Vwhw})^{0.412} \quad \text{.....(2-5)}$$

Where V_{eroded}, volume of material eroded from the dam embankment in cubic meter; V_{out}, volume of water that passes through the breach in cubic meter can be calculated in terms of storage volume at time of breach plus volume of inflow after breach begins minus any spillway and gate flow after breach begins; h_w, depth of water above the bottom of the breach in meters; t_f, breach formation time in hours; B, bottom width of the breach in meters; h_b, height from the top of the dam to bottom of breach in meters; C, crest width of the top of dam in meter; $Z_3 = Z_1 + Z_2$; Z_1, average slope (Z_1:1) of the upstream face of dam; Z_2, average slope (Z_2:1) of the downstream face of dam and Z_b, side slope of the breach (Z_b:1), Qp, peak breach outflow discharge in cubic meter per second, and Vw, reservoir volume at time of failure in cubic meter.

2.10.2. Von Thun and Gillette 1990 Regression Approach

Von Thun and Gillette used 57 historic dam failures data sets to develop the equation for average breach width and breach formation time. Von Thun and Gillette 1990 developed two different sets of equations for breach development time; which is breach development time as a function of water depth above the breach bottom and also breach development time as a function of water depth above the breach bottom and average breach width. The average breach side slopes is proposed as 0.5H: 1V (for overtopping and piping).

$$Bavg = 2.5\ hw + Cb \quad \text{(2- 6)}$$

Table 2-3: Value of C_b as a function of reservoir storage

Reservoir size (m^3)	C_b (m)
$< 1.23\times 10^6$	6.1
$1.23\times 10^6 - 6.17\times 10^6$	18.3
$6.17\times 10^6 - 1.23\times 10^7$	42.7
$>1.23\times 10^7$	54.9

Source: (Davide and Canale, 2016).

Breach development time equation as a function of water depth above the breach bottom for erosion resistant and easily erodible respectively as follows:

$$tf = 0.02\ hw + 0.25 \quad \text{(2-7)}$$

$$tf = 0.015\ hw \quad \text{(2-8)}$$

Breach development time equation as a function of water depth above the breach bottom and average breach width for erosion resistant and easily erodible respectively as follows:

$$tf = \frac{Bavg}{4\ hw} \quad \text{(2-9)}$$

$$tf = \frac{Bavg}{4\ hw+61} \quad \text{(2-10)}$$

$$Qp = 0.863\ Vw^{0.335} Hd^{1.833} Bavg^{-0.663} \quad \text{(2-11)}$$

Where, B_{avg}, average breach width in meters, h_w, depth of water above the bottom of the breach in meters, C_b, coefficient which is a function of a reservoir size in meters, and t_f, breach

development time in hours, Qp, peak breach outflow discharge in cubic meter per second, Vw, reservoir volume at time of failure in cubic meter, and Hd, dam height in meter

2.10.3. Froehlich 1995 Regression Approach

Froehlich utilized 63 earthen, zoned earthen, earthen with a clay core and rock fill dams historic dam failures data sets to develop equations for prediction of average breach width, side slopes and failure time. Froehlich 1995 states that the average breach side slope should be 1.4H: 1V for overtopping failure and 0.9H: 1V for piping failure and also the height of the breach is normally calculated by assuming the breach goes from the top of the dam all the way down to the natural ground elevation at the breach location.

$$Bavg = 0.1803\ Ko\ Vw^{0.32} hb^{0.19} \quad \text{(2-12)}$$

$$tf = 0.00254\ Vw^{0.53} hb^{-0.9} \quad \text{(2-13)}$$

$$Qp = 0.6\ Vw^{0.295} hb^{1.24} \quad \text{(2-14)}$$

Where, B_{avg}, average breach width in meters; K_o, constant (1.4 for overtopping failures and 1 for piping); V_w, reservoir volume at time of failure in cubic meter; h_b, height of the final breach in meter, t_f, breach formation time in hours and Qp, peak breach outflow discharge in cubic meter per second.

2.10.4. Froehlich 2008 Regression Approach

Froehlich updated his breach equations based on the addition of new data and then utilized 74 earthen dam, zoned earthen dam, earthen with a clay core and rock fill historic dam failures data sets to develop equations for prediction of average breach width, side slopes and failure time. Froehlich 2008 states that the average breach side slope should be 1H: 1V for overtopping failure and 0.7H: 1V for piping failure and also the height of the breach is normally calculated by assuming the breach goes from the top of the dam all the way down to the natural ground elevation at the breach location.

$$Bavg = 0.27\ Ko\ Vw^{0.32}\ hb^{0.04} \quad \text{(2-15)}$$

$$tf = 63.2\sqrt{\frac{Vw}{g(hb)^2}} \quad \text{(2-16)}$$

$$Qp = 3.1 Bavg\ hw^{1.5}\left(\frac{\gamma}{\gamma + tf\sqrt{hw}}\right)^3 \quad \text{(2-17)}$$

Where, B_{avg}, average breach width in meters; K_o, constant (1.3 for overtopping failures and 1 for piping); V_w, reservoir volume at time of failure in cubic meter; h_b, height of the final breach in meter; g, gravitational acceleration (9.81) in meter per second squared, t_f, breach formation time in hours, γ, instantaneous flow reduction factor expressed as $\gamma = 23.4\left(\frac{As}{Bavg}\right)$, and As, Surface area of the reservoir in acres corresponding to hw. In order to simulate the dam break, the break size should be initially determined quantitatively. The estimations of the break including location, size, and development time parameters are important to make an accurate estimate of the outflow hydrographs and downstream flood inundation. For estimating break parameters such as average break width and break development time which are input data for HEC-RAS model, Parameters can be specified using regression approach generating from historical dam break occurrence data suggested by Froehlich 2008 (Ekaningtyas, 2017).

One of the recent studies on dam breach is presented by Froehlich 2008 which can be considered as a further enhancement of his breach equations by increasing the historic dam failures data sets and states that the average breach side slopes are equal to 1H:1V for overtopping failure and 0.7H:1V for piping. The breach development time is related inversely to the breach height and directly to reservoir volume, that means for a given reservoir volume, dams with greater height tend to produce shorter failure times (Basheer *et al.*, 2017).

The performances of Von Thun and Gillette 1990, Froehlich 1995, Froehlich 2008, equations in predicting the average breach width and in predicting the breach failure time, is indicated by comparing the observed breach values (average width and failure time) and predicted breach values (average width and failure time). The highest accuracy in predicting the average breach width and failure time is obtained by Froehlich 2008 equations. Also the performance of Froehlich method 2008 is relatively better than the other methods for the dam breach width and dam failure time estimation (Sammen *et al.*, 2017).

Regarding the flood and the dam failure simulation the HEC-RAS model is used. For the study of the overtopping and piping failure mode, the most important parameters of the breach like average breach width and breach failure time is calculated using the empirical equations developed by Froehlich 2008 (Urzica *et al.*, 2019).

2.11. Dam Break Analysis using HEC-RAS

HEC-RAS is designed to perform one dimensional steady flow and one dimensional and two dimensional unsteady flow river hydraulics calculations for full network of natural and constructed channels, and overbank or floodplain areas (Brunner, 2016).

HEC-RAS model helps to rout the inflow hydrograph through the reservoir and rout the outflow hydrograph results from dam failure through the downstream of the river in dam break analysis purpose. Routing inflow flood hydrograph via reservoir, can be carried out using any of the methods such as full saint venant equation (one dimensional unsteady flow routing), full saint venant equation or diffusion wave equation (two dimensional unsteady flow routing), or level pool routing. In full unsteady flow routing (one or two dimensional unsteady flow routing), the water surface slope through the pool is captured as the inflow hydrograph reaches in addition to the variation in the water surface slope that happens during a break of the dam. The figure 2-4 shows one dimensional full Dynamic Routing. Level pool routing is used when the water supplied to the dam will come from the storage area and the storage area elevation will drop as a level pool as water flows out of the breach. In level pool routing approach, the water surface in the reservoir is always assumed horizontal. The figure 2-5 shows the level pool routing. The dam is modeled with the Inline structure option in HEC-RAS (Muhammad and Rasheed, 2016).

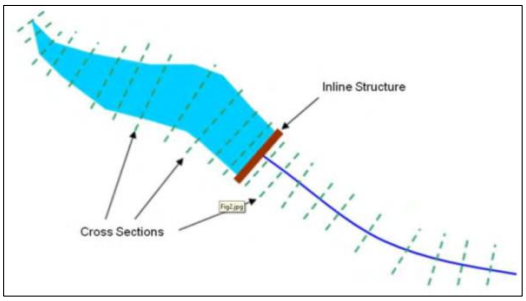

Figure 2-4: One-Dimensional Full Dynamic Routing, Source: (Muhammad and Rasheed, 2016).

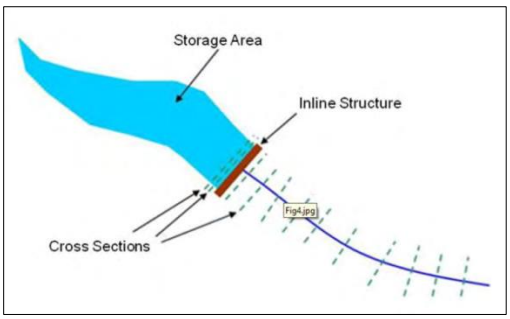

Figure 2-5: Level Pool Routing, Source: (Muhammad and Rasheed, 2016).

While developing an unsteady flow simulation for dam break study in the HEC-RAS model, the points should be considered are: Cross sections, Manning's Roughness Coefficient, inline structures, upstream boundary condition and downstream boundary condition (Abdulrahman, 2014). HEC-GeoRAS develops geometric data for HEC-RAS model from Digital elevation model and the model results calculated in HEC-RAS can be post processed in GIS to know the floodplain depths and extents for flood inundation map (Cameron and Ackerman, 2012).

2.12. Dam Hazard classification

The hazard potential classification of a dam, along with its size (height and capacity) is used by State agencies to regulate dam design and dam breach modeling. Federal and state dam safety agencies categorize a dam based on the potential effects of a dam break on downstream areas. The hazard potential classification does not reflect in any way on the current condition of the dam corresponding safety and structural integrity (FEMA, 2013).

FEMA guidance recommends a three classifications levels that includes low, medium and high hazard potential classifications depending on the potential for loss of life, economic loss, and environmental damage resulting from a hypothetical dam failure. Dams assigned the low hazard potential classification are those where failure results in no probable loss of human life, low economic and environmental losses. If the dam failure consequences can cause economic loss and environmental damage, the dam is categorized as medium hazard potential and Dams assigned the high hazard potential classification are those where failure will probably cause loss of human life.

2.13. Previous Studies

In Various literatures dam break analysis of certain dams have been conducted by several researchers as the world. The case histories of dam failures in the worldwide indicated that, embankment dams are under worst condition of overtopping and piping failure scenarios. Therefore analysis of any embankment dams break due to overtopping and piping at any time is essential to reduce the risk due to its break. The most recent time models used for dam breach study are DAMBRK MODEL, FLDWAV, SMPDBK, and HEC-RAS. The most acceptable and recent time model for dam breach analysis from these models is HEC-RAS model. The HEC-RAS model allows only simulating overtopping and piping failure scenarios of embankment dams (Pandya and Thakor, 2016).

The experience of analyzing dam breach conditions prior to its possibly fail was some extent contributed to constructed dam in Ethiopia. Since number of dam constructed in the country was dominantly embankment dam, many researches have been done for embankment dam fail analysis via different researchers.

(Duressa and Jubir, 2018) conducted their study on dam break analysis of Fincha'a Rock fill dam located in Horro Guduru Wollega Zone Oromiya Region, Ethiopia. (Leoul and Kassahun, 2019) presented the study on dam break analysis of Kesem Kebena embankment dam located at the southern end of the Afar depression in Afar regional state, Ethiopia 225 km East of Addis Ababa. Not only Fincha'a Dam and Kesem Kebena dam, dam breach modeling and downstream risk analysis of Arjo dedesa embankment dam located in East Wollega Zone Oromia Region and dam breach analysis of Mhtsab Azmati Embankment dam located northern part of Ethiopia in the Tigray region have been done by the two researchers (Lejissa, 2015) and (Yohannes, 2019) respectively. Dire dam under case study is also embankment dam which possibly fails and affects downstream areas by flooding. In order to prevent irreversible failure of the dam and flood resulting in the downstream areas in the event of its breach, analyzing Dire dam breach is very important.

3. MATERIALS AND METHODS

3.1. Study Area Description

3.1.1. Location of the Study Area

The Dire Watershed with the respective dam was located 30 km to the east of Addis Ababa city within the boundary of the Oromia Region. Geographically the dam was bounded between 38°56′02″ E longitude and 9°08′53″ N latitude. Dire dam Watershed area considered for this study was 427 km^2. It is sub-catchment of the Akaki river basin which flows in a northeast-southwest direction and is portion of the drainage system that forms the northwest corner of the Awash River basin. The dam was constructed in the year 1999 along the Legedadi River for the purpose of providing potable water for Addis Ababa city in order to meet increasing demand for water in the metropolitan area.

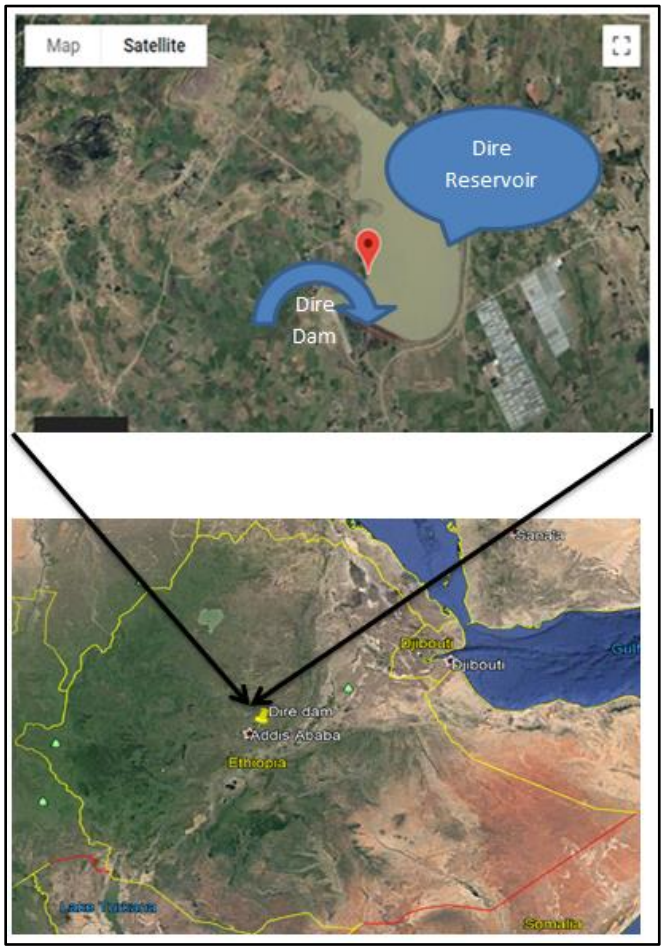

Figure 3-1: Satellite image of the Study Area, Source: Google Earth

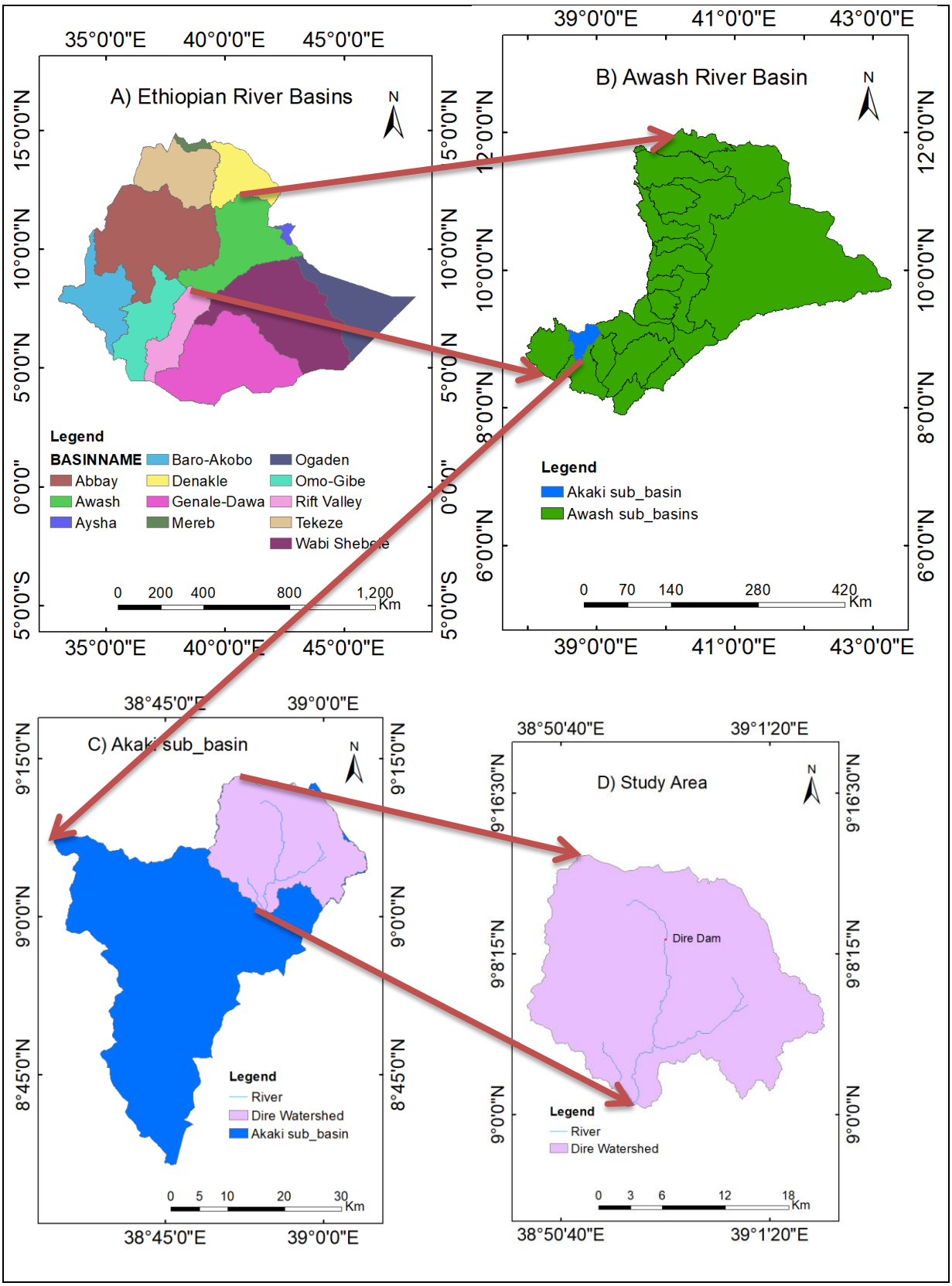

Figure 3-2: Location of the Study Area

3.1.2. Climate of the Study Area

The rainfall configurations in the region of the study area have a bimodal profile with strong peaks in the summer season and minor rainfalls in the March and April. During summer seasons, predominantly from July to September, a robust air current moves in the direction of the southwest to the northeast. The mean annual rainfall range in this study area is 1230 -1,300 mm. The weather of the study area is comparatively cool in the wet season of July to September at what time the highest rains fall, and the more or less rainless season of October to June has warmer temperatures.

3.1.3. Topography of the Study Area

The elevation in the Dire Watershed ranges from 2,277 m to 3,237 m. The 960 m elevation difference exhibits the steepness of the watershed. Figure 3-3 represented the elevations of Dire Watershed.

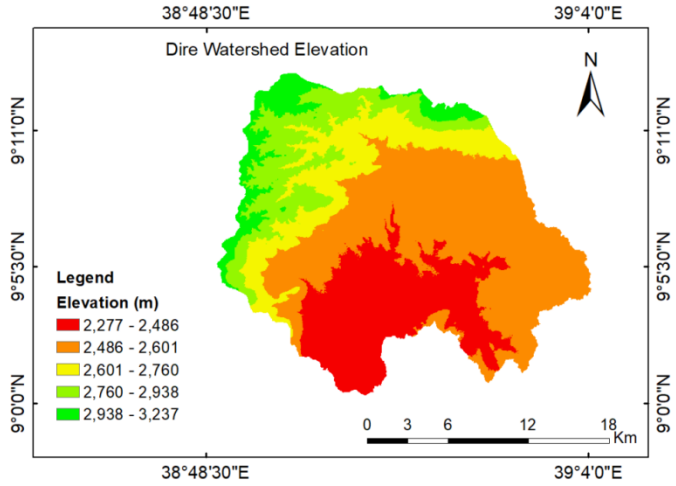

Figure 3-3: Elevation map of the study area

3.1.4. Land Slope of the Study Area

The main physiographic units on which the various study area land cover types found were the mountains of Bura, Tenkole, and Bereh, separated side slopes of mountains, hills, steep to undulating foot-slopes, gullies, valleys, and undulating plains and flat to almost flat plains. Therefore the land slope of the study area was steep slope and showed in the figure 3-4 below.

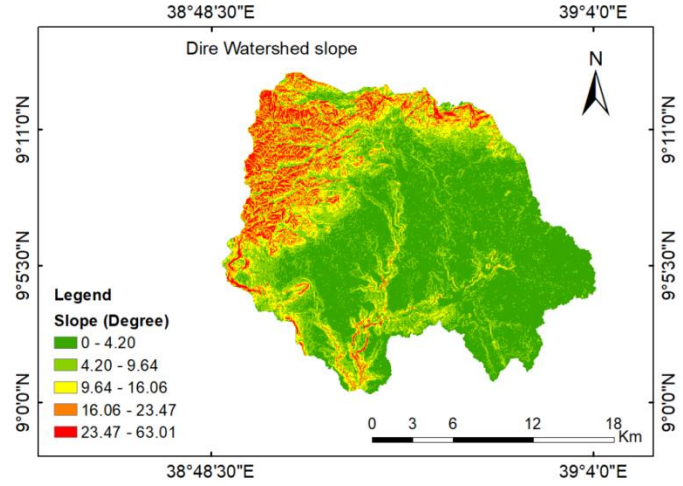

Figure 3-4: Land slope of the study area

3.1.5. Land Use/Land Cover of the Study Area

The land uses land covers in the Dire Dam Watershed comprises Cropland with grassland savanna and shrub land, grassland with cropland and shrub land, Montane Broadleaf Evergreen woodland, Tropical plantations and settlements. The land uses land covers in the Watershed were exhibited in figure 3-5.

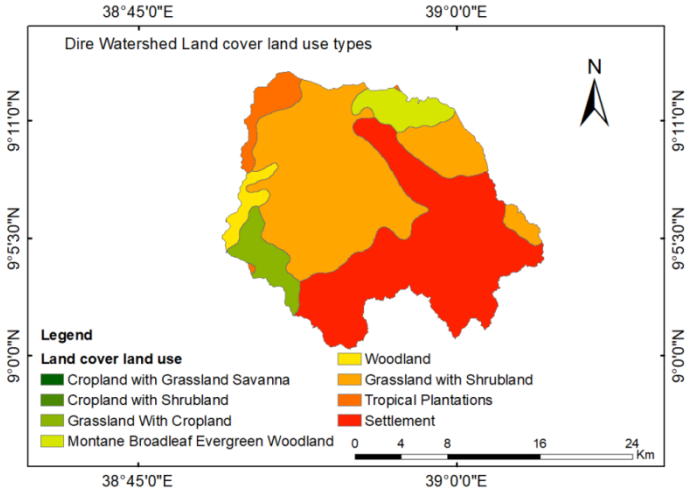

Figure 3-5: Land use land cover map of the study area

3.1.6. Soil of the Study Area

The soil types in the Dire Watershed were considered to be more prone to soil erosion. The major soil types in this study area are Calcic xerosols, Chromic cambisols, Chromic luvisols, Leptosols, Orthic solonchaks and pellic vertisols and figure 3-6 below showed the soil types in the Dire Watershed.

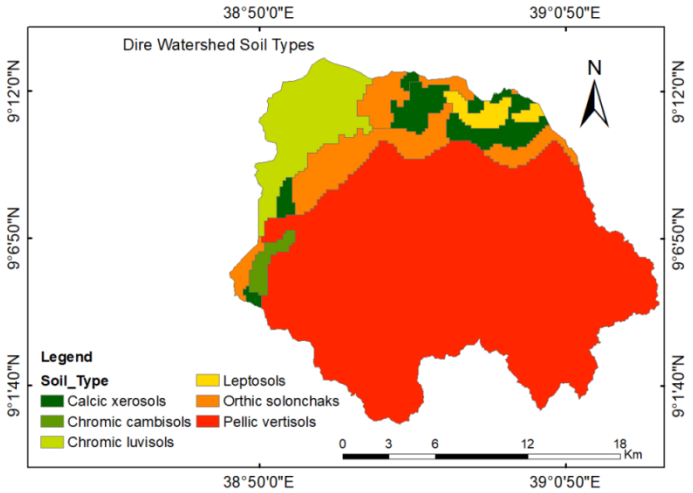

Figure 3-6: Soil map of the study area

3.1.7. Dire Dam and Reservoir

Dire dam was a zoned rock fill dam with an impermeable central clay core. The raw water in the Dire reservoir is supplied to the Legedadi Water treatment plant. The dam encompasses intake structure, bottom outlet, the spillway, and the conveyance pipeline for carrying the water to the Legedadi Water Treatment Plant. The intake structure comprises intake tower, bottom gate, conveyance structure located downstream. The un-gated overflow type spillway structure was constructed on the right bank and was designed to convey flood discharge of about 500m^3/s. The main characteristics of the dam and reservoir were given in the table 3-1.

Table 3-1: The main characteristics of Dire dam and Dire reservoir

Dam crest elevation (m a.m.s.l)	2559.8
Dam height (m)	41.8
Dam crest length (m)	2000
Dam crest width (m)	7
Upstream Embankment slope	4:1
Downstream Embankment slope	2.5:1
Spillway flood discharge (m^3/s)	500
Peak Probable maximum flood (m^3/s)	570
River bed level (m a.m.s.l)	2518
Normal water level or full supply level (m a.m.s.l)	2557
Low water level (m a.m.s.l)	2529.5
Maximum water level (m a.m.s.l)	2558.25
Reservoir area (m^2)	$1.75*10^6$
Reservoir Volume at the maximum water surface elevation (m^3)	$23.5*10^6$
Reservoir Volume at full supply level (m^3)	$19.55*10^6$

Source: (Addis Ababa Water and Sewerage Authority, 2016).

3.2. Data Collection

In order to conducting this study, a number of data should be available as required. The study was based on existing hydrologic and topographic data. The data required for the study were topographic data, hydrologic data and dam geometric data.

3.2.1. Topographic Data

Topographic data for the study area was collected in the form of Digital Elevation Model (DEM). DEM symbolizes elevation values over a topographic surface or represents elevation data of the reservoir, dam and cross sections of a river. For this study elevation data of Legadadi river channel, banks and cross sections were developed from high resolution 12.5m × 12.5m DEM of Dire watershed collected from the website http://vertex.daac.asf.alaska.edu/. Figure 3-7 presented DEM of the Dire watershed which province to limit the analysis area for the watershed.

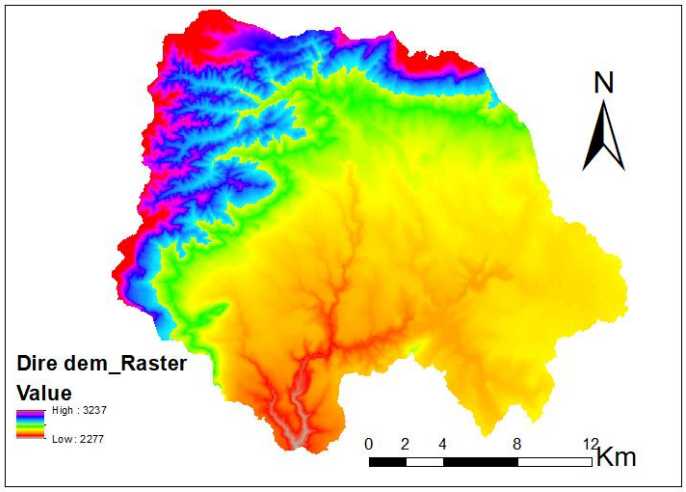

Figure 3-7: Digital Elevation Model of the study area

3.2.2. Hydrologic Data

Hydrologic data of Legadadi River including PMF Inflow flood hydrograph, reservoir capacity, and reservoir storage versus elevation data were collected from Addis Ababa Water and Sewerage Authority (AAWSA).

3.2.3. Dam Geometric Data

Dire Dam geometric data which represents physical characteristics of the dam such as dam height, dam crest length, dam top width, dam side slopes, and dam crest elevation were collected from Addis Ababa Water and Sewerage Authority (AAWSA).

3.3. Data Analysis

The main important issue of data analysis was to obtain evidence from the collected data. In this study, the data that was collected from different organizations needs analysis in order to generate evidence that ensures the result that was developed through the study. Data required for this study including Hydrologic data and Dam Geometric data were analyzed by concerned organizations and elevation data of Legadadi River was analyzed through HEC-GeoRAS model.

3.4. Methodology

Dam break analysis can be performed using the flood routing techniques suggested by St. Venant's equations with level pool routing for unsteady flow. St. Venant's equations solve both the continuity and momentum equations. Solution of the equation is governed by the number of cross sections. Since solving the entire equation simultaneously is difficult, the so called one dimensional HEC-RAS hydraulic model has been selected. St. Venant's Equations of both Continuity Equation and Momentum Equation expressed as in the equations 3-1 and 3-2.

St. Venant's Equations:

Continuity Equation

$$\frac{\partial Q}{\partial x} + \frac{\partial A}{\partial t} = 0 \quad \text{.....(3-1)}$$

Momentum Equation

$$\frac{1}{A}\frac{\partial Q}{\partial t} + \frac{1}{A}\frac{\partial}{\partial x}\left(\frac{Q^2}{A}\right) + g\frac{\partial y}{\partial x} - g(So - Sf) = 0 \quad \text{.....(3-2)}$$

Where: Q, discharge in cubic meter per second; A, cross-sectional area of flow in meter squared; y, water surface elevation in meters; x, distance along the channel or waterway in meters; t, time in second; g, gravitational acceleration in meter per second squared; So, expansion contraction slope and Sf, friction slope.

In level pool routing method, the water starts to breach the dam comes from the storage area and the storage area level drop as a level pool as water flows through the breach. In order to model dire reservoir, using level pool routing in HEC-RAS, the pool area was modeled with the storage area that was connected to the downstream Legadadi River reach and the River reach had two cross sections inside the reservoir pool. In HEC-RAS, Dire dam was modeled as an inline

structure which requires one cross section in the upstream side. The first cross section inside the reservoir pool was tied to dire reservoir and the second cross section inside the reservoir pool was tied to dire dam.

3.4.1. General Process of Dire Dam Break Analysis

Dire dam breach analysis in one dimensional HEC-RAS involves several procedures in order to attain the objectives. The important procedures carried out were: identifying dam break scenario, dam break parameters estimation, preparing geometric data, unsteady flow simulation and preparing a downstream flood inundation map. The dam break scenario for the dam under the case study was assumed as overtopping and piping failure. The dam break parameters (bottom breach width and breach formation time) were estimated through Parametric regression methods of MacDonald & Langridge-Monopolis 1984, Von Thun and Gillette 1990, Froehlich 1995, and Froehlich 2008. However these methods were used for estimating breach parameters, the values found by Froehlich 2008 were selected for dire dam breach analysis while comparing to others.

Geometric data involves: required information about physical characteristics of stream center line, bank line, flow path line, cross sections, inline structure, and storage area. This data was created in GIS via HEC-GeoRAS from Dire DEM represented by TIN and imported in to HEC-RAS. Unsteady flow simulation was carried out in HEC-RAS through processing unsteady flow data and the geometric data. The downstream flood inundation map was prepared in GIS. Afterward the unsteady flow analysis was performed in HEC-RAS model; the water surface elevation, the maximum flow depth and velocity were exported in to GIS and assimilated with the Aerial map in order to envisage the inundation map extent advanced from the breached dam through overtopping and piping failure modes. Figure 3-8 below presented the overall workflow diagram for the study.

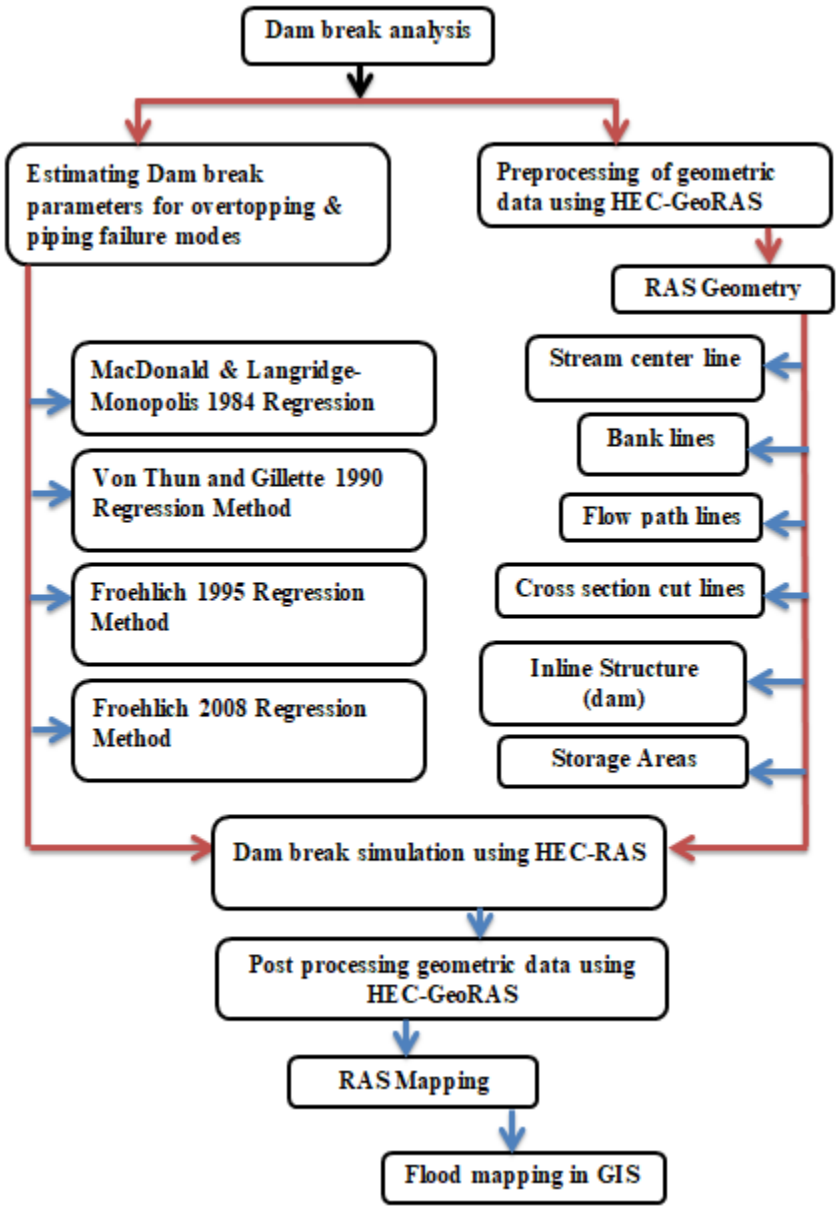

Figure 3-8: The Overall Workflow diagram of the Study

3.4.2. MacDonald & Langridge-Monopolis 1984 Regression Method

As reviewed in the literatures, the dam breach parameters such as bottom breach width (B), breach formation time (tf) and peak breach outflow discharge (Qp) can be estimated using MacDonald & Langridge-Monopolis 1984 method as represented in the equations 3-3, 3-4, and 3-5 respectively.

$$B = \frac{Veroded - hb^2\left(CZb + \frac{hbZbZ_3}{3}\right)}{hb\left(C + \frac{hbZ_3}{2}\right)} \quad \text{.....(3-3)}$$

$$tf = 0.0179(Veroded)^{0.364} \quad \text{.....(3-4)}$$

$$Qp = 1.153\ (Vwhw)^{0.412} \quad \text{.....(3-5)}$$

In the equation (3-3) and (3-4) above, Veroded denotes volume of material eroded from the dam embankment in cubic meter which is the function of volume of water that passes through the breach (V_{out}) in cubic meter and depth of water above the bottom of the breach (h_w) in meter. It is expressed as follows for earth fill dam as, $Veroded = 0.0261(Vout \times hw)^{0.769}$ and for earth fill dam with core material or rock fill dam as, $Veroded = 0.00348(Vout \times hw)^{0.852}$; Hb, height of the breach in meter, Zb, breach side slope, Z3 is the function of upstream (Z1) and downstream face of dam side slopes (Z2), (Z3 = Z1+Z2), and C, crest width of the top of dam in meter. In the equation (3-5) above, Vw represents reservoir volume at time of failure in cubic meter. The units for B, tf, and Qp in the above equations are meter, hour and cubic meter per second respectively.

3.4.3. Von Thun and Gillette 1990 Regression Method

As reviewed in the literatures, the dam breach parameters such as Average breach width (Bavg), breach formation time (tf) and peak breach outflow discharge (Qp) can be estimated using Von Thun and Gillette 1990 method as expressed in the equations 3-6, 3-7, 3-8, 3-9, 3-10, and 3-11 below.

$$Bavg = 2.5\ hw + Cb \quad \text{.....(3-6)}$$

$$tf = 0.02\ hw + 0.25 \quad \text{.....(3-7)}$$

$$tf = 0.015\ hw \quad \text{.....(3-8)}$$

$$tf = \frac{Bavg}{4\ hw} \quad \text{.....(3-9)}$$

$$tf = \frac{Bavg}{4\ hw+61} \quad \text{.....(3-10)}$$

$$Qp = 0.863\ Vw^{0.335} Hd^{1.833} Bavg^{-0.663} \quad \text{.....(3-11)}$$

In the expressions of the above equations, hw, denotes depth of water above the bottom of the breach in meter, and Hd, indicates dam height in meter. Vw, represents reservoir volume at time of failure in cubic meter, and C_b, coefficient which is a function of a reservoir size in meter

shown in the table 2-3 under literature review part. Equations (3-7) and (3-8) expresses the breach formation time as a function of water depth above the breach bottom for erosion resistant and easily erodible respectively, and also Equations (3-9) and (3-10) expresses the breach formation time as a function of water depth above the breach bottom and average breach width for erosion resistant and easily erodible respectively. The units for Bavg, tf, and Qp in the above equations are meter, hour and cubic meter per second respectively.

3.4.4. Froehlich 1995 Regression Method

As reviewed in the literatures, the dam breach parameters such as Average breach width (Bavg), breach formation time (tf) and peak breach outflow discharge (Qp) can be estimated using Froehlich 1995 method as represented in the equations 3-12, 3-13, and 3-14 respectively.

$$Bavg = 0.1803\ Ko\ Vw^{0.32} hb^{0.19} \quad \text{(3-12)}$$

$$tf = 0.00254\ Vw^{0.53} hb^{-0.9} \quad \text{(3-13)}$$

$$Qp = 0.6\ Vw^{0.295} hb^{1.24} \quad \text{(3-14)}$$

In the equation (3-12) above, Ko represents, constant (1.4 for overtopping failures and 1 for piping) and also in the equations (3-12), (3-13), and (3-14); V_w and h_b denote reservoir volume at time of failure in cubic meter, and height of the final breach in meter respectively. The units for Bavg, tf, and Qp in the above equations are meter, hour and cubic meter per second respectively.

3.4.5. Froehlich 2008 Regression Method

This method was appreciable to compute dam break parameters (breach width and breach formation time) based on past historic dam breach data sets. Since the method was utilizing the evidence of 74 earth fill dams of past historic dam break data sets and the method had high performance and highest accuracy in estimating break parameters while comparing to other approaches, the method was selected for this study. Then the break parameters average break width (Bavg) and break development time (tf) and also peak breach outflow discharge (Qp) were expressed through Froehlich 2008 Regression equation as follows respectively.

$$Bavg = 0.27\ Ko\ Vw^{0.32}\ hb^{0.04} \quad \text{(3-15)}$$

$$tf = 63.2\sqrt{\frac{Vw}{g(hb)^2}} \quad \text{(3-16)}$$

$$Qp = 3.1 Bavg\ hw^{1.5}\left(\frac{\gamma}{\gamma + tf\sqrt{hw}}\right)^3 \quad \text{(3-17)}$$

In the equation (3-15) above, ko signifies, constant (1.3 for overtopping failure mode and 1 for piping failure mode) and also in the equations (3-15), (3-16), and (3-17); V_w and h_b denote reservoir volume at time of failure in cubic meter, and height of the final breach in meter respectively. Also γ, instantaneous flow reduction factor expressed as $\gamma = 23.4\left(\frac{As}{Bavg}\right)$, and As, Surface area of the reservoir in acres corresponding to hw. In the equation (3-16), g indicates gravitational acceleration (9.81) in meter per second squared. The units for Bavg, tf, and Qp in the above equations are meter, hour and cubic meter per second respectively.

3.4.6. Hydraulic model: HEC-RAS Model

HEC-RAS (Hydrologic Engineering Centers River Analysis System) is an integrated package of hydraulic analysis programs, in which the user interacts with the system through the use of a graphical user interface (GUI). The model has the key function to calculate water surface elevation at the location of interest for either a particular set of steady flow simulation or unsteady flow simulation. The results of the model can be applied to floodplain management and flood protection studies (ShahiriParsa *et al.*, 2016).

This model allows to simulate both overtopping and piping (through dam body) failure modes of dam break for embankment dam with the failure trigger being water surface elevation. The HEC-RAS requires dam break parameters, dam geometric data, reservoir elevation-volume data, unsteady flow data, and River geometric data to perform dam breach modeling (Brunner, 2014).

For this study HEC-RAS hydraulic model performed unsteady flow simulation in order to estimate breach outflow hydrograph and to map the downstream flood inundation areas. The estimation of breach outflow hydrograph was carried out in HEC-RAS and mapping of downstream flood inundation area was performed in GIS.

3.4.7. Geographic information system

GIS software was used to delineate study area, generate triangulated irregular network (TIN) from DEM of Dire watershed for creating of Legadadi river networks and developing dire dam downstream areas flood inundation map. In GIS the progress of creating Legadadi river networks were done through HEC-GeoRAS and the progress of developing flood plain map was

performed after exporting the water surface elevation, the maximum flow depth and velocity from HEC-RAS into GIS. The triangulate irregular network generated in GIS from Dire DEM was shown in figure 3-9.

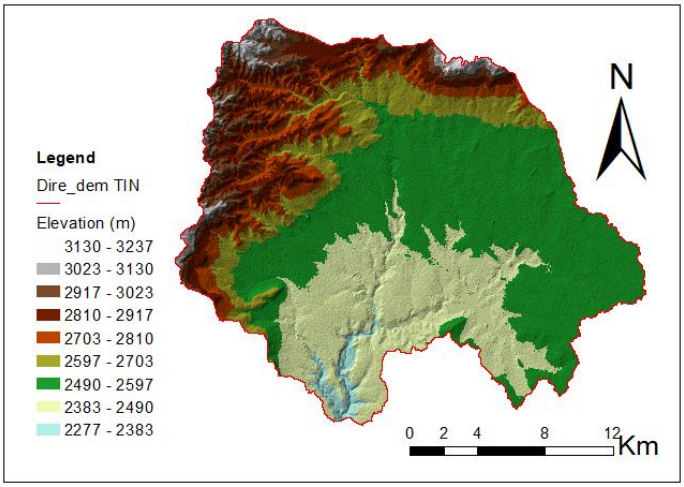

Figure 3-9: Triangulate irregular network map of the study area

3.4.8. HEC-GeoRAS model

HEC-GeoRAS (Hydrologic Engineering Centers-Geographic River Analysis System) is a set of GIS tools especially designed to process geospatial data for use with the HEC-RAS. In HEC-GeoRAS geometric data is created from GIS layers and from a DEM represented by a triangulate irregular network (TIN). The layers are referred to collectively as the RAS layers. Geometric data are established based on the intersection of the RAS layers (Cameron and Ackerman, 2012).

For this study, HEC-GeoRAS was used to create Legadadi River Network such as stream line, banks, flow paths, cross-section and inline structure with storage area from the Dire DEM represented by TIN. The Legadadi River Networks created were imported into HEC-RAS for unsteady flow simulation.

3.5. HEC-RAS Model Development

For developing dam breach analysis using HEC-RAS model, unsteady flow simulation should be performed. Unsteady flow simulation requires the major input data such as river profile, cross-section data, inline structure, storage area, manning's roughness coefficient values and unsteady flow data. The geometric data were extracted from the Dire DEM represented by TIN in GIS through HEC-GeoRAS and the flow data were taken from hydrologic study results formerly conducted in the study area.

3.5.1. Creation of the Geometric Data

The geometric data comprises combined information nearby the physical characteristics of the river channels, banks elevations, hydraulic structures, and cross sections. The geometric data creation was done in GIS via HEC- GeoRAS before being imported in to HEC-RAS. The created attributes in HEC- GeoRAS were stored in a distinct feature group represented as RAS layer. The RAS layers used were: stream centerline, banks, flow paths, cross section Cut Lines, Inline Structures and Storage.

Table 3-2: Summary of HEC-GeoRAS layers

RAS layers	Description
Stream Centerlines	Used to identify the connectivity of the river network and assign river stations to computation points
Cross-Sectional Cut Lines	Used to extract elevation transects from the DEM at specified locations and other cross-sectional properties
Bank Lines	Used in conjunction with the cut lines to identify the main channel from overbank areas
Flow Path Centerlines	Used to identify the center of mass of flow in the main channel and overbanks to compute the downstream reach lengths between cross sections
Inline Structures	Used to extract the weir profile from the DEM for inline structures (dams)
Storage Areas	Used to define the extent of detention areas and develop the elevation - volume relationship from the DEM

Source: (Cameron and Ackerman, 2012).

3.5.2. Legadadi River

The Legadadi River profile was created in GIS through HEC-GeoRAS from Dire DEM represented by TIN. This profile was created starting from the upstream end of Legadadi River at Dire dam location up to downstream end of Legadadi River about 12 km located downstream of Dire dam. After this kilometer, the river is joined with Sendafa River and flows to Akaki River. The Legadadi River profile created via HEC-GeoRAS was imported in to HEC-RAS model for model development. Stream Centerline (river), Bank Lines and Flow Path layers of Legadadi River that were digitized in GIS through HEC-GeoRAS were shown in figure 3-10.

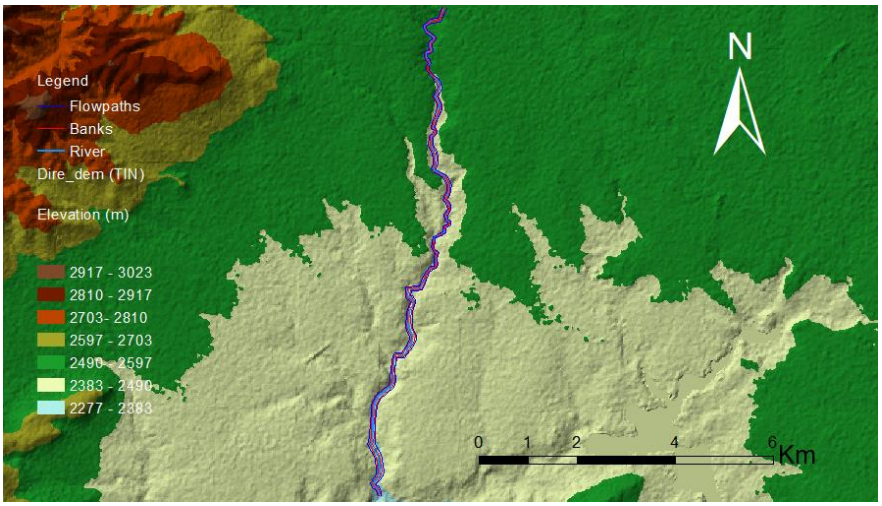

Figure 3-10: Digitized Legadadi River profile in HEC-GeoRAS

3.5.3. Legadadi River Cross Sections

Cross section is one of the important input data to HEC-RAS model for unsteady flow simulation and is digitized in GIS through HEC-GeoRAS. The digitized Cross section is imported into HEC-RAS model along with other geometric data. Cross section cut lines are used to extract elevation data from the terrain to generate a ground profile across channel flow. The cut lines intersect with RAS layers such as river centerline and flow path lines to calculate bank station (locations that separate the main channel from both left over bank and right over bank), and downstream reach length (distance between cross sections). The cross sections are valuable for the computations of water surface elevations. While digitizing the cross sections the spacing between cross-sections should be at appropriate interval and lesser spacing at inline structure boundary cross-sections for accurate computation. The recommended value of cross section spacing is up to 200m (Ekaningtyas, 2017).

Therefore, for this study cross sections were digitized along the downstream of Legadadi River from the Dire dam up to the downstream boundary about 12km from the dam and were digitized from Dire DEM represented by TIN. The total cross sections digitized perpendicular to the stream center line along the longitudinal profile of Legadadi River was 121 in numbers. Out of 121 total numbers of cross-sections, 119 cross-sections were at downstream of the Dire dam and 2 cross-sections were in the Dire reservoir.

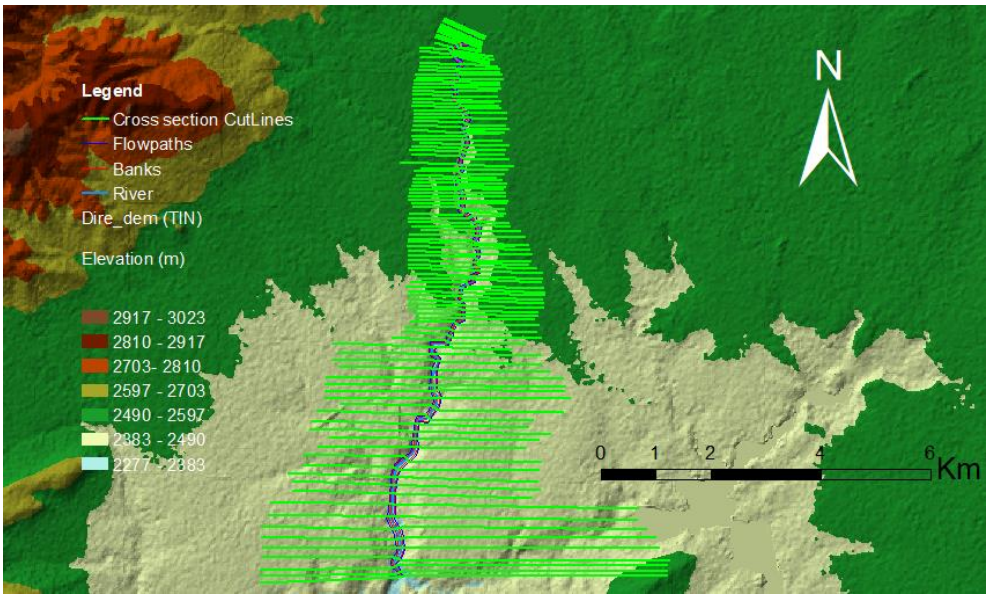

Figure 3-11**:** Digitized Legadadi River cross sections in HEC-GeoRAS

3.5.4. Dire Dam and Reservoir

The Dire dam was modeled as an inline structure in HEC-RAS. The dam profile was created in GIS through HEC-GeoRAS from Dire DEM represented by TIN. The Dire reservoir was created as storage areas via HEC-GeoRAS with Legadadi River Network from Dire DEM represented by TIN and was routed as storage area in HEC-RAS model using level pool routing. The Dire Dam and Reservoir created in HEC-GeoRAS with Legadadi River Network shown in figure 3-12. The created Dire dam and reservoir data with Legadadi River Networks were later imported in to HEC-RAS model for model development. Elevation- volume data of dire reservoir was shown in table 3-3.

Table 3-3: Dire reservoir Elevation- volume data

Elevation (m) a.m.s.l	Volume (10^6 m^3)
2518.00	0.000
2529.50	0.003
2532.50	0.326
2534.00	0.650
2536.50	1.354
2538.50	2.088
2540.50	2.970
2543.00	4.260
2545.50	5.911
2547.00	7.085
2548.500	8.404
2550.50	10.420
2552.50	12.840
2554.50	15.651
2555.50	17.160
2557.00	19.550
2558.25	23.550

Source: (Addis Ababa Water and Sewerage Authority, 2016).

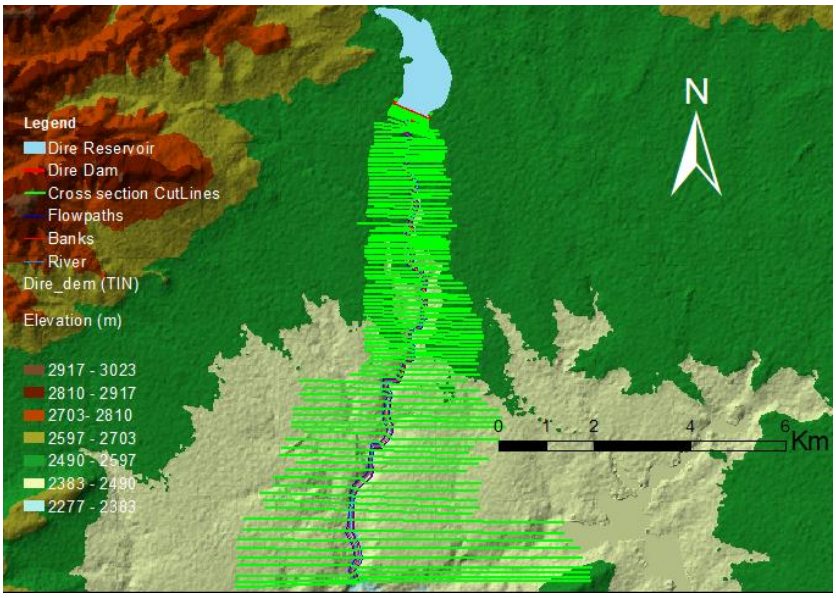

Figure 3-12: Dire Dam and Reservoir created in HEC-GeoRAS with Legadadi River Networks

For dam breach analysis, the geometric data created in HEC-GeoRAS were imported in to HEC-RAS model. The analysis was carried out through performing unsteady flow simulation. Figure 3-13 revealed geometric data imported in to HEC-RAS model.

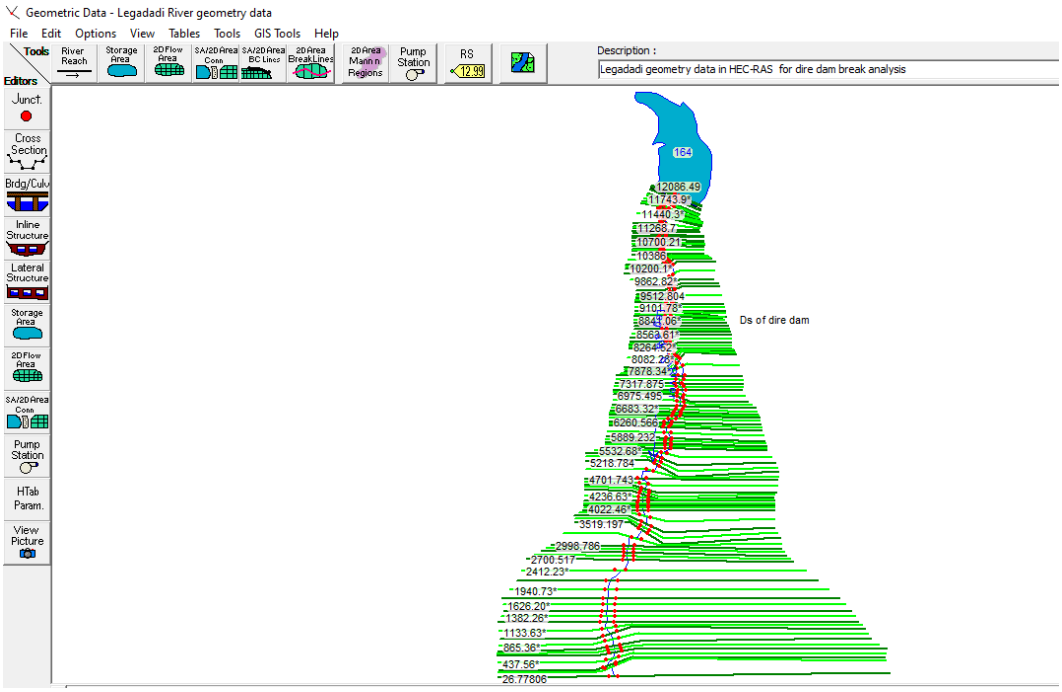

Figure 3-13: Geometry data in HEC-RAS window

3.5.5. Manning Roughness Coefficient

The manning roughness coefficient is necessary to enter into HEC-RAS model for each River channel and river bank cross section. Roughness coefficients characterize the resistance to flow and flood plains. Manning's n coefficient is used in the manning equation to calculate discharge in the open channel. Selection of the suitable Manning's n value is very imperative for an accurate computation of water surface profiles. The value of Manning's n is highly flexible and depends upon a number of elements including; channel irregularities, channel surface roughness, size and shape of channel, scour and deposition, vegetation, obstructions, suspended materials and bed load materials.

(Brunner, 2016) have presented the range of manning's roughness coefficients value for natural streams which has stone river bed channels covers with grass banks. The manning's roughness coefficient range for river bed channel is 0.035-0.05 and for banks is 0.03-0.05. Since Legadadi River under the case study was characterized by stone river bed channel and grass banks, the manning's roughness coefficients value were adopted in the ranges of 0.035-0.05 and 0.03-0.05 for both river channel and banks respectively.

3.5.6. Unsteady Flow Analysis

Dam break is most applicably modeled in HEC-RAS through unsteady flow simulation. For this case study, HEC-RAS model was used to simulate unsteady flow due to overtopping and piping (through dam body) dam failure mode. The dam breach parameters, Dire dam geometric data, Legadadi River geometric data, Dire reservoir elevation-volume data, and unsteady flow data were used in HEC-RAS model to perform unsteady flow simulation. Unsteady flow data required in HEC-RAS was boundary conditions.

3.5.7. Boundary Conditions

Boundary conditions are essential to describe the upstream and downstream ends of the river system. These Boundary conditions were upstream boundary condition and downstream boundary condition.

3.5.8. Upstream Boundary Condition

The upstream area of the dam reservoir can either be modeled with cross-sections or by means of storage area. HEC-RAS model performs full unsteady flow routing through the reservoir pool and downstream of the dam when cross-sections are used. HEC-RAS model uses level pool routing for unsteady flow routing via the reservoir and downstream of the dam when storage area is used. The upstream boundary condition for this study was the PMF inflow flood hydrograph. The 24 hour PMF inflow flood hydrograph of Legadadi River conducted during feasibility study of Dire Dam design project in the year of 1994 was taken as in the table 3-4 below.

Table 3-4: PMF inflow flood hydrograph of Legadadi River

Time (hrs)	Inflow (m^3/s)	Time (hrs)	Inflow (m^3/s)
0	45	13	180
1	98	14	130
2	160	15	100
3	300	16	77
4	500	17	65
5	570	18	50
6	560	19	39.5
7	520	20	30
8	480	21	21
9	405	22	13
10	355	23	8
11	305	24	5
12	235		

Source: (Addis Ababa Water and Sewerage Authority, 2016).

3.5.9. Downstream Boundary Condition

For unsteady flow analysis, the downstream boundary condition is normal depth. Normal depth is most commonly used as downstream boundary condition for open ended river reach. In this study, normal depth was used as downstream boundary condition. While using normal depth, it was required to enter a friction slope for the reach in the locality of the boundary condition. The water surface slope is often a good estimate of the friction slope. Therefore frictional slope 0.01655 was used as normal depth for downstream boundary condition and found from the profile graph for frictional slope computation of the Legadadi River profile shown in figure 3-14 below.

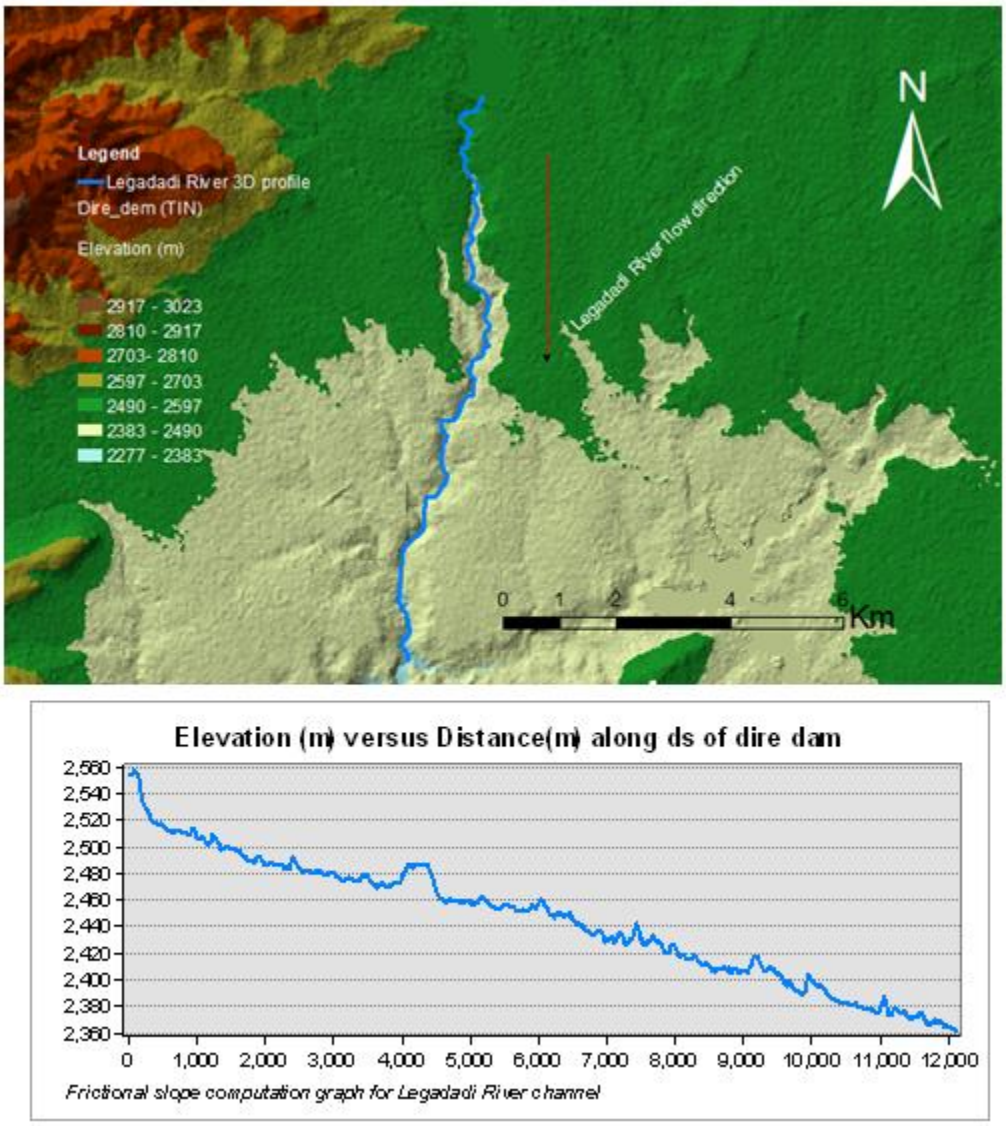

Figure 3-14: Legadadi River profile and frictional slope computation profile graph

3.6. Dam Break Simulation in HEC-RAS Model

For dam break Simulation in HEC-RAS model, the model uses the parameters include failure location, failure mode, shape, formation time, trigger condition, Weir coefficients, and pipe flow coefficients.

3.6.1. Failure Location

The dam break failure location is centerline stationing of the break in the dam. As high hydrostatic pressure is present at the center of bottom break width of the dam, for the dam under this case study the failure location was assumed to be at the center of bottom break width of the dam and develop equally in both break sides.

3.6.2. Failure Mode

The failure mode can be defined as the mechanism for beginning and developing the breach. The HEC-RAS model break hydraulic computations comprise both overtopping and piping failure modes. Therefore the selected failure modes for the dire dam under the case study were assumed as overtopping and piping failure mode.

3.6.3. Break Formation Time

The break formation time is described as the duration from which the break commences to have some substantial erosion, and to the full growth of the break. The HEC-RAS break start time for overtopping failure is considered to be while the erosion process has migrated to the upstream dam face. At this point, the outflow from the dam will begin to increase due to the dam breach. The end of the break formation time is when the break is fully developed and significant erosion has ceased. The break formation ending time should not involve the time to entirely drain the reservoir pool. The HEC-RAS break start time for piping failure is considered to be while a substantial amount of flow and materials are coming out of the pipe formed. The HEC-RAS break ending time is considered when the break is fully developed for most party. The estimation of the break formation time for both overtopping and piping failure mode for this study was calculated outside of the HEC-RAS model through Froehlich 2008 empirical method.

3.6.4. Trigger Mechanism

Trigger mechanism is demarcated as reservoir pool elevation; reservoir pool elevation plus duration of dam failure. For the dam under this study, reservoir pool elevation was used as trigger mechanism and inserted as input in to HEC-RAS model.

3.6.5. Break Shape Definition

Break shape description in HEC-RAS model involves the bottom break width, height of the break, and break side slopes. These values characterize the maximum break size. The break width is termed as the average break width (Bavg). HEC-RAS uses the break bottom width as an input data. The break bottom width is computed by using side slopes recommended by regression approaches. The break height (hb) is the vertical extent from the top of the dam to the invert elevation of the break and the height of the water (hw) that is the vertical extent from the maximum water surface above the dam crest to the invert elevation of the break. The breach shape during dam break can be triangular, rectangular, or trapezoidal. The shape of the break was trapezoidal in several case studies. Dam break simulation in HEC-RAS model was done by widening a trapezoidal-shaped break with time in accordance with the particular progression and geometry. Hence, trapezoidal shape was selected for this case study as presented in figure 3-15.

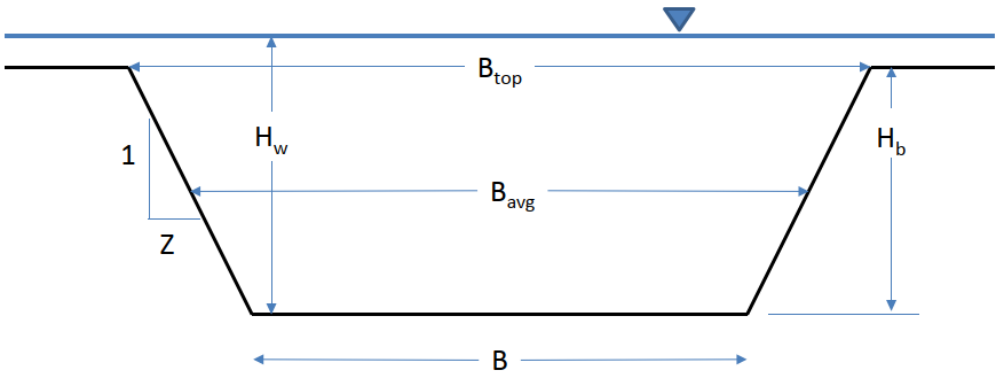

Figure 3-15: Break shape and break parameters, Source: (Wahl, 2014).

3.6.6. Break Weir Coefficient

Water going over the dam crest during an overtopping failure process of an earthen dam is modeled as weir type of flow. Break Weir Coefficient directly affect the magnitude of peak outflow hydrograph for any given break. An earthen dam with medium to very large storage volumes upstream have a weir coefficient (C) typical of a broad crested weir with a long crest length (i.e. C= 2.6). However dams with relatively low volume of water have a weir coefficient

(C) typical of a sharp-crested weir (i.e. C= 3.2). Dams that have a clay core and totally constructed of clay material much more pronounced head cut process and have higher weir coefficient (i.e. C=3.2), whereas Dams that are constructed of gravel or sand less pronounced head cut process and have less weir coefficient (i.e. C= 2.6).

Table 3-5: Dam breach weir coefficients

Dam types	Over flow or weir coefficients
Earthen clay or clay core	2.6 – 3.3
Earthen sand and gravel	2.6 – 3.0
Concrete Arch	3.1 – 3.3
Concrete Gravity	2.6 – 3.0

Source: (Brunner, 2014).

Since Dire embankment dam was constructed of earthen clay core material, the selected value of weir coefficient was assumed as 2.65 for overtopping mode of failure.

3.6.7. Break Piping Flow Coefficient

The movement of water through the dam during piping (through dam body) failure process is modeled as pressurized orifice flow type. This coefficient depicts the measure of how efficiently the flow can get in to the pipe orifice. Piping flow coefficients recommended values are in the range of 0.5 to 0.6.

Table 3-6: Dam breach piping flow coefficients

Dam types	Piping or pressure flow coefficients
Earthen clay or clay core	0.5 – 0.6
Earthen sand and gravel	0.5 – 0.6
Concrete Arch	0.5 – 0.6
Concrete Gravity	0.5 – 0.6

Source: (Brunner, 2014).

Since Dire embankment dam was constructed of clay core material, the selected value of piping flow coefficient was assumed as 0.55 for piping mode of failure.

3.7. Overtopping Mode of Dam Break Simulation in HEC-RAS Model

HEC-RAS model for dam break simulation allows simulating overtopping failure mode of embankment dam in addition to piping (through dam body) failure using the required input data. Overtopping take place when the surface elevation of water in the reservoir exceeds the dam crest elevation thereby water can then flow over the top crest of the dam, inadequacy of spillway capacity to free by pass over resulting flood event, inadequacy of reservoir storage capacity to

handle resulting flood event, inadequacy of freeboard and also when a reservoir's outlet structure is not functioning suitably, in so doing raising the surface elevation of water in the dam reservoir.

Overtopping failure for embankment dams starts when water behind the dam flow over its crest begins flowing over the downstream dam face and begins to erode the face of the dam. The continuous eroding of dam face results expands in generally to trapezoidal shape of the dam breach and the water flow via the expanding breach act as a weir flow. The most common failure mode for embankment dams is overtopping due to flooding.

In this study for overtopping failure, the most critical agent was while the reservoir was at full reservoir situation and when surplus flood passes over the dam crest. The capacity of the Dire dam spillway was 500m^3/s which less than the peak floods passing over the dam. Since the Dire dam spillway was uncontrolled spillway type, the peak floods greater than spillway capacity passes over the dam. So having this evidence the hypothetical failure of Dire dam due to overtopping was analyzed in HEC-RAS model using required input data of Dire dam break parameters, final breach bottom elevation and maximum water surface elevation in the reservoir. The initial water surface elevation for the dam break was 2558.25m a.m.s.l and finally it extends up to final breach bottom elevation which was 2518m a.m.s.l. Figure 3-16 showed Dire dam breach model in HEC-RAS.

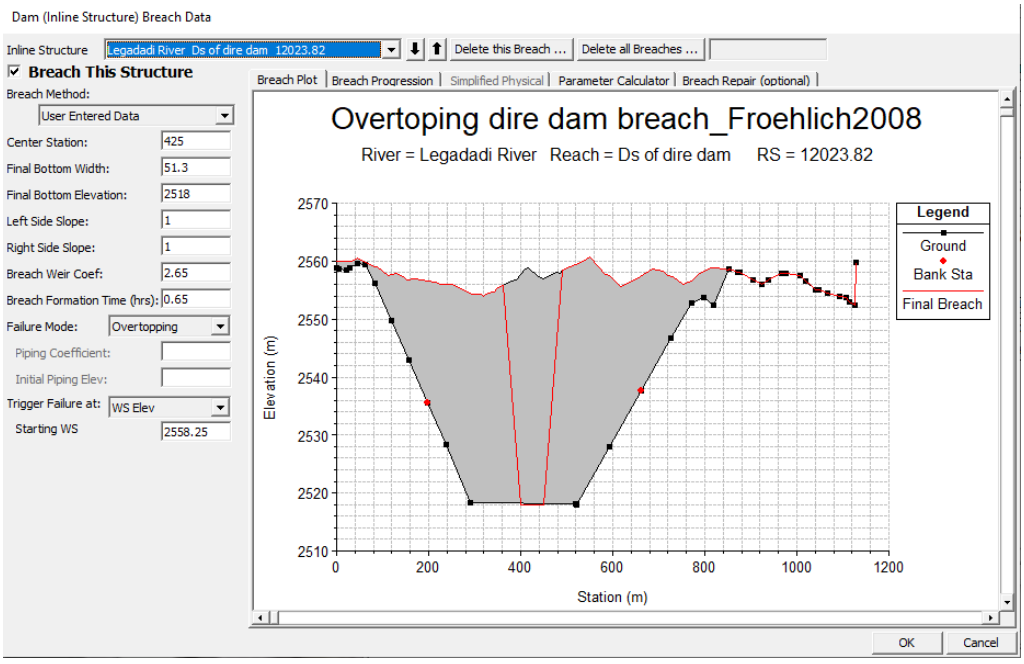

Figure 3-16: Dire dam breach model in HEC-RAS due to overtopping

3.8. Piping Mode of Dam Break Simulation in HEC-RAS Model

HEC-RAS model for dam break simulation allows simulating piping (through dam body) failure mode of embankment dam in addition to overtopping failure using the required input data. Piping mode of failure is also the major causes of embankment dam failures which cause erosion and saturation in the dam body and causes it to lose strength. Dam piping failure occurs when water stored in the upstream of the dam reservoir gradually seep in to the dam body and forms large hole which ensures so as to massive materials is transported out of the dam and starts to erode the downstream face of the dam.

The movement of water via the dam body is modeled in terms of a pressurized orifice type flow. The continuous eroding of downstream dam face consequences expands in generally to trapezoidal shape of the dam breach. The Piping failure can start at any elevation of water in the reservoir and grow to the maximum extents. The most critical condition for piping failure is at normal reservoir condition. Then for this study, the most critical condition for piping failure was at normal water level in the reservoir which was 2557m a.m.s.l and lastly it extends up to final breach bottom elevation which was 2518m a.m.s.l. The initial piping elevation for piping mode of failure was assumed to be at 2554m a.m.s.l. The Dire dam breach was modeled in HEC-RAS through the required input data as shown in figure 3-17.

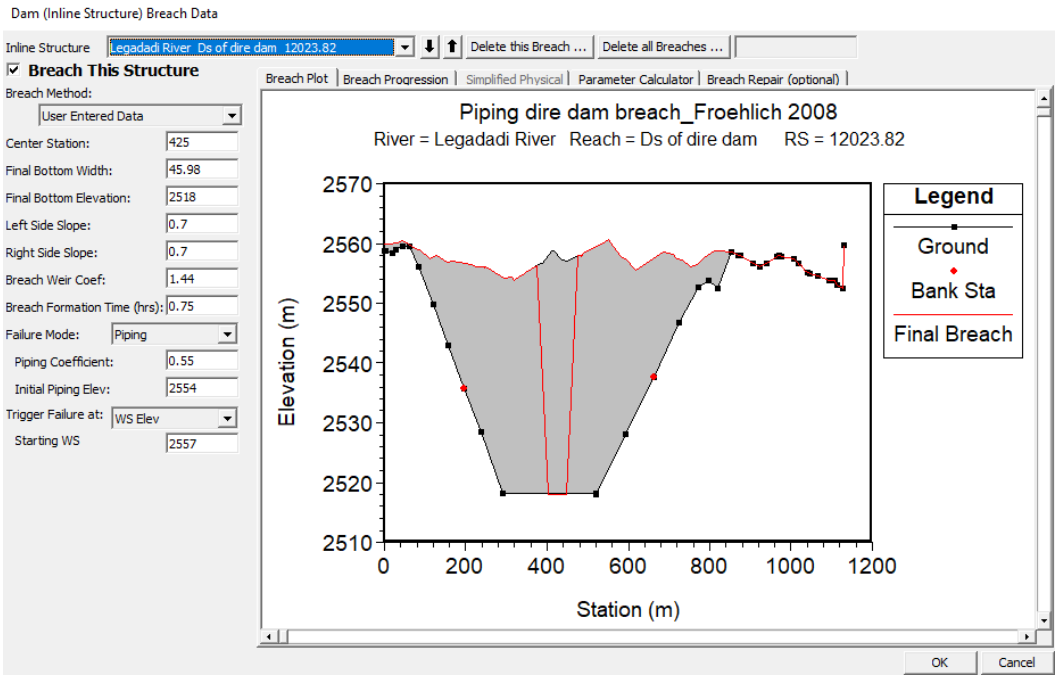

Figure 3-17: Dire dam breach model in HEC-RAS due to piping

3.9. Envelope Curves

Envelope curves represent the peak breach outflow computed from the past historic dam failure data using empirical peak breach outflow equations. The peak breach outflow equations were derived from historic dam failure data for zoned earthen dam, earthen dam with impervious core of clay, concrete, and rock fill dam. After breach outflow hydrograph is calculated in HEC-RAS model, the calculated peak flow from this model is compared with an envelope curves established by different peak flow regression equations as a test for checking the reality of simulated value by the model. For best fit value, the peak breach outflow discharge simulated by the HEC-RAS model is comparable with the peak breach outflow discharge computed by empirical peak breach outflow equations or should be below envelope curve (Brunner, 2014). The hydraulic depth available for comparison over the envelope curve is observed from the HEC-RAS model at dam site when dam breach occurs and finally converted from meter (m) to feet (ft). Envelope curves of different peak flow regression equation that used for comparison with the calculated peak flow in the HEC-RAS model was shown in figure 3-18.

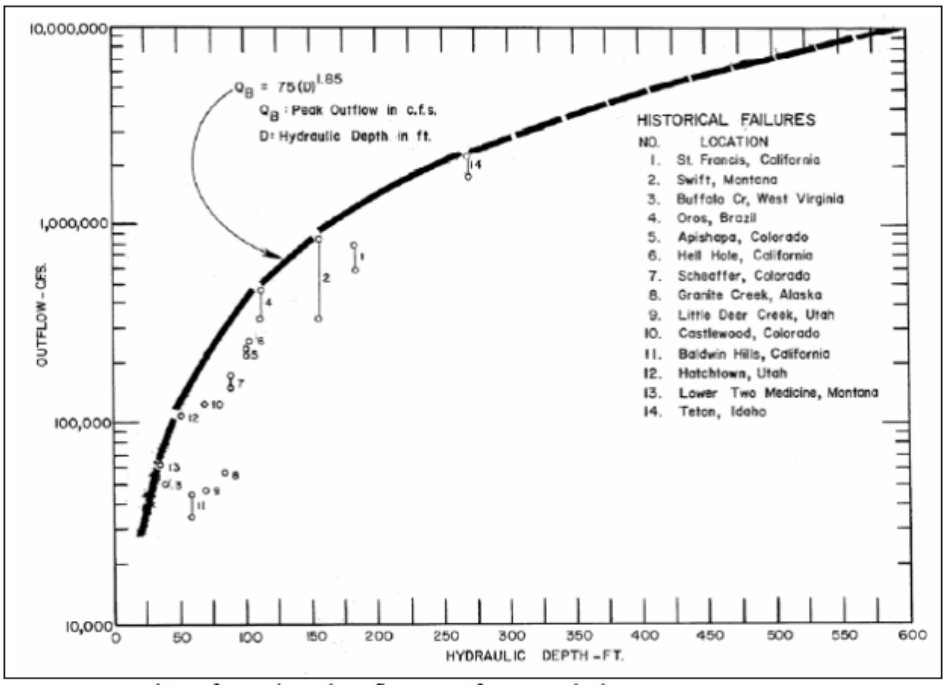

Figure 3-18: Envelope curve of experienced outflow rates from breached Dams, Source: (Brunner, 2014).

3.10. Flood Inundation Mapping

Dam break flood inundation map shows area with the intention of floods as a result of a dam break. The maps are used by thick scope of end users for planning and as a reaction instrument to decide the effect of dam break in downstream areas. In addition, the incremental areas flooded as a consequence of dam break were considered for a dam classification exercise (Balaji and Kumar, 2018). The flood map embodies, areas where there is a risk of flooding and helps for warning the population and preparatory work of flood hazard map distribution among them proves to be effective to mitigating flood damage and reduce the numbers of casualties (Boussekine and Djemili, 2016).

For this study, the area located downstream of the dam that would be inundated were small house collecting and housing wires from piezometers, Legadadi town with different infrastructures. Then in order to reduce flood risk to dire dam downstream areas for the time where the dam fails, knowing the extent and depth of flood is very essential. Inundation map of dire dam downstream flood areas was developed in GIS after water surface elevation, maximum flood depth and velocity were imported in to GIS from HEC-RAS model.

4. RESULTS AND DISCUSSIONS

This study passed through important procedures to achieve the overall objective and specific objectives. Depending on the appropriate methodology including the selected model and all the significant procedures undertaken, the Dire dam breach analysis was performed. The following sections describe the results found and its discussions through the objectives of the study.

4.1. Dam Break Parameters

In order to achieve the point of dam break analysis first estimating the parameters of dam break are the core. The break parameters estimated were break dimensions, break formation time, and breach outflow peak discharge for both overtopping and piping mode of failure. The parameters of breach bottom width, breach formation time, and breach side slope were used as an input data in HEC-RAS model for the Dire dam breach simulation. These parameters were estimated out of the model through empirical methods using the required Dire dam and reservoir data.

4.1.1. Dam Break Parameters Estimation for Overtopping Failure Mode

The dam breach parameters for dire dam were estimated through empirical methods of MacDonald & Langridge-Monopolis 1984, Von Thun and Gillette 1990, Froehlich 1995, and Froehlich 2008. The estimated breach parameters values of breach bottom width (B), breach formation time (tf), and breach side slopes (bss) for overtopping failure mode through regression approaches were shown in table 4-1.

Table 4-1: Break parameters for dire dam due to overtopping failure mode by different methods

		Dire Dam breach parameters		
S/N	Regression Approaches	B (m)	tf (hr)	bss
1	MacDonald & Langridge-Monopolis 1984	12	1.39	0.5
2	Von Thun and Gillette 1990	127.3	0.64	0.5
3	Froehlich 1995	58.83	0.71	1.4
4	Froehlich 2008	51.3	0.65	1

The values of breach parameters are important for simulating peak breach outflow discharge in HEC-RAS model. (Brunner, 2014) have presented the break parameters like break size, and break formation time will directly affect the prediction of the peak breach outflow discharge coming out of the dam. Since computing of the peak breach outflow discharge was based on these parameters, the magnitude of the parameter determines the discharge.

As reviewed from different publications, Froehlich 2008 empirical method was the more appreciable method for estimating dam breach parameters. (Sammen *et al.*, 2017) presented the Froehlich 2008 empirical method had high accuracy and high performance in estimating dam breach parameters while comparing to other methods. Therefore, the method was selected for this study. The breach parameters (breach bottom width, breach formation time, and breach side slopes) estimated through this method was used as an input data for unsteady flow simulation due to Overtopping and piping failure mode in HEC-RAS model.

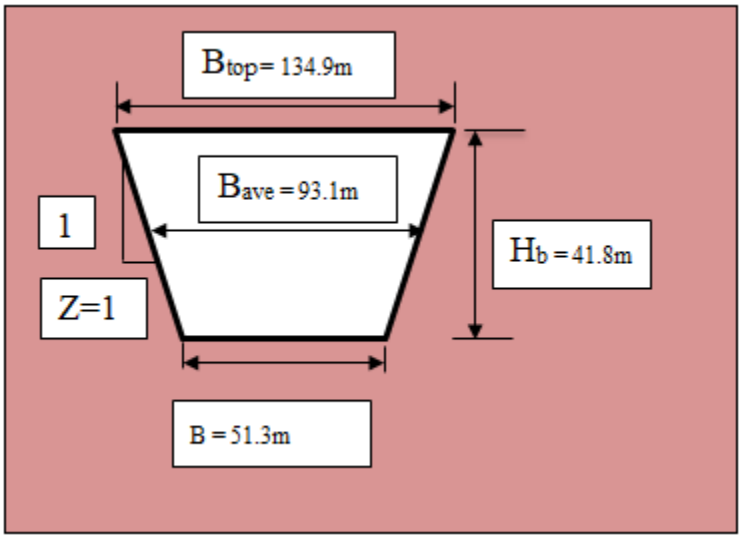

Figure 4-1: Breach trapezoidal shape and breach parameters for Dire Dam by overtopping failure

Table 4-2: Summary of Break parameters for dire dam due to overtopping failure mode

S/N	Dam breach parameters	Froehlich 2008 Empirical method
1	Breach bottom width (m)	51.3
2	Breach side slopes	1
3	Breach formation time (hr)	0.65

4.1.2. Dam Break Parameters Estimation for Piping Failure Mode

The dam breach parameters for dire dam due to piping failure mode were also estimated through empirical methods including MacDonald & Langridge-Monopolis 1984, Von Thun and Gillette 1990, Froehlich 1995, and Froehlich 2008. The breach parameters values of breach bottom width (B), breach formation time (tf), and breach side slopes (bss) for piping failure mode through regression approaches were shown in in table 4-3.

Table 4-3: Break parameters for dire dam due to piping failure mode by different methods

		Dire Dam breach parameters		
S/N	Regression Approaches	B (m)	tf (hr)	bss
1	MacDonald & Langridge-Monopolis 1984	9	1.34	0.5
2	Von Thun and Gillette 1990	114.7	0.65	0.5
3	Froehlich 1995	48.96	0.81	0.9
4	Froehlich 2008	45.98	0.75	0.7

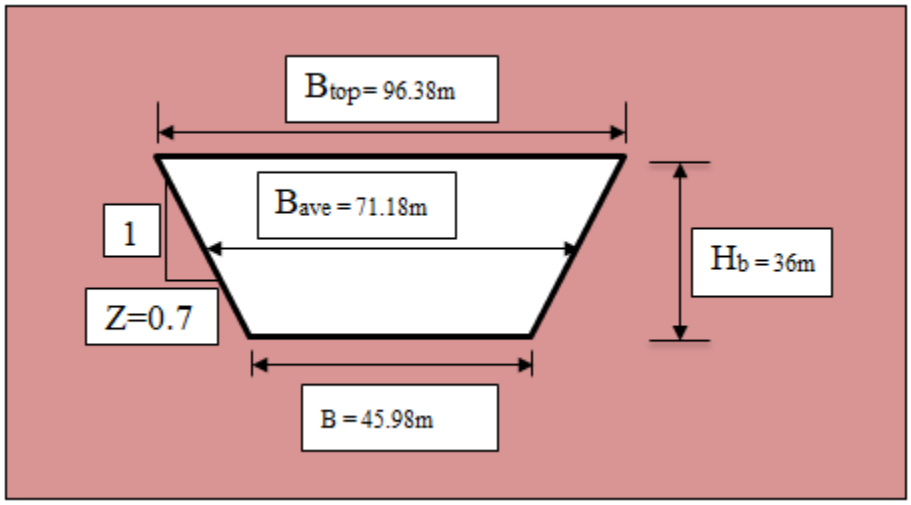

Figure 4-2: Breach trapezoidal shape and breach parameters for Dire Dam by piping failure

Table 4-4: Summary of Break parameters for dire dam due to piping failure mode

S/N	Dam breach parameters	Froehlich 2008 Empirical method
1	Breach bottom width (m)	45.98
2	Breach side slope	0.7
3	Breach formation time (hr)	0.75

According to (Ekaningtyas, 2017) the magnitude of breach bottom width and breach formation time determines dam breach conditions. Therefore, this breach parameters value indicated that, the dam would breach at large size by overtopping than that of piping based on the value of breach bottom width and also the dam would breach former due to overtopping than that of piping depending on the breach failure time.

4.2. Unsteady Flow Analysis

For dam breach analysis, the essential task to be done is unsteady flow simulation in which flood from the dam to the downstream boundary is routed. Unsteady flow analysis is important for estimating dam breach outflow discharge and routing this discharge to the downstream of dam. HEC-RAS can perform unsteady flow analysis using required data as an input data. Unsteady flow analysis can be initiated after inserting boundary conditions for the farthest upstream and

downstream cross sections in to HEC-RAS model. For this study, unsteady flow analysis was done using the required unsteady flow data including PMF inflow flood hydrograph of Legadadi River at the upstream river end cross section (RS 12086.49) and normal depth of the farthest downstream vicinity (RS 26.77806) as the boundary conditions. The dam breach parameters, dam geometric data, Legadadi River geometric data, and reservoir elevation-volume data were also inserted in the model for completing unsteady flow analysis. Unsteady flow analysis for both overtopping and piping failure mode were performed in HEC-RAS model.

4.2.1. Unsteady Flow Analysis of Overtopping Failure Mode

The simulation of unsteady flow of dam overtopping failure for this study was done in HEC-RAS model. The simulation results of unsteady flow of dam overtopping failure for MacDonald & Langridge-Monopolis 1984, Von Thun and Gillette 1990, Froehlich 1995, and Froehlich 2008 were done in HEC-RAS model. The maximum breach outflow discharges for these methods at the dam site (RS 12086.49) were attached on appendix A. The maximum breach outflow discharge due to overtopping was occurred for the computation method of Froehlich 2008 while comparing to the others method. Therefore the breach outflow discharge simulated through Froehlich 2008 in HEC-RAS was accepted for routing the simulated breach outflow discharges via downstream of Dire dam and also used for developing the flood inundation map. The routing of breach outflow discharges by overtopping for dire dam was done starting from the upstream end RS of 12086.49 (dam site) to the downstream end RS of 26.77806. Figure 4-3 showed the simulated unsteady flow result for Froehlich 2008 by overtopping in HEC-RAS window.

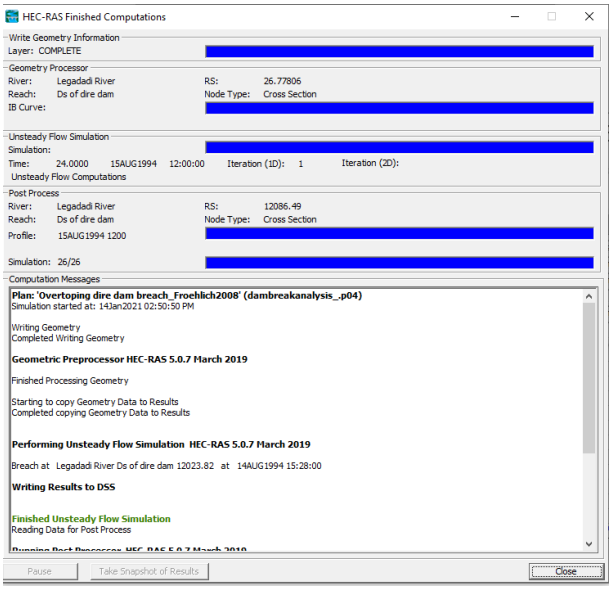

Figure 4-3: Unsteady flow simulation result for overtopping failure mode in HEC-RAS model

The peak breach outflow discharge simulated in HEC-RAS model for Dire dam due to overtopping through regression methods of MacDonald & Langridge-Monopolis 1984, Von Thun and Gillette 1990, Froehlich 1995, and Froehlich 2008 at the upstream end river station of 12086.49 (dam site) were presented in table 4-5.

Table 4-5: Peak breach outflow discharges by overtopping at upstream end RS (12086.49)

S/N	Regression Approaches	Peak discharge (m^3/s) at RS= 12086.49
1	MacDonald & Langridge-Monopolis 1984	5842.5
2	Von Thun and Gillette 1990	8658.3
3	Froehlich 1995	9182.7
4	Froehlich 2008	9285.3

According to the study conducted on Attabad Lake dam break analysis due to overtopping scenario (Muhammad and Rasheed, 2016) the results of the hydraulic models for simulating breach outflow discharge are comparable with available results computed by emperical method to ensure the accuracy of the model. Therefore, the results found for Dire dam breach study was also acceptable since the peak breach outflow discharges simulated in HEC-RAS model were comparable with that of peak breach outflow discharges computed by the empirical methods. This ensures reliability of the model accuracy in the simulation of the discharges. The peak breach outflow discharge simulated by Froehlich 2008 method was greater than the peak breach outflow discharge simulated by the other three methods. Figure 4-4 exhibited the Flood hydrograph routed at upstream end River station of 12086.49 (dam site) by overtopping for different regression approaches.

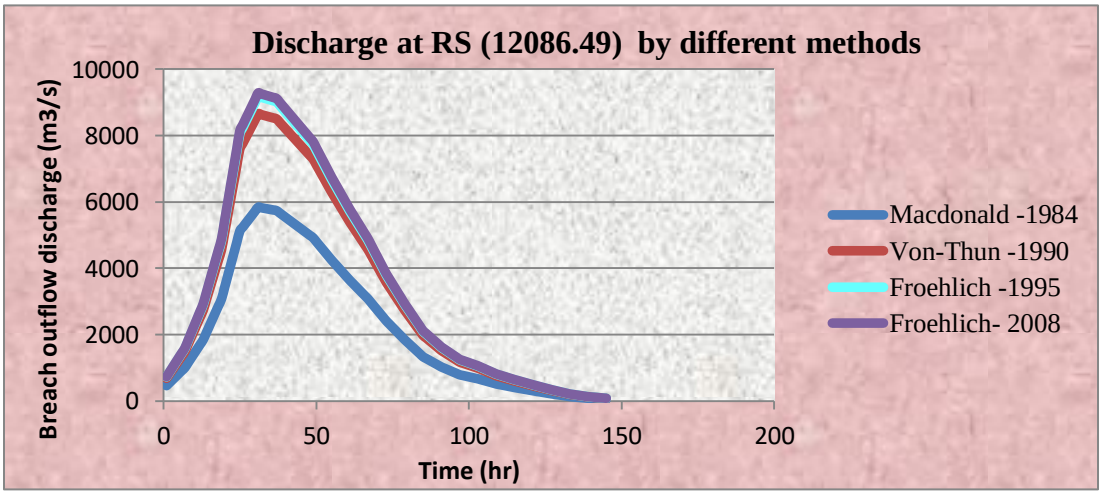

Figure 4-4: Flood hydrograph routed at upstream end River station of 12086.49 by overtopping for different regression approaches

(Hossain, 2015) have presented flood routing as techniques to determine the outflow hydrograph at a point downstream in a river (or reservoir) as a function of the inflow hydrograph at a point upstream. As flood waves move downstream they are attenuated and delayed. That is, the peak flow of the hydrograph decreases and the time base of the hydrograph escalations. Then for this study, routing of flood hydrographs from the upstream end RS of 12086.49 (dam site) to the downstream end RS of 26.77806 were analyzed. The routed flood discharges at different river stations of RS (12086.49), RS (8924.878), RS (4701.743), and RS (26.77806) were attached on appendix B. The peak breach outflow discharge simulated in HEC-RAS model due to overtopping at the upstream end RS of 12086.49 and at the downstream of Dire dam of RS (8924.878), RS (4701.743), and RS (26.77806) were presented in table 4-6. The results found showed that, the peak breach outflow discharge at RS (12086.49) was greater than that of the peak discharges at the different river stations and peak discharge attenuation was taken place along the downstream of the dam.

Table 4-6: Peak breach outflow discharges by overtopping at different River stations

S/N	River stations	Peak discharge (m^3/s) at different River stations
1	12086.49	9285.3
2	8924.878	9248.65
3	4701.743	9181.45
4	26.77806	9165.80

The routing of breach outflow discharges at different river stations of RS (12086.49), RS (8924.878), RS (4701.743), and RS (26.77806) were shown in figure 4-5.

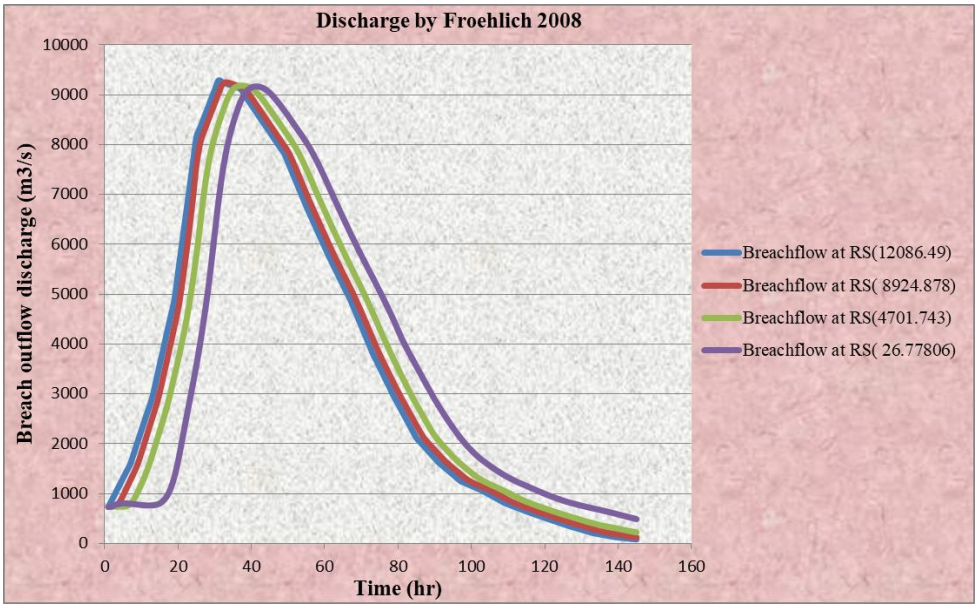

Figure 4-5: Flood hydrographs routed at different River stations by overtopping

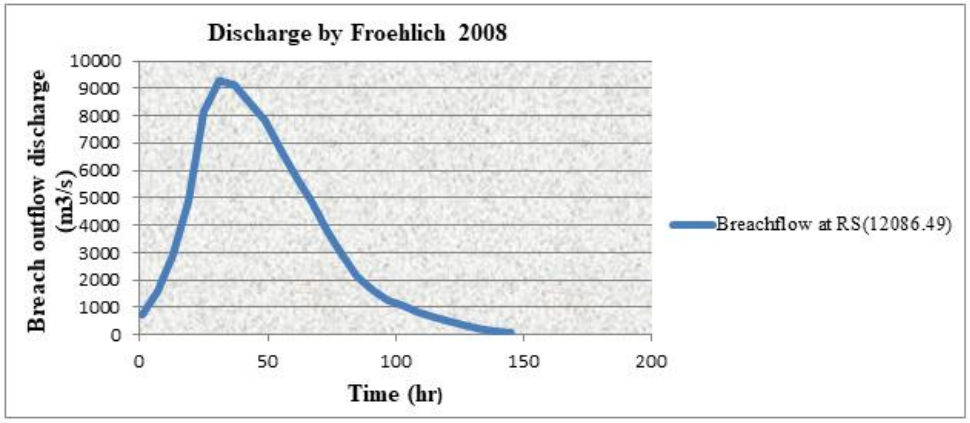

Figure 4-6: Flood hydrograph routed at RS (12086.49) by overtopping

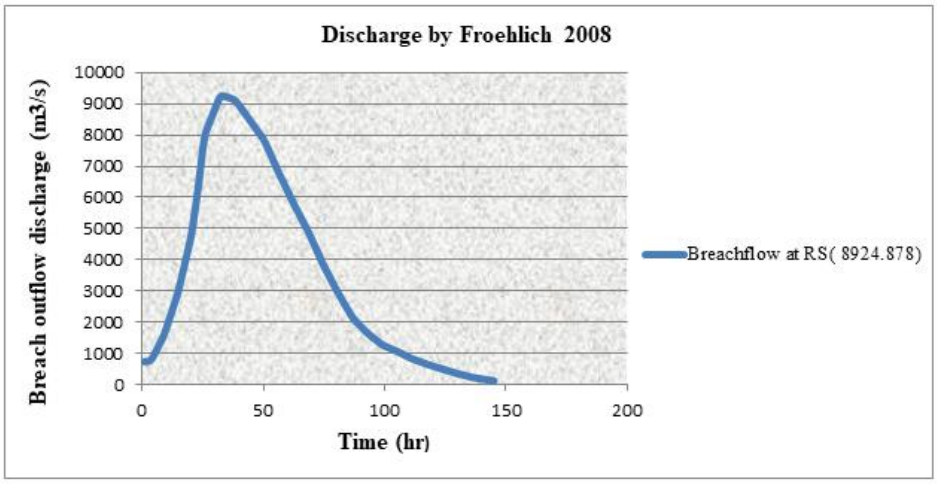

Figure 4-7: Flood hydrograph routed at RS (8924.878) by overtopping

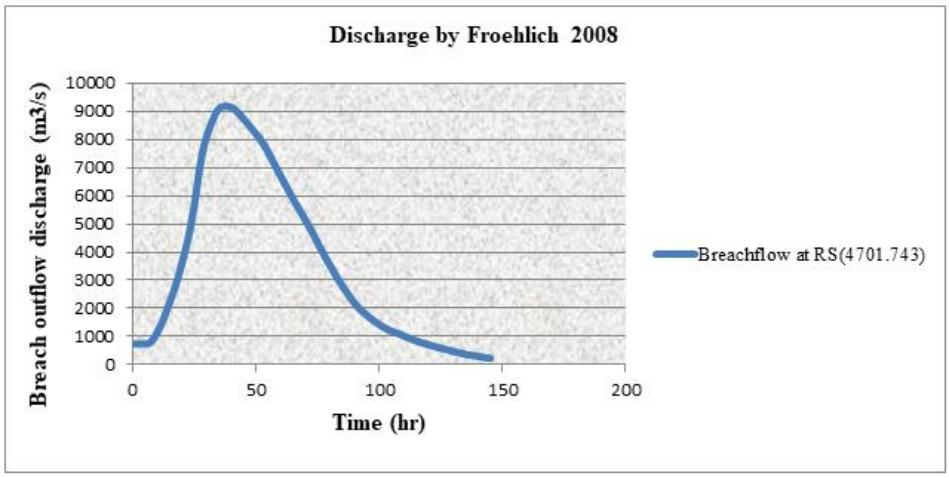

Figure 4-8: Flood hydrograph routed at RS (4701.743) by overtopping

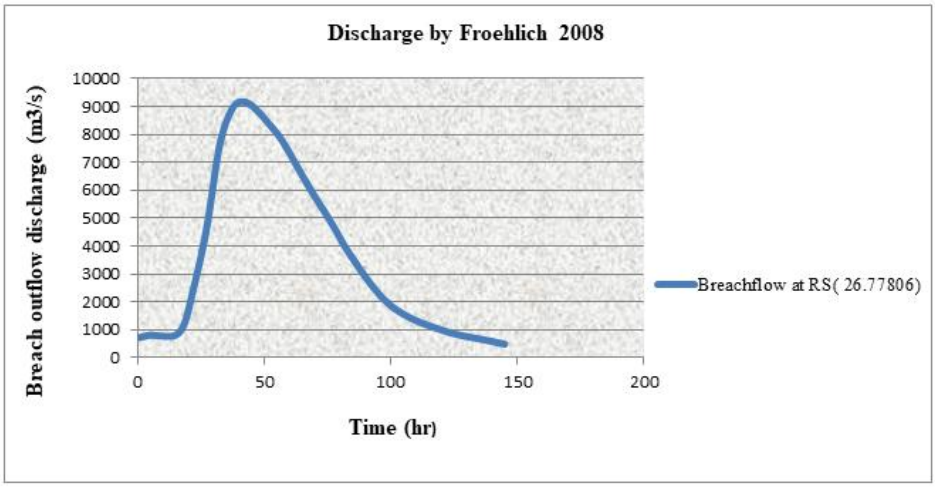

Figure 4-9: Flood hydrograph routed at RS (26.77806) by overtopping

4.2.2. Unsteady Flow Analysis of Piping Failure Mode

Unsteady flow simulation of dam body piping failure was performed in HEC-RAS model. The simulation results of unsteady flow of dam body piping failure for MacDonald & Langridge-Monopolis 1984, Von Thun and Gillette 1990, Froehlich 1995, and Froehlich 2008 was done in HEC-RAS. The maximum breach outflow discharges for these methods at the dam site (RS 12086.49) were attached on appendix C. The maximum breach outflow discharge due to piping was occurred for the computation method of Froehlich 2008 while comparing to the others method. As a result, breach outflow discharge simulated through Froehlich 2008 in HEC-RAS was selected for routing of the simulated breach outflow discharge via downstream of dire dam and also used for developing the flood inundation map. The routing of breach outflow discharge due to piping for the dam under the case study was performed starting from the upstream end RS of 12086.49 to the downstream end RS of 26.77806. Figure 4-10 showed the simulated unsteady flow result for Froehlich 2008 due to piping in HEC-RAS window.

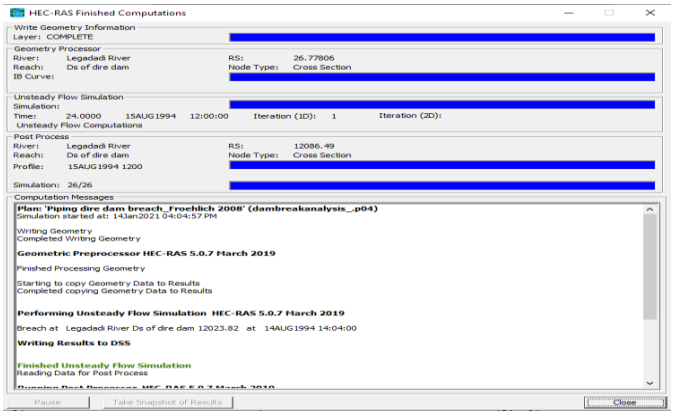

Figure 4-10: Unsteady flow simulation result for piping failure mode in HEC-RAS model

The peak breach outflow discharges simulated in HEC-RAS due to piping for MacDonald & Langridge-Monopolis 1984, Von Thun and Gillette 1990, Froehlich 1995, and Froehlich 2008 at the upstream end RS of 12086.49 were presented in table 4-7. The results revealed that, the peak breach outflow discharges simulated in HEC-RAS were quite comparable with that of peak breach outflow discharges computed by the empirical methods and this ensures reliability of the model accuracy in simulation of the breach outflow discharges.

Table 4-7: Peak breach outflow discharges by piping at upstream end RS (12086.49)

S/N	Regression Approaches	Peak discharge (m^3/s) at RS (12086.49)
1	MacDonald & Langridge-Monopolis 1984	5472
2	Von Thun and Gillette 1990	7090.8
3	Froehlich 1995	7626.6
4	Froehlich 2008	7712.1

Figure 4-11 presented the Flood hydrograph routed at upstream end River station of 12086.49 (dam site) by piping for different regression approaches.

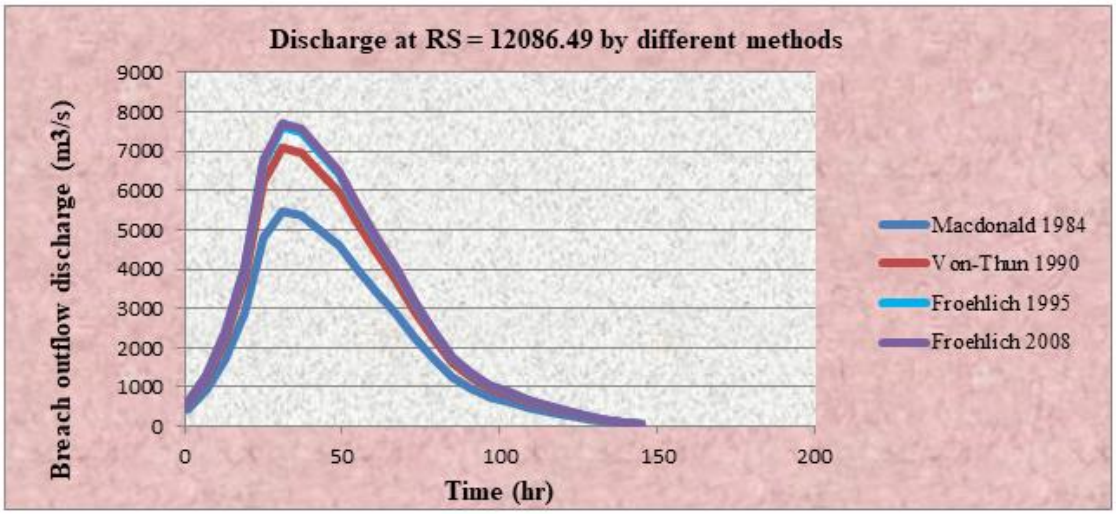

Figure 4-11: Flood hydrographs routed at upstream end River station of 12086.49 by piping for different regression approaches.

The routing of flood hydrographs from the upstream end RS of 12086.49 (dam site) to the downstream end RS of 26.77806 were done. The routed flood discharges at different river stations of RS (12086.49), RS (8924.878), RS (4701.743), and RS (26.77806) were attached on appendix D. The peak breach outflow discharges simulated in HEC-RAS model due to piping for Froehlich 2008 at the upstream end RS of 12086.49, at the downstream of Dire dam of RS (8924.878), RS (4701.743), and RS (26.77806) were presented in table 4-8. The results indicated that, the peak breach outflow discharge at RS (12086.49) was greater than that of the peak breach

outflow discharges at the different RS and peak discharge attenuation was taken place along the downstream of the dam.

Table 4-8: Peak breach outflow discharges by piping at different River stations

S/N	River stations	Peak discharge (m^3/s) at different River stations
1	12086.49	7712.10
2	8924.878	7681.21
3	4701.743	7626.23
4	26.77806	7611.54

The routing of flood discharges at different river stations of RS (12086.49), RS (8924.878), RS (4701.743), and RS (26.77806) were shown in figure 4-12.

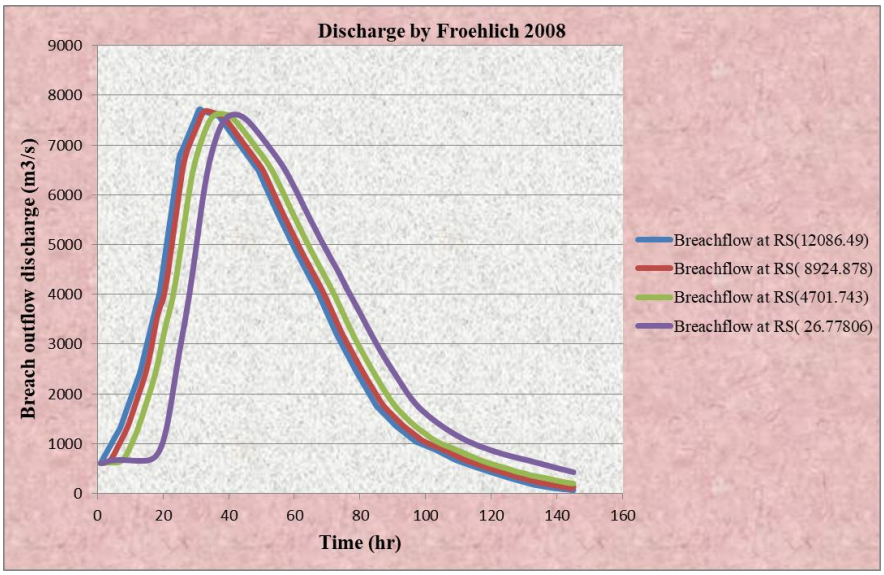

Figure 4-12: Flood hydrographs routed at different River stations by piping

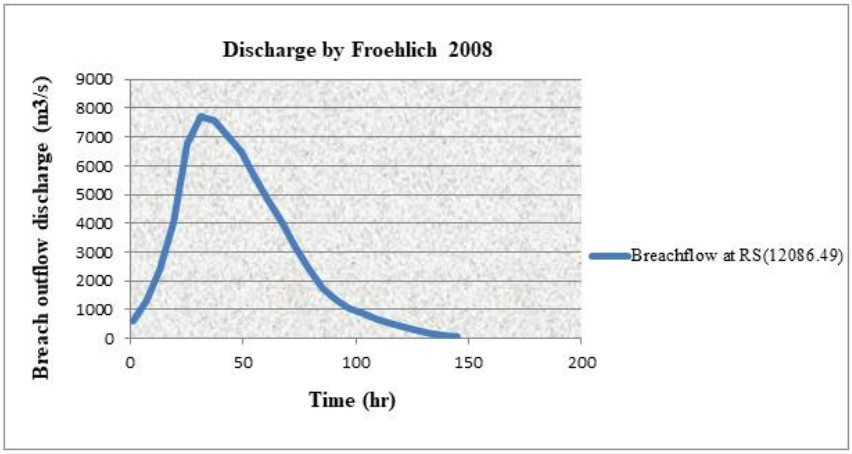

Figure 4-13: Flood hydrograph routed at River station 12086.49 by piping

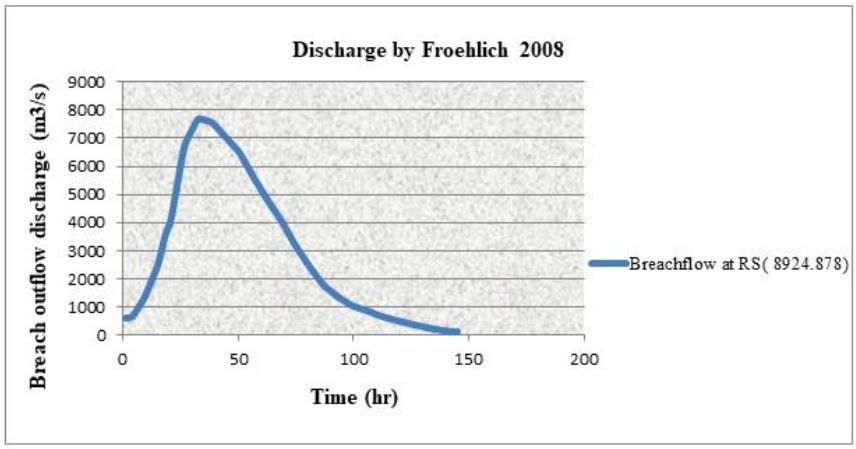

Figure 4-14: Flood hydrograph routed at River station 8924.878 by piping

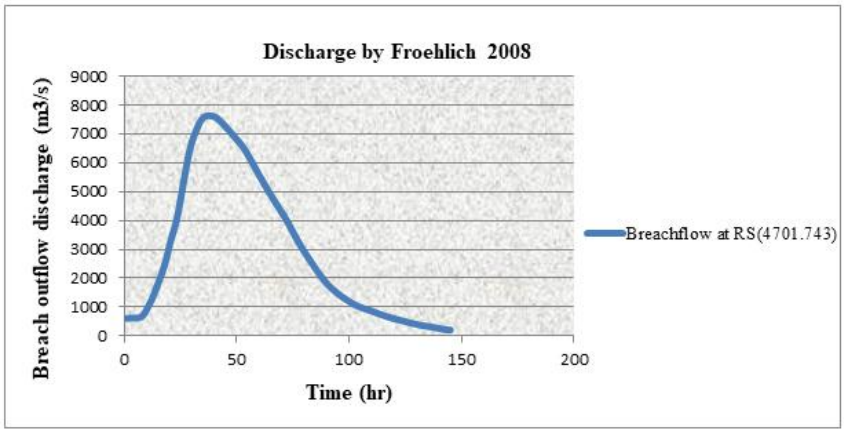

Figure 4-15: Flood hydrograph routed at River station 4701.743 by piping

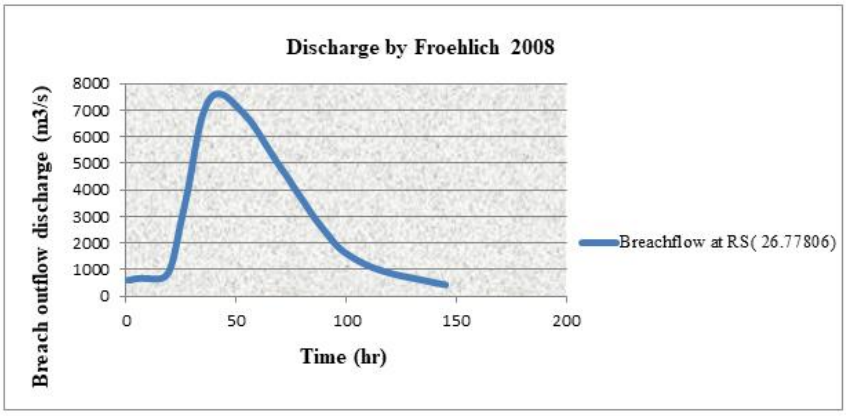

Figure 4-16: Flood hydrograph routed at River station 26.77806 by piping

As observed from study conducted (Lejissa, 2015) on Arjo-Dedesa dam breach using HEC-RAS, the peak breach outflow discharge due to overtopping of 180,690.8 m^3/s is greater than that of dam body piping 163,026.8 m^3/s and the flood risk to the downstream area is greater due to

overtopping than piping. For Dire dam, the results found from unsteady flow analysis due to overtopping and piping showed that, the peak breach outflow discharges found from unsteady flow simulation in HEC-RAS model were 9285.3m^3/s and 7712.1m^3/s respectively. The results demonstrated that, as the breach outflow discharges due to overtopping was greater than that of piping, the resulting flood from the breached dam by overtopping would affect downstream areas of the dam than that of the resulting flood from the breached dam by piping failure.

4.3. Reliability checking of the Peak breach outflow discharge

For Dire dam, both unsteady flows due to overtopping and piping were analyzed. The peak breach outflow discharges at the dam location for both failure modes were taken to the dam downstream flood analysis. The peak breach outflow discharges simulated in HEC-RAS model for Froehlich 2008 due to overtopping and piping at the dam location were 9285.3 m^3/s and 7712.1 m^3/s respectively. (Brunner, 2014) have presented the accuracy of the simulated breach outflow discharge in HEC-RAS is governed under the experienced envelope curve. Therefore, in order to ensure the reality of the peak breach outflow discharges result from the breached dam, checking the simulated peak discharge with the experienced envelope curve is very significant. This task was carried out through connecting the hydraulic depth value due to breached dam and the peak envelope discharge via referencing the experienced envelope curve. The calculation of hydraulic depth was done through the HEC-RAS model. For best reality of the result, the simulated peak discharge value should be located within the boundary of the experienced envelope curve. Hence, the peak breach outflow discharge simulated for Dire dam due to overtopping and piping was located within the envelope curve boundary. This showed that, the HEC-RAS model have capable of simulating breach outflow discharge from the breached dam. Figure 4-17 and 4-18 showed reality checking of peak breach outflow discharge with experienced envelope curve from breached dam due to overtopping and piping respectively.

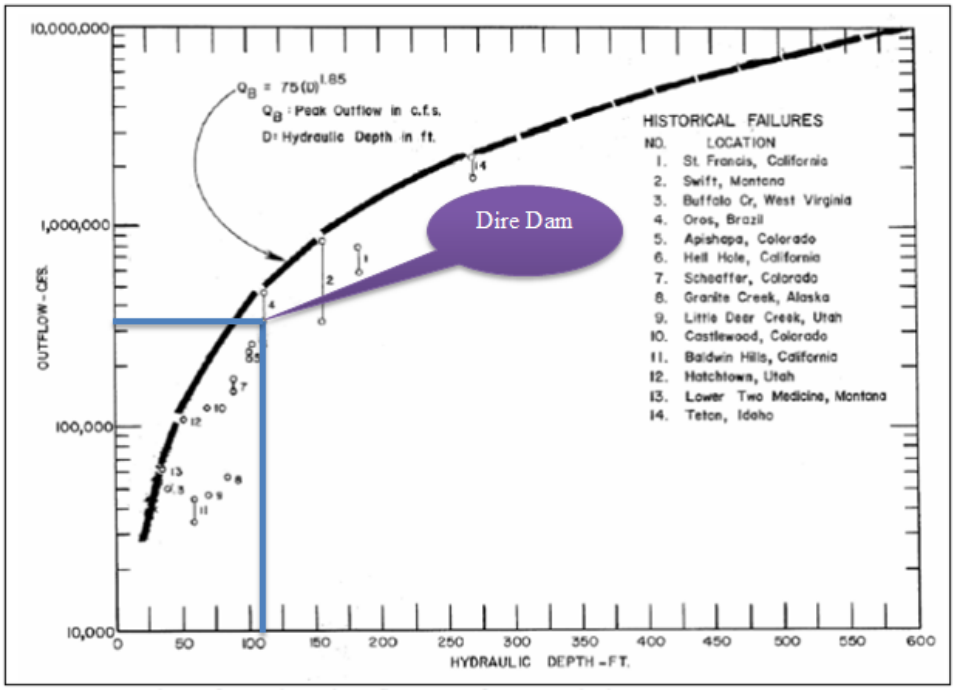

Figure 4-17: Dire dam location on envelope of experienced outflow rates from breached dam due to overtopping

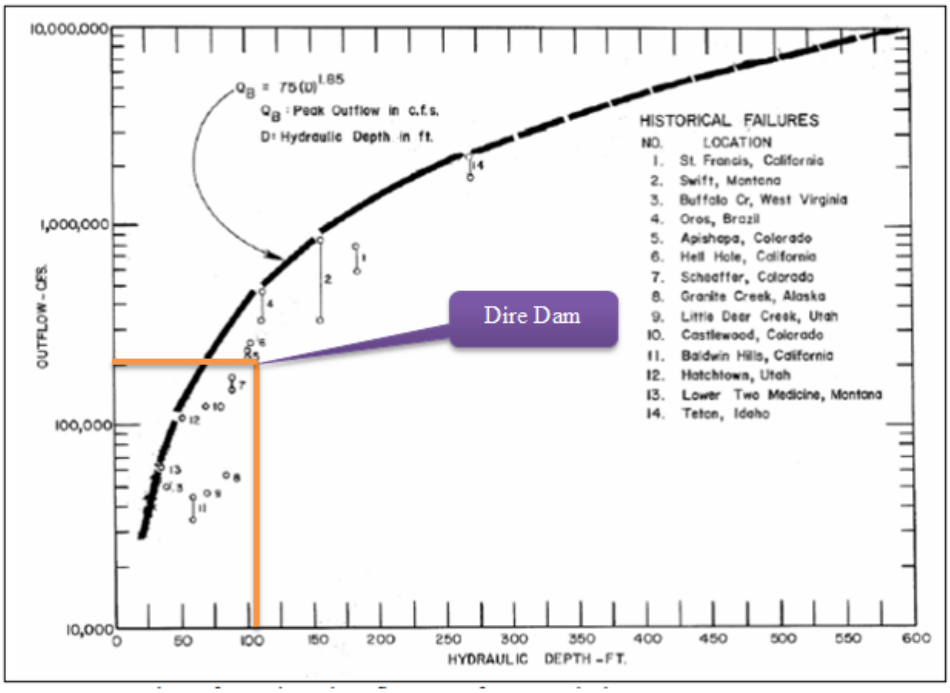

Figure 4-18: Dire dam location on envelope of experienced outflow rates from breached dam due to piping

4.4. Longitudinal Profile of the Legadadi River

The River longitudinal profile comprises the various characteristics of river through its reach length. The Legadadi River longitudinal profile consist of the water surface elevation, the base elevation, the energy grade elevation, and the main channel distance from the upstream boundary condition to the downstream boundary condition. These river channel characteristics were found after the computation of unsteady flow due to overtopping and piping failure mode in HEC-RAS model. Figure 4-19 presented the longitudinal profile of Legadadi River.

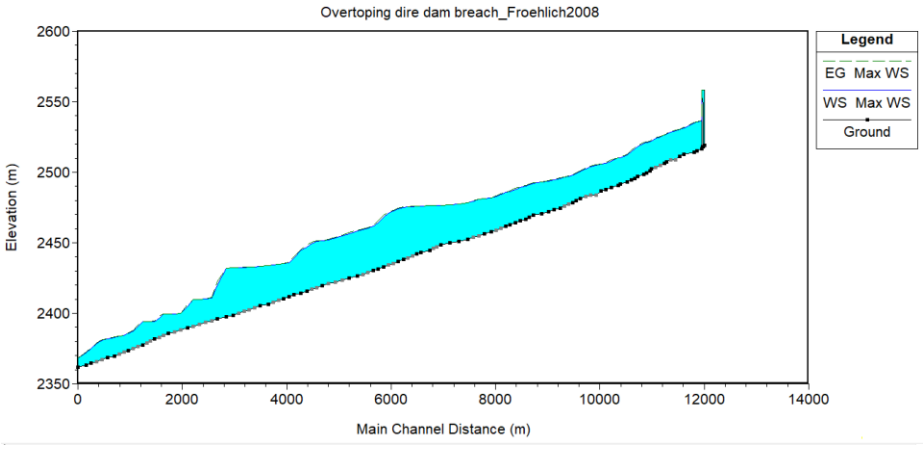

Figure 4-19: Longitudinal bed profile of Legadadi River

As observed from the above figure 4-19, at the dam location the maximum flood profile of the Legadadi River have various characteristics. Table 4-9 depicted the maximum flood profile of Legadadi River at the dam location for both overtopping and piping failure mode.

Table 4-9: The maximum flood profile of Legadadi River at the dam location

S/N	Legadadi river characteristics	by dam Overtopping	by dam piping
1	Energy grade elevation (m)	2558.30	2557.03
2	Maximum channel depth (m)	38.93	37.71
3	Maximum water surface elevation (m)	2558.24	2557.02
4	Top width (m)	1107.12	845.79
5	Minimum channel elevation (m)	2519.31	2519.31

(Basheer *et al.*, 2017) presented the flood water distribution has strong relation with top width. Then as observed from the results in the table 4-9, water distribution extent due to the flood discharge occurred by overtopping breach scenario was greater than that of the piping breach mode since the top width or free water surface distribution of flood water due to overtopping was larger than the flood water due to piping failure mode.

4.5. Cross Sectional Profile of the Legadadi River

The Cross sectional profile of river shows a cross-section of a river's channel and banks at certain points in the river's reach length. The cross sectional profile of Legadadi River was analyzed during dam breach due to overtopping and piping failure mode. This cross sectional profile of the river contains maximum energy grade surface and maximum water surface. The maximum depth of flood and top width over the banks at different river stations of RS (8924.878), RS (4701.743), and RS (26.77806) were analyzed. Table 4-10 presented the maximum depth of flood and top width over the banks at river stations of RS (8924.878), RS (4701.743), and RS (26.77806).

Table 4-10: The maximum depth of flood and top width over the banks at different river stations

S/N	River stations	flood depth (m)		Top width (m)	
		by overtopping	by piping	by overtopping	by piping
1	RS (8924.878)	10.97	9.88	946.18	869.25
2	RS (4701.743)	13.11	12.07	1740.92	1656.45
3	RS (26.77806)	11.24	10.45	1629.27	1550.28

The results in the table 4-10 showed that, the maximum flood depth from breached dam due to overtopping was larger than due to piping and the flood risk due to overtopping would be high to the downstream area of the dam. The top width from breached dam showed flood water distribution extent along the downstream of the dam. Then the flood water distribution extent due to overtopping was widespread than that of the piping.

Table 4-11: The flood arrival time at different river stations

S/N	River stations	flood arrival time (minutes)	
		by overtopping	by piping
1	RS (8924.878)	20	20
2	RS (4701.743)	70	60
3	RS (26.77806)	100	110

Figure 4-20 up to 4-22 showed the cross sectional profile of Legadadi River from breached dam by overtopping at different river stations of RS (8924.878), RS (4701.743), and RS (26.77806).

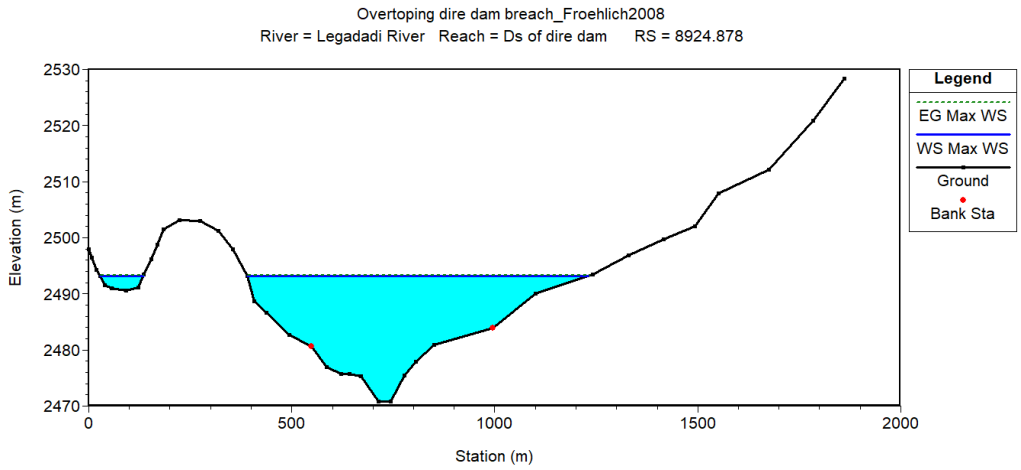

Figure 4-20: Cross sectional profile of Legadadi River by overtopping of RS (8924.878)

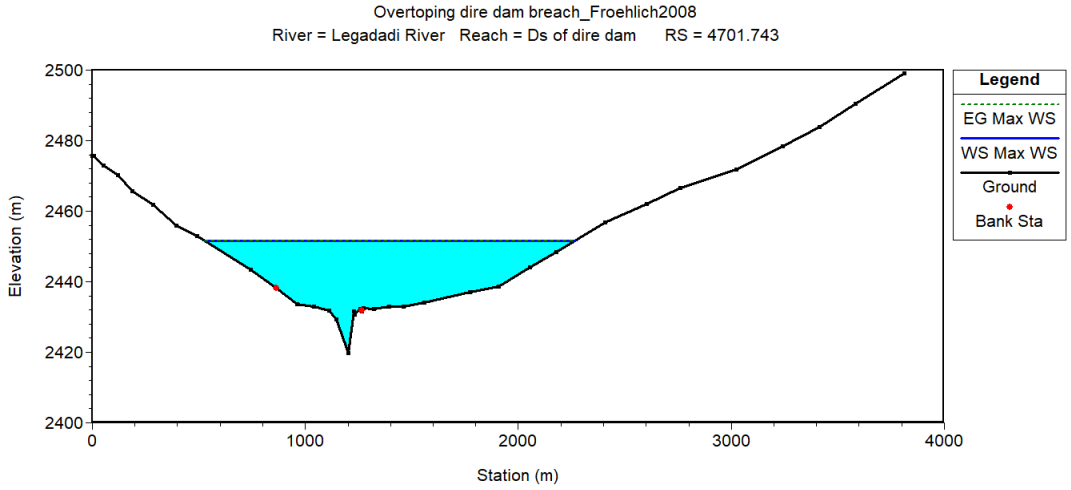

Figure 4-21: Cross sectional profile of Legadadi River by overtopping of RS (4701.743)

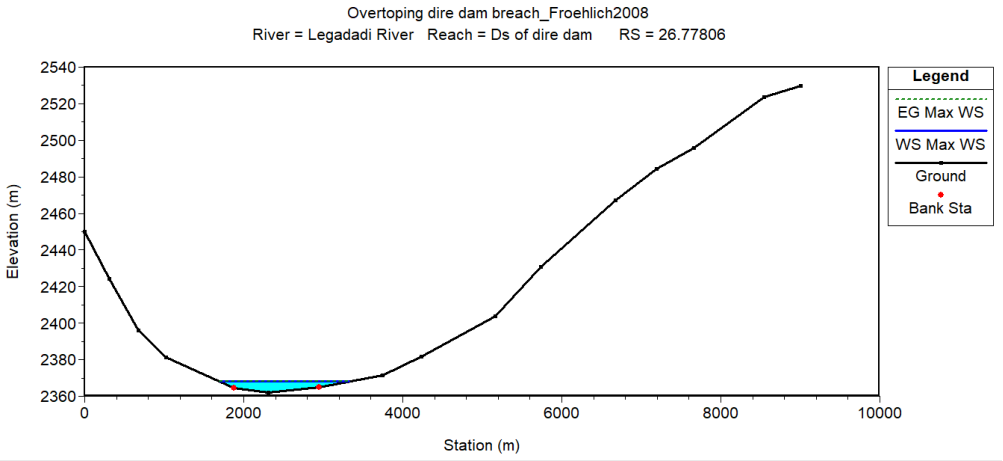

Figure 4-22: Cross sectional profile of Legadadi River by overtopping of RS (26.77806)

The cross sectional profile of Legadadi River from breached dam by piping at different river stations of RS (8924.878), RS (4701.743), and RS (26.77806) were demonstrated in figure 4-23 up to 4-25.

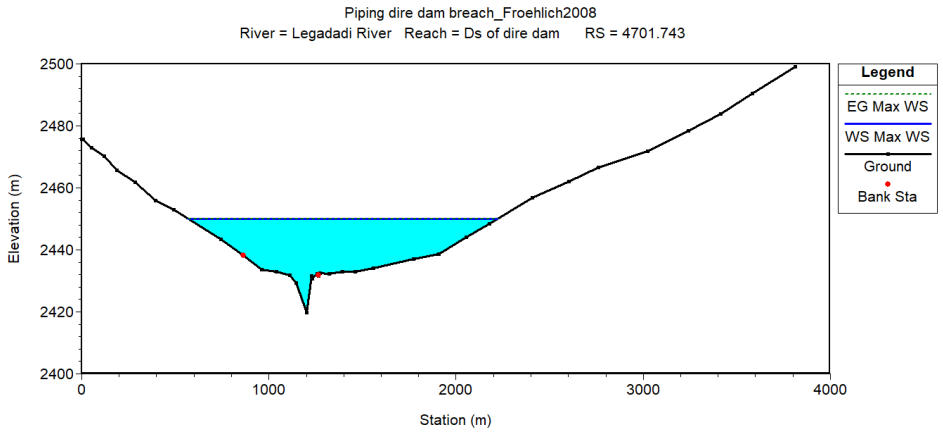

Figure 4-23: Cross sectional profile of Legadadi River by piping of RS (8924.878)

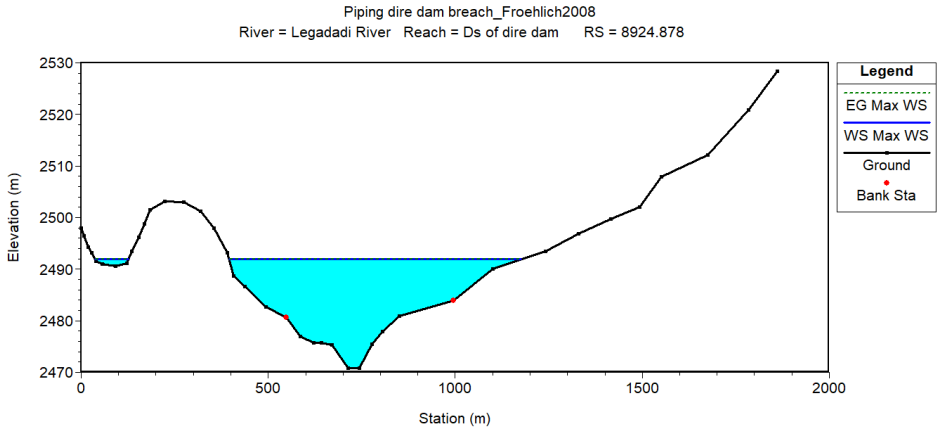

Figure 4-24: Cross sectional profile of Legadadi River by piping of RS (4701.743)

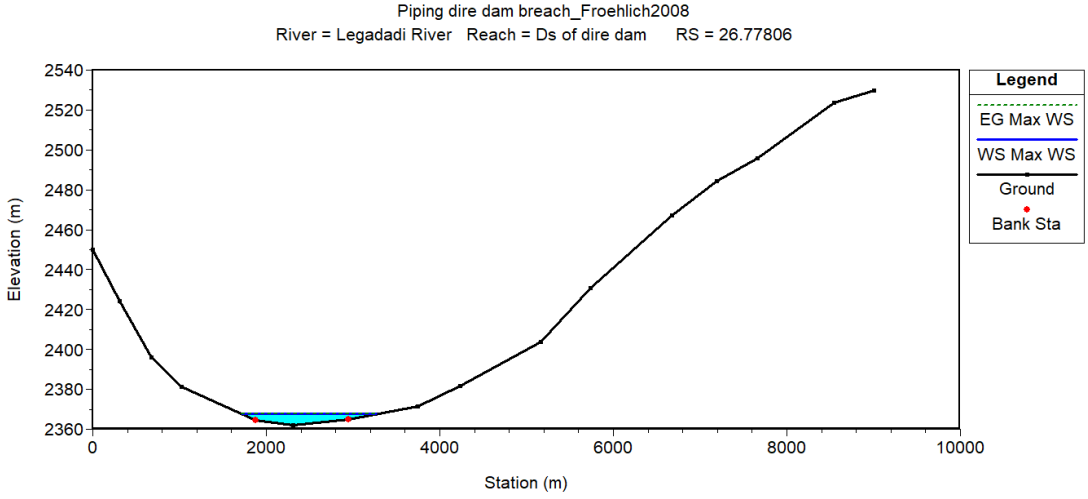

Figure 4-25: Cross sectional profile of Legadadi River by piping of RS (26.77806)

4.6. Flood Inundation Map Development

Inundation map is a map demarcating the area that would be flooded by a specific flood event and comprises the ground surfaces downstream of dam showing the probable impingement by water released because of failure of dam or from unusual flood flows released through dam's spillway and other appurtenant structures. In the analyzing of downstream risk assessment and their consequence classification, development of an inundation map resulted from the computation of flow depth and flow velocity have a great role (FEMA, 2013). The flood map for the Dire dam was done through the flood resulting by overtopping and piping mode of failure.

For this study, the area located downstream of the dam that would be inundated were small house collecting and housing wires from piezometers, Legadadi town with different infrastructures. Some of these areas were presented on google Map, World Street Map, and World topographic Map. Figure 4-26 up to 4-28 indicated the downstream areas of Dire dam.

Figure 4-26: Downstream areas of Dire dam, source: Google Map

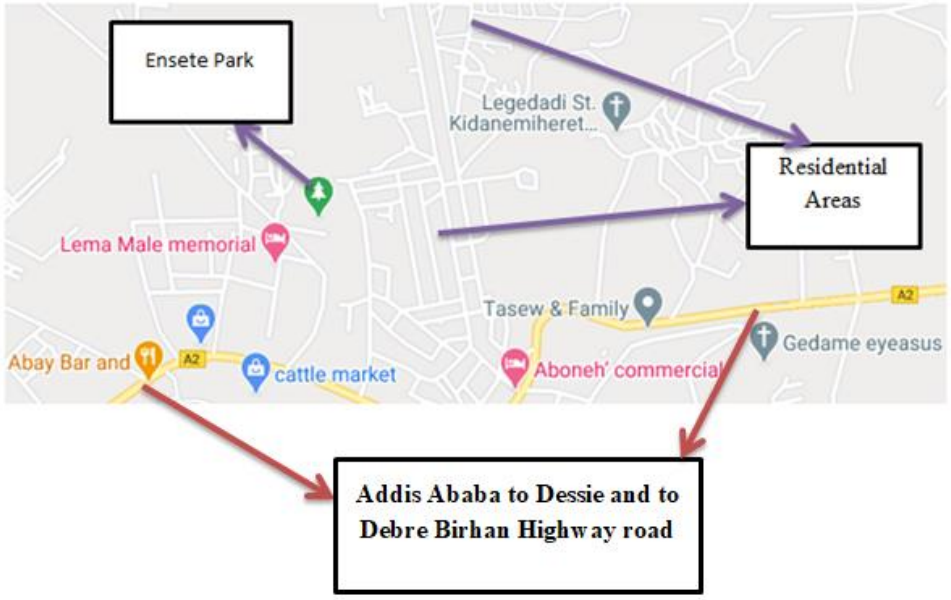

Figure 4-27: Residential areas and Infrastructures located at the downstream of Dire dam, source: World Street Map

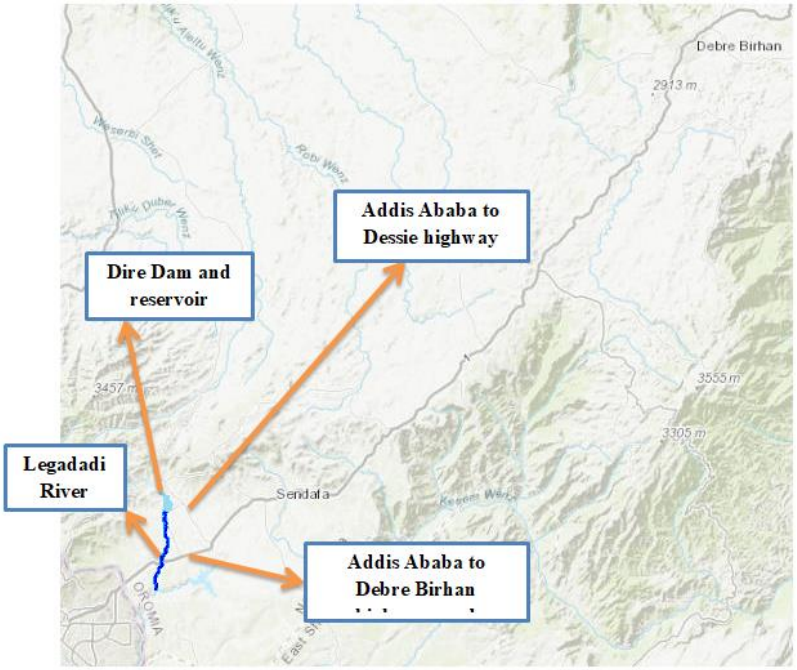

Figure 4-28: Addis Ababa to Debre Birhan and to Dessie highway roads located downstream of Dire dam, source: World topographic Map

In addition to estimating breach outflow hydrograph, another task performed during dam breach analysis was flood mapping of downstream area of dam that would be inundated by the flood resulting from breach of the dam. This task was carried out through unsteady flow simulation.

Afterward unsteady flow analysis was performed in HEC-RAS model; the water surface elevation, the maximum flow depth and velocity were exported in to GIS and assimilated with the Aerial map in order to envisage the inundation map extent advanced from the breached dam due to overtopping and piping failure modes. Therefore the downstream areas that would be inundated by the flood resulting from the breached Dire dam were covered about 30.927 km^2. It was calculated in GIS from polygon created for the flood coverage of the downstream of the dam. Figure 4-29 revealed the flood polygon area at downstream of the Dire dam.

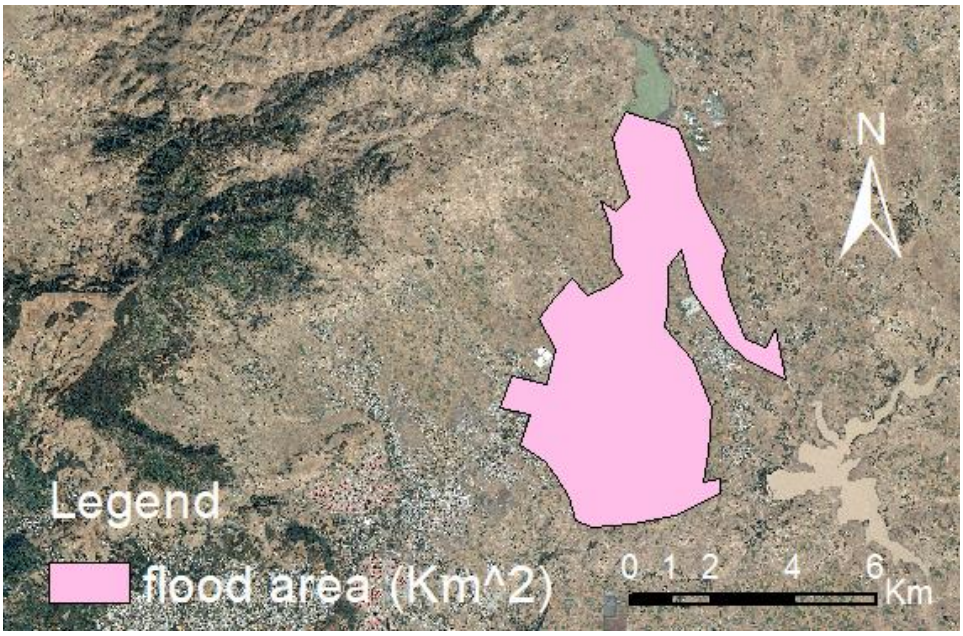

Figure 4-29: Flood coverage area for downstream of Dire dam

(Shahrim and Ros, 2020) conducted dam break study using HEC-RAS model on Temenggor Dam, Malaysia for overtopping and piping worst case. The maximum flood depth resulted from the breach of the dam for overtopping and piping are 56.1 m and 52.1 m respectively and also the maximum flood velocity resulted from the breach of the dam for overtopping and piping are 29.4 m/s and 28.6 m/s respectively.

For Dire dam, the maximum flood depth and maximum flood velocity due to overtopping were 16.41 m and 22.74 m/s respectively. The flood map through downstream of Dire dam flooded area due to maximum flood depth and maximum flood velocity for overtopping was shown in figure 4-30 and 4-31.

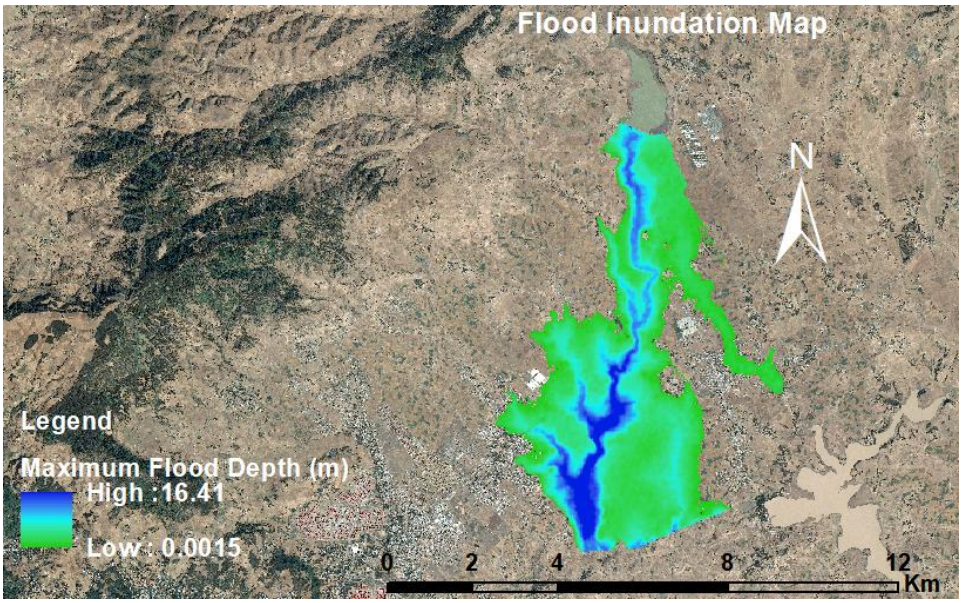

Figure 4-30: Flood map due to maximum depth from breached dam by overtopping

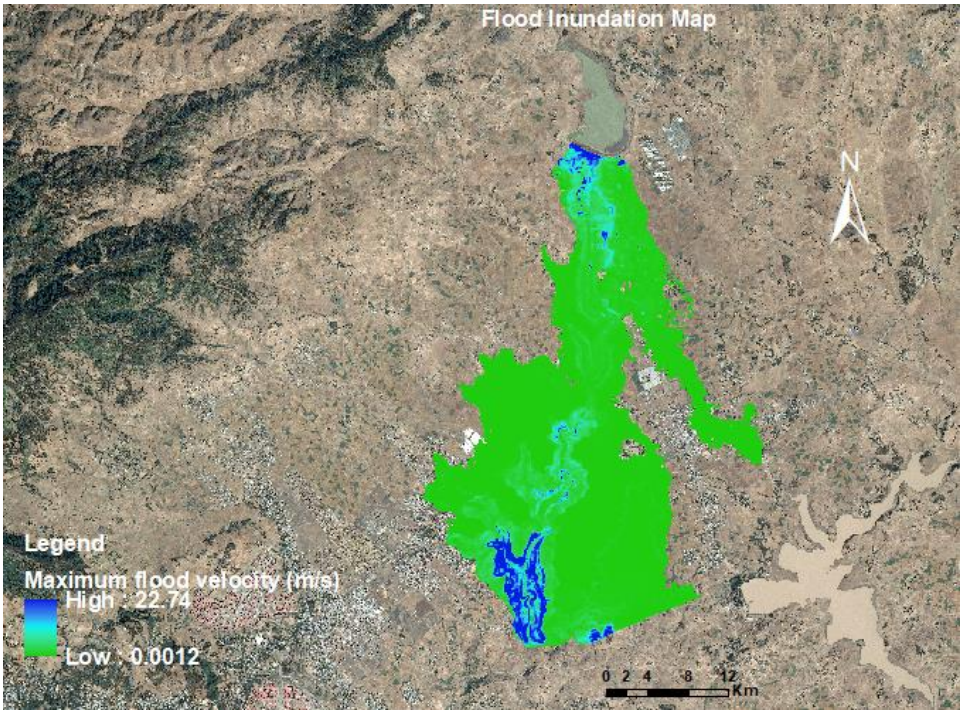

Figure 4-31: Flood map due to maximum velocity from breached dam by overtopping

Figure 4-32 below presented the infrastructure of the highway road serving for transportation from Addis Ababa to Dessie and to Debre Birhan located downstream of Dire dam after it would be inundated by flood resulting from the failure of Dire dam due to overtopping.

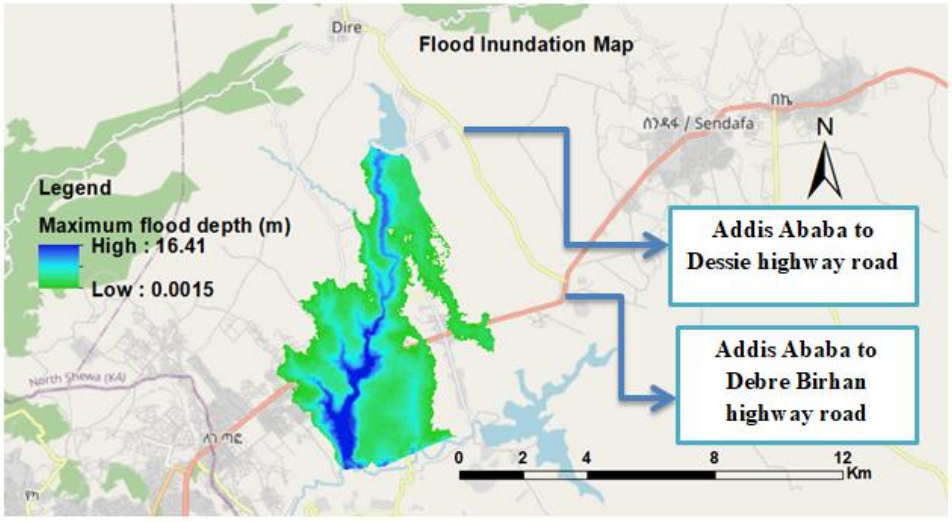

Figure 4-32: Addis Ababa to Dessie and to Debre Birhan Highway road that would be inundated from the breached dam due to Overtopping

The maximum flood depth and maximum flood velocity due to piping were 14.43 m and 19.56 m/s respectively. The flood map through downstream of dire dam flooded area due to maximum flood depth and maximum flood velocity for piping was shown in figure 4-33 and 4-34.

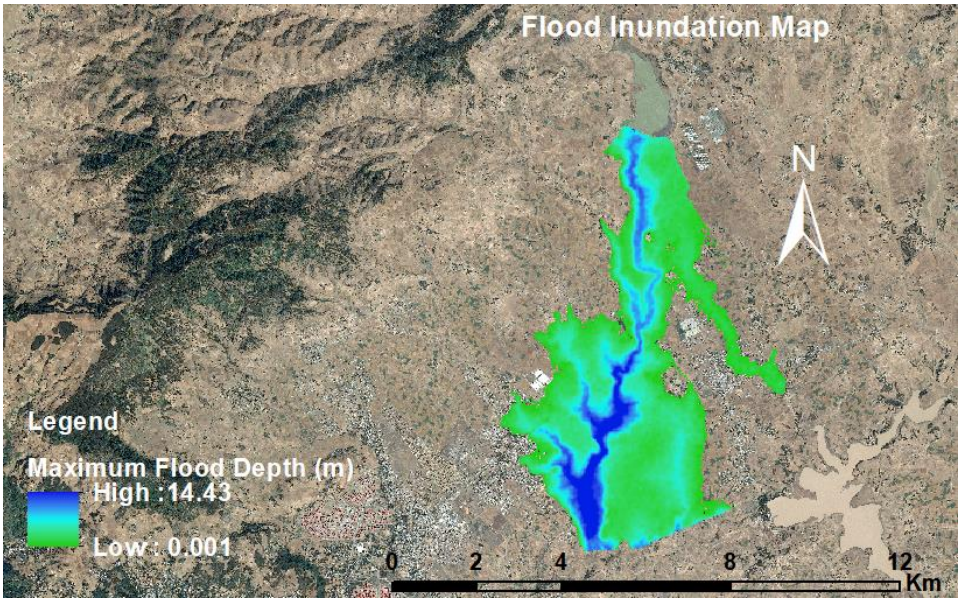

Figure 4-33: Flood map due to maximum depth from breached dam by piping

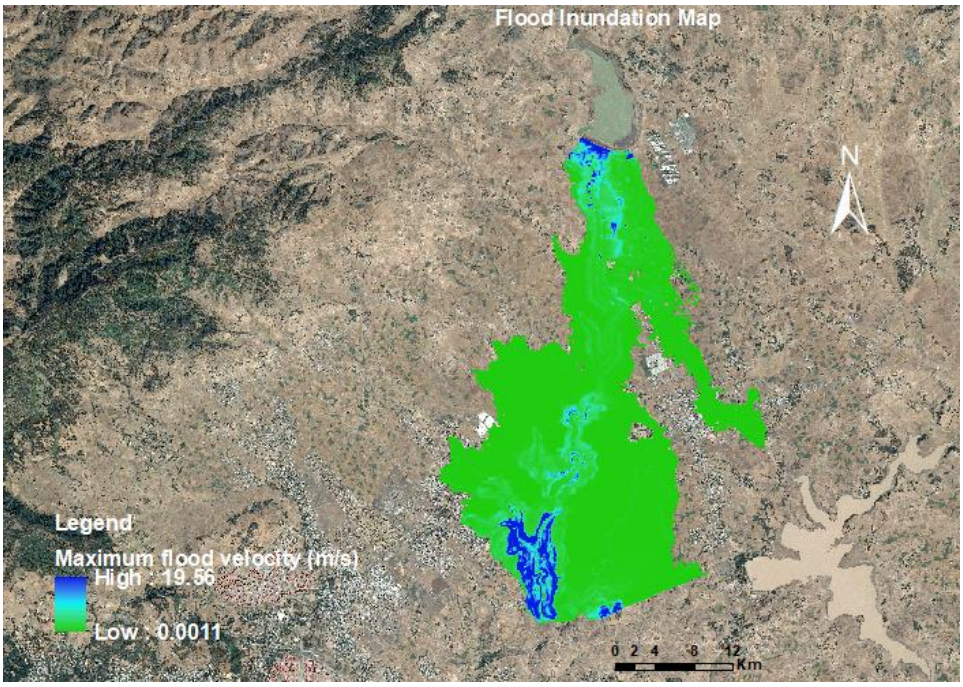

Figure 4-34: Flood map due to maximum velocity from breached dam by piping

The infrastructure of the highway road serving for transportation from Addis Ababa to Dessie and to Debre Birhan located downstream of Dire dam after it would be inundated by flood resulting from the failure of Dire dam due to piping was displayed in figure 4-35.

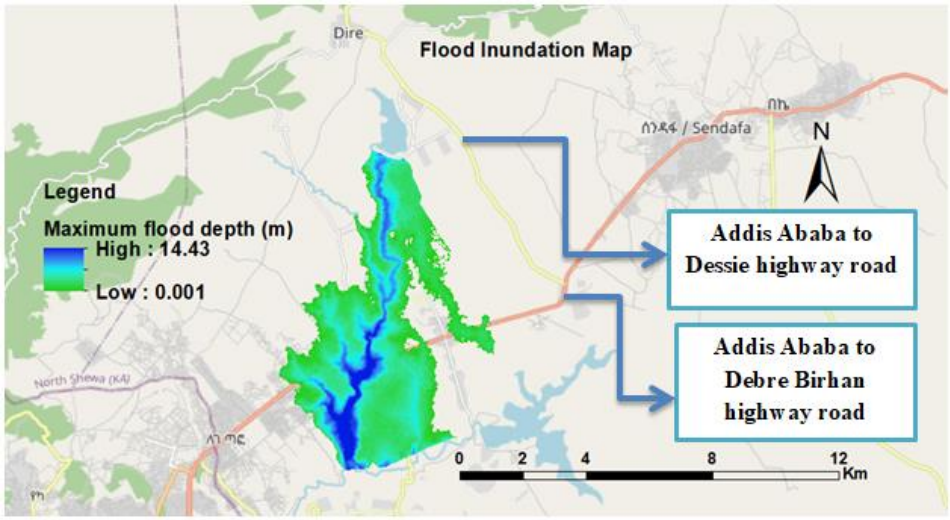

Figure 4-35: Addis Ababa to Dessie and to Debre Birhan Highway road that would be inundated from the breached dam due to Piping

4.7. Flood Hazard Mapping

The risk to public safety and to situate infrastructures damage triggered through floods based mostly upon the velocity and depth of flood occurred from breached dam. The larger these elements become, the larger the hazard to downstream civilian population and infrastructures. This hazard is categorized as high hazard, medium hazard and low hazard based on the risk related to magnitude of flood hazard detection factors. Figure 4-36 showed depth-velocity hazard classification diagram basis for flood hazard mapping in this study.

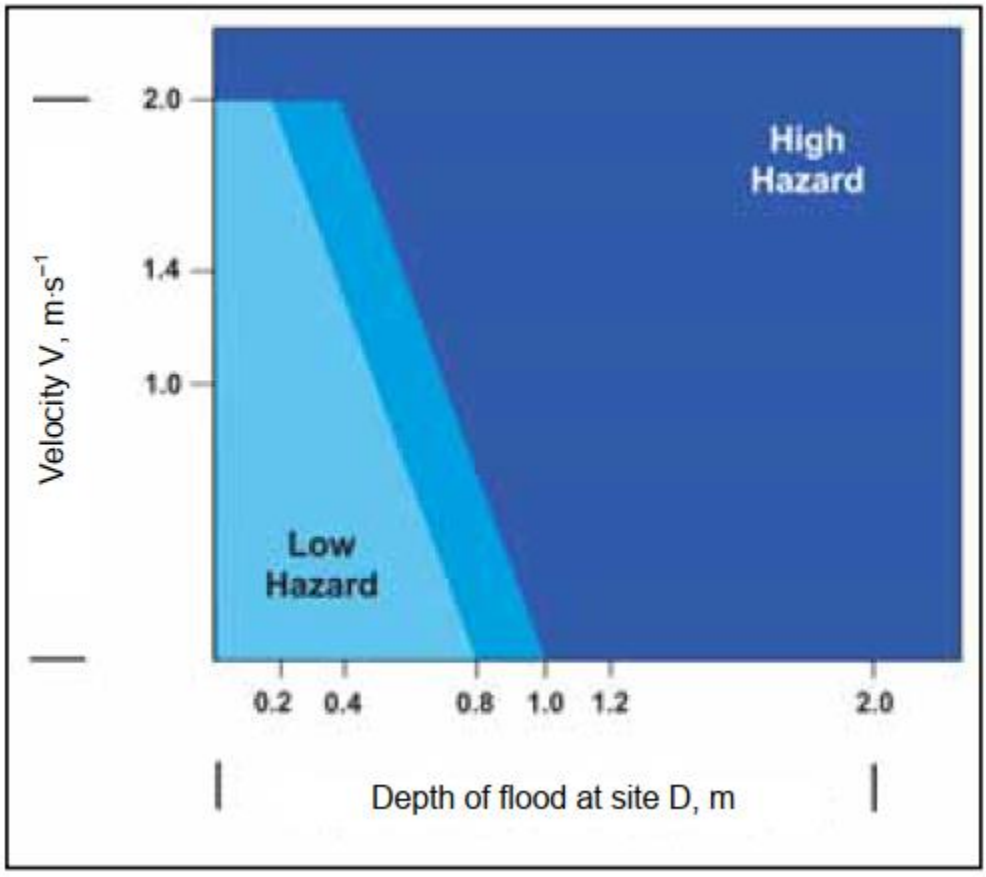

Figure 4-36: Flood Hazard zone classification as a function of velocity and water depth; source: (Derdous *et al.*, 2015).

The flood hazard map was developed in the GIS through combining depth and velocity maps. Figure 4-37 showed the downstream hazard flood map subsequent from the breach of Dire dam due to overtopping and piping.

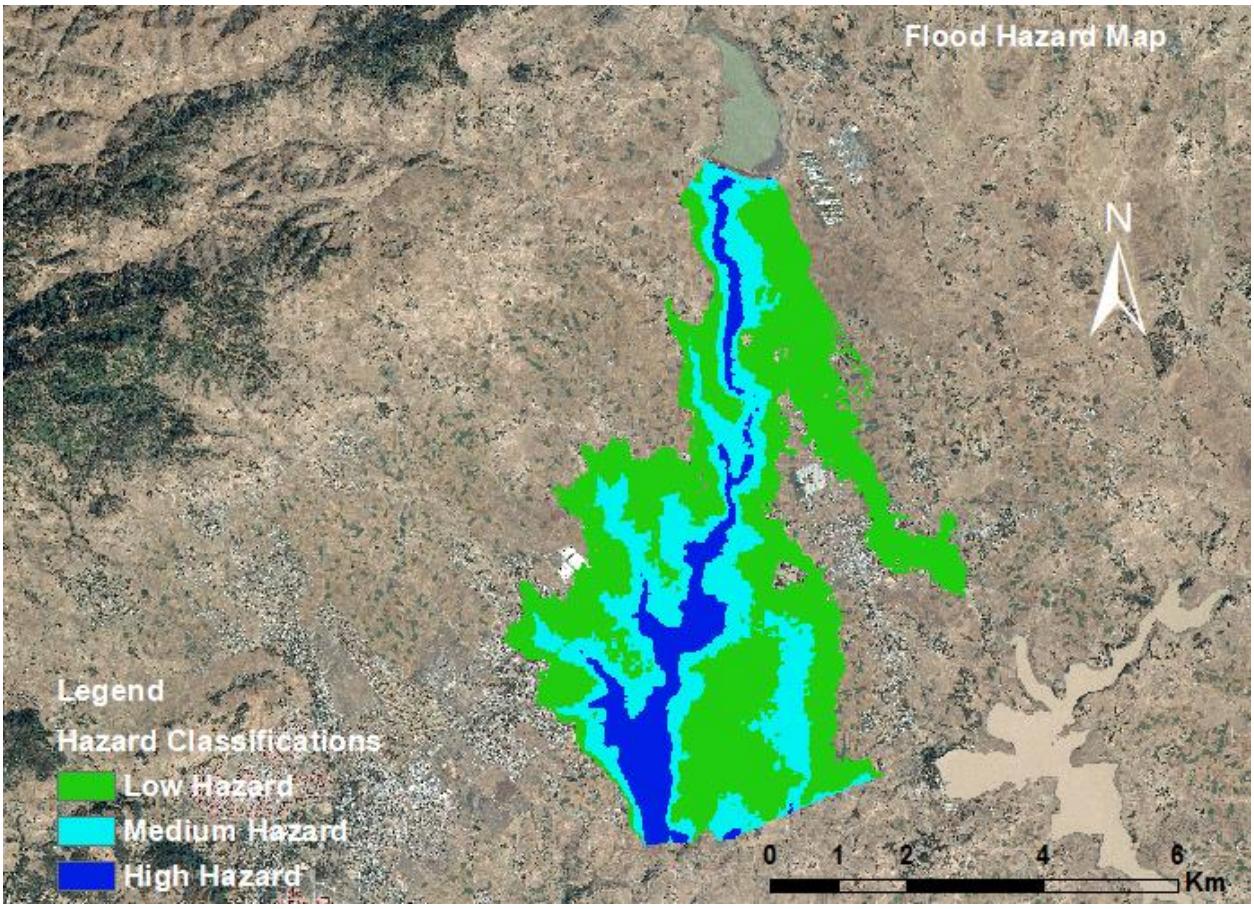

Figure 4-37: Flood hazard map resulting from the failure of Dire dam

Based on (FEMA, 2013) dam hazard classification as observed from the flood hazard map, at the point of low hazard symbolized by green color, the inundated flood on the downstream areas of Dire dam would results no probable loss of community life and low economic and environmental losses. For Medium hazard class represented by aqua color, the flood occur would probably cause economic loss and environmental damage, and also for high hazard class symbolized by blue color, the flood would probably cause loss of community life.

5. CONCLUSION AND RECOMMENDATION

5.1. CONCLUSION

This study mainly focused on breach analysis of dire dam located at 30 km to the east of Addis Ababa city within the boundary of the Oromia region. The dam failure modes for this study were assumed to be overtopping and piping. In order to meet this objective, the one dimensional HEC-RAS model played a great role incorporates with GIS, and HEC-GeoRAS. In HEC-RAS model, unsteady flow simulation was performed for the assumed dam failure modes after all important data including Dire dam breach parameters, Dire dam geometric data, Dire reservoir elevation-volume data, unsteady flow data, and geometric data of Legadadi River were inserted in the model as an input data. The dam breach parameters were computed through the Froehlich 2008 empirical method while comparing to others methods. The method was selected based on the criteria of high performance and accuracy in estimating breach parameters. In HEC-GeoRAS, Legadadi River geometry data were extracted from study area DEM represented by TIN.

The breach parameters value of breach bottom width (B), breach formation time (tf), and breach side slopes (bss) for overtopping failure mode were 51.3m, 0.65hr, and 1. The breach parameters value of breach bottom width (B), breach formation time (tf), and breach side slopes (bss) for piping failure mode were 45.98m, 0.75hr, and 0.7. The peak breach outflow discharges found from the breach dam after the completion of unsteady flow simulation in HEC-RAS model were 9285.3m^3/s and 7712.1m^3/s by overtopping and piping failure respectively. The results demonstrated that, as the breach outflow discharges due to overtopping was greater than that of piping, the resulting flood by overtopping would damages downstream areas of the dam than that of the resulting flood by piping failure. The maximum flood depth and maximum flood velocity occurred due to dam overtopping failure were 16.41m and 22.74m/s respectively. The maximum flood depth and maximum flood velocity occurred due to dam piping failure were 14.43m and 19.56m/s respectively.

The flood inundation map for Dire dam downstream areas for resulting flood due to overtopping and piping failure were developed in GIS after water surface elevation, maximum flood depth and maximum velocity were imported in to GIS from HEC-RAS model. The simulation outcomes presented that in the event of Dire dam breach due to the assumed dam break modes, some Dire dam downstream areas were observed as having high flood hazard due to the significant flood water depth and velocity values.

5.2. RECOMMENDATION

The findings of the study indicated that the dire dam would be breached under failure scenarios of overtopping and piping and also there would be downstream flooding from the resulting flood due to the breached dam. As a result, some recommendations were forwarded depending on the findings of the study.

Since the dam would be failed due to overtopping and piping, dam owner, operating personnel, and maintenance personnel must be skilled of these potential problems which can lead to dam failure. These bodies can reduce the failure by observing the structure through its service life to recognize these potential problems.

The study results presented that, some areas located downstream of dire dam would be flooded from resulting flood in the event of dire dam break. These areas located near the Legadadi River flood plains would be damaged by the flood as observed from flood hazard map and better if the residential houses and infrastructures are built at the minimum distance of 350m from the left bank and 200m from the right bank.

The maximum flood depth found among both the overtopping and piping breach scenarios was 16.41 m, therefore people living very close to Legadadi river banks in downstream area needs to build their houses above this level. For more improvement of the results found, the dam owner should also have conducted further study by collecting downstream elevation data for lessening the deviation from the actual one.

REFERENCES

Abdulrahman, K. Z., 2014 ‘Case Study of the Chaq-Chaq Dam Failure : Parameter Estimation and Evaluation of Dam Breach Prediction Models’, International Journal of Engineering Research and Applications, 4(5), pp. 109–116.

Afsal, K.P., Anjali, P., Peter, J.,Vinaya, S.M., 2016 ‘Dam Break Analysis of Idukki Dam Using FLDWAV River Mechanics’, International Research Journal of Engineering and Technology (IRJET), 03(05), Pp. 304–307.

Addis Ababa Water and Sewerage Authority, 2016 ‘Legadadi and Dire Dam Rehabilitation Project Final Design Rerort‘.

Balaji, B., and Kumar, S., 2018 ‘Dam break analysis of kalyani dam using HEC-RAS’, International Journal of Civil Engineering and Technology, 9(5), pp. 372–380.

Basheer, T. A., Wayayok, A., Yusuf, B., Kamal, MD. R., 2017 ‘Dam breach parameters and their influence on flood hydrographs for mosul dam’, Journal of Engineering Science and Technology, 12(11), pp. 2896–2908.

Boussekine, M., and Djemili, L., 2016 ‘Modelling approach for gravity dam break analysis’, Journal of Water and Land Development, 30(1), pp. 29–34.

Brunner, G., 2014 ‘Using HEC-RAS for Dam Break Studies, TD-39’, Us Army Corps of Engineers Hydrologic Engineering Center (Hec), (August), p. 74.

Brunner, G., 2016 ‘HEC-RAS, River Analysis System Version 5.07 Hydraulic Reference Manual‘, Us Army Corps of Engineers Hydrologic Engineering Center.

Cameron, T., and Ackerman, P. E., 2012 'HEC-GeoRAS GIS Tools for Support of HEC-RAS User’s Manual'.

Davide, W., and Canale, L., 2016 ‘Dam break analysis for Serra degli Ulivi dam’, International Conference paper on Dam break.

Derdous, O., Djemili, L., Bouchehed, H., Tachi, S.E., 2015 ‘A GIS based approach for the prediction of the dam break flood hazard - A case study of Zardezas reservoir “skikda, Algeria”’, Journal of Water and Land Development, 27(1), pp. 15–20.

Duressa, J. N., and Jubir,A. K., 2018 ‘Dam Break Analysis and Inundation Mapping, Case Study of Fincha’a Dam in Horro Guduru Wollega Zone, Oromiya Region, Ethiopia’, Science Research, 6(2), p. 29.

Ekaningtyas, L. R., 2017 ‘Flood Inundation Prediction of Logung River due to the Break of Logung Dam’, Journal of the Civil Engineering Forum, 3(2), p. 331.

FEMA, 2013 ‘Federal Guidelines for Inundation Mapping of Flood Risks Associated with Dam Incidents and Failures.

Hong, W., and Changzhi, L., 2014 ‘Dam Break Flood Risk Assessment for Laiyang City’, Journal of Geological Resource and Engineering, 2(4), pp. 189–199.

Hossain, M. M., 2015 ‘Analysis of Flood Routing’, Dhaka University Journal of Science, 62(2), pp. 69–73.

Joshi, M. M., 2017 ‘Study of Two Dimensional Dam Break Analysis Using HEC-RAS for Vir Dam’, International Journal of Engineering Technology Science and Research, 4(8), pp. 982–987.

Joy, D., 2016 ‘Dam Break Analysis Using HEC-RAS', International Research Journal of Engineering and Technology, 3(5), pp. 308–309.

Kulkarni, S.R., Jagtap, S.A., 2017 ‘Dam Break Analysis of Pawana Dam’, International Journal of Recent Advances in Engineering & Technology (IJRAET), 5(1).

Kumar, S., Jaswal, A., Pandey, A.,Sharma, N., 2017 ‘Literature Review of Dam Break Studies and Inundation Mapping Using Hydraulic Models and GIS’, International Research Journal of Engineering and Technology, 4(4).

Lejissa, H., 2015 'Dam Breach Modelling and Downstream Risk Analysis (For Arjo-Dedessa Dam)' , Addis Ababa University, Addis Ababa Institute of Technology.

Leoul, A., and Kassahun, N., 2019 ‘Dam Breach Analysis Using HEC-RAS and HEC-GeoRAS: The Case of Kesem Kebena Dam’, Open Journal of Modern Hydrology, 09(04), pp. 113–142.

Maria, L., 2016 ‘Safety of Dams: A Pathological Approach of Qualitative and Quantitative Risks’, Journal of Civil Engineering and Architecture, 10(9), pp. 1032–1051.

Morris, M. and Hassan, M., 2018 ‘A guide to breach prediction’, Dams and Reservoirs, 28(4), pp. 150–152.

Muhammad, U., and Rasheed, M., 2016 ‘Dam Break Modeling by using HEC-RAS A Case Study of Attabad Lake Dam on Hunza River’, Journal of Engineering and Scientific Research, 4(1), pp. 26–31.

Nema, M., and Desmukh, T. S., 2016 ‘Dam break-A Review’, International Journal of Advanced Engineering Research and Science (IJAERS), 3(6), pp. 130–134.

Pandya, P. H., and Thakor, D. J., 2016 ‘A Brief Review of Method Available for Dam Break Analysis’, Indian Journal of Research, 2(4), pp. 117–118.

Razack, R., 2014 ‘Dam Break Analysis using GIS Applications’, International Journal of Engineering Research & Technology (IJERT), 3(3), pp. 1157–1161.

Saleh, M., and Kareem, R., 2011 ‘Predicting the breach hydrograph resulting due to hypothetical failure of haditha dam’, Jordan Journal of Civil Engineering, 5(3), pp. 392–400.

Sammen, S.S., Mohamed, T.A., Ghazali, A.H., Sidek, L.M., El-Shafie, A., 2017 ‘An evaluation of existent methods for estimation of embankment dam breach parameters’, Natural Hazards. Springer Netherlands, 87(1), pp. 545–566.

ShahiriParsa, A., Noori, M., Heydari, M., Rashidi, M., 2016 ‘Floodplain zoning simulation by using HEC-RAS and CCHE2D models in the Sungai Maka river’, Air, Soil and Water Research, 9, pp. 55–62.

Shahrim, M., and Ros, F., 2020 ‘Dam Break Analysis of Temenggor Dam Using HEC-RAS’, IOP Conference Series: Earth and Environmental Science.

Sharma, P., 2016 ‘Dam Break Analysis Using HEC-RAS and HEC-GeoRAS – A Case Study of Ajwa Reservoir’, Journal of Water Resources and Ocean Science, 5(6), pp. 108–113.

Sharma, R. P., and Kumar, A., 2013 ‘Case Histories of Earthen Dam Failures’, in Seventh International Conference on Case Histories in Geotechnical Engineering, p. 8.

Urzica, A., Hutanu, E., Mihu-Pintilie, A., Stoleriu, C.C., 2019 ‘Dam break analysis using HEC-RAS techniques. Case study: Cal Alb dam (NE Romania)’, 16th International Conference on

Environmental Science and Technology. Rhodes, Greece, pp. 2–3.

Wahl, T. L., 2014 ‘Evaluation of Erodibility-Based Embankment Dam Breach Equations‘, Hydraulic Laboratory Report HL-2014-02.

Xoing, Y., 2011 ‘A Dam Break Analysis Using HEC-RAS’, Journal of Water Resource and Protection, 3(6), pp. 370–379.

Yohannes, H. F., 2019 'Dam Breach Analysis and Emergency Action Plan Case Study of Mhtsab Azmati Dam', Addis Ababa University, Addis Ababa Institute of Technology.

APPENDICES

Appendix – A: The Maximum breach outflow discharges (m^3/s) by different methods at the dire dam site due to overtopping breach scenario.

Date		Flow (m^3/s) **Macdonald 1984**	Flow (m^3/s) **Von-Thun 1990**	Flow (m^3/s) **Froehlich 1995**	Flow (m^3/s) **Froehlich 2008**
14Aug1994	1200	461.25	683.55	724.95	733.05
14Aug1994	1210	551.79	817.73	867.25	876.94
14Aug1994	1220	642.33	951.91	1009.56	1020.84
14Aug1994	1230	732.87	1086.09	1151.87	1164.74
14Aug1994	1240	823.42	1220.26	1294.17	1308.63
14Aug1994	1250	913.96	1354.44	1436.48	1452.53
14Aug1994	1300	1004.5	1488.62	1578.78	1596.42
14Aug1994	1310	1144.58	1696.22	1798.95	1819.05
14Aug1994	1320	1284.67	1903.81	2019.12	2041.68
14Aug1994	1330	1424.75	2111.41	2239.29	2264.31
14Aug1994	1340	1564.83	2319.01	2459.46	2486.94
14Aug1994	1350	1704.92	2526.6	2679.63	2709.57
14Aug1994	1400	1845	2734.2	2899.8	2932.2
14Aug1994	1410	2050	3038	3222	3258
14Aug1994	1420	2255	3341.8	3544.2	3583.8
14Aug1994	1430	2460	3645.6	3866.4	3909.6
14Aug1994	1440	2665	3949.4	4188.6	4235.4
14Aug1994	1450	2870	4253.2	4510.8	4561.2
14Aug1994	1500	3075	4557	4833	4887
14Aug1994	1510	3416.67	5063.33	5370	5430
14Aug1994	1520	3758.33	5569.67	5907	5973
14Aug1994	1530	4100	6076	6444	6516
14Aug1994	1540	4441.67	6582.33	6981	7059
14Aug1994	1550	4783.33	7088.67	7518	7602
14Aug1994	1600	5125	7595	8055	8145
14Aug1994	1610	5244.58	7772.22	8242.95	8335.05
14Aug1994	1620	5364.17	7949.43	8430.9	8525.1
14Aug1994	1630	5483.75	8126.65	8618.85	8715.15
14Aug1994	1640	5603.33	8303.87	8806.8	8905.2
14Aug1994	1650	5722.92	8481.08	8994.75	9095.25
14Aug1994	1700	5842.5	8658.3	9182.7	9285.3
14Aug1994	1710	5825.42	8632.98	9155.85	9258.15
14Aug1994	1720	5808.33	8607.67	9129	9231
14Aug1994	1730	5791.25	8582.35	9102.15	9203.85
14Aug1994	1740	5774.17	8557.03	9075.3	9176.7
14Aug1994	1750	5757.08	8531.72	9048.45	9149.55

14Aug1994	1800	5740	8506.4	9021.6	9122.4
14Aug1994	1810	5671.67	8405.13	8914.2	9013.8
14Aug1994	1820	5603.33	8303.87	8806.8	8905.2
14Aug1994	1830	5535	8202.6	8699.4	8796.6
14Aug1994	1840	5466.67	8101.33	8592	8688
14Aug1994	1850	5398.33	8000.07	8484.6	8579.4
14Aug1994	1900	5330	7898.8	8377.2	8470.8
14Aug1994	1910	5261.67	7797.53	8269.8	8362.2
14Aug1994	1920	5193.33	7696.27	8162.4	8253.6
14Aug1994	1930	5125	7595	8055	8145
14Aug1994	1940	5056.67	7493.73	7947.6	8036.4
14Aug1994	1950	4988.33	7392.47	7840.2	7927.8
14Aug1994	2000	4920	7291.2	7732.8	7819.2
14Aug1994	2010	4808.96	7126.64	7558.27	7642.72
14Aug1994	2020	4697.92	6962.08	7383.75	7466.25
14Aug1994	2030	4586.88	6797.52	7209.22	7289.77
14Aug1994	2040	4475.83	6632.97	7034.7	7113.3
14Aug1994	2050	4364.79	6468.41	6860.17	6936.82
14Aug1994	2100	4253.75	6303.85	6685.65	6760.35
14Aug1994	2110	4151.25	6151.95	6524.55	6597.45
14Aug1994	2120	4048.75	6000.05	6363.45	6434.55
14Aug1994	2130	3946.25	5848.15	6202.35	6271.65
14Aug1994	2140	3843.75	5696.25	6041.25	6108.75
14Aug1994	2150	3741.25	5544.35	5880.15	5945.85
14Aug1994	2200	3638.75	5392.45	5719.05	5782.95
14Aug1994	2210	3544.79	5253.21	5571.38	5633.63
14Aug1994	2220	3450.83	5113.97	5423.7	5484.3
14Aug1994	2230	3356.88	4974.72	5276.03	5334.98
14Aug1994	2240	3262.92	4835.48	5128.35	5185.65
14Aug1994	2250	3168.96	4696.24	4980.68	5036.33
14Aug1994	2300	3075	4557	4833	4887
14Aug1994	2310	2963.96	4392.44	4658.47	4710.52
14Aug1994	2320	2852.92	4227.88	4483.95	4534.05
14Aug1994	2330	2741.88	4063.32	4309.42	4357.57
14Aug1994	2340	2630.83	3898.77	4134.9	4181.1
14Aug1994	2350	2519.79	3734.21	3960.37	4004.62
14Aug1994	2400	2408.75	3569.65	3785.85	3828.15
15Aug1994	0010	2314.79	3430.41	3638.17	3678.82
15Aug1994	0020	2220.83	3291.17	3490.5	3529.5
15Aug1994	0030	2126.88	3151.92	3342.82	3380.17
15Aug1994	0040	2032.92	3012.68	3195.15	3230.85
15Aug1994	0050	1938.96	2873.44	3047.48	3081.53

15Aug1994	0100	1845	2734.2	2899.8	2932.2
15Aug1994	0110	1759.58	2607.62	2765.55	2796.45
15Aug1994	0120	1674.17	2481.03	2631.3	2660.7
15Aug1994	0130	1588.75	2354.45	2497.05	2524.95
15Aug1994	0140	1503.33	2227.87	2362.8	2389.2
15Aug1994	0150	1417.92	2101.28	2228.55	2253.45
15Aug1994	0200	1332.5	1974.7	2094.3	2117.7
15Aug1994	0210	1281.25	1898.75	2013.75	2036.25
15Aug1994	0220	1230	1822.8	1933.2	1954.8
15Aug1994	0230	1178.75	1746.85	1852.65	1873.35
15Aug1994	0240	1127.5	1670.9	1772.1	1791.9
15Aug1994	0250	1076.25	1594.95	1691.55	1710.45
15Aug1994	0300	1025	1519	1611	1629
15Aug1994	0310	985.71	1460.77	1549.25	1566.56
15Aug1994	0320	946.42	1402.54	1487.49	1504.11
15Aug1994	0330	907.12	1344.32	1425.74	1441.67
15Aug1994	0340	867.83	1286.09	1363.98	1379.22
15Aug1994	0350	828.54	1227.86	1302.23	1316.78
15Aug1994	0400	789.25	1169.63	1240.47	1254.33
15Aug1994	0410	768.75	1139.25	1208.25	1221.75
15Aug1994	0420	748.25	1108.87	1176.03	1189.17
15Aug1994	0430	727.75	1078.49	1143.81	1156.59
15Aug1994	0440	707.25	1048.11	1111.59	1124.01
15Aug1994	0450	686.75	1017.73	1079.37	1091.43
15Aug1994	0500	666.25	987.35	1047.15	1058.85
15Aug1994	0510	640.63	949.38	1006.88	1018.13
15Aug1994	0520	615	911.4	966.6	977.4
15Aug1994	0530	589.38	873.42	926.32	936.68
15Aug1994	0540	563.75	835.45	886.05	895.95
15Aug1994	0550	538.12	797.47	845.77	855.22
15Aug1994	0600	512.5	759.5	805.5	814.5
15Aug1994	0610	494.56	732.92	777.31	785.99
15Aug1994	0620	476.62	706.33	749.11	757.48
15Aug1994	0630	458.69	679.75	720.92	728.98
15Aug1994	0640	440.75	653.17	692.73	700.47
15Aug1994	0650	422.81	626.59	664.54	671.96
15Aug1994	0700	404.88	600.01	636.34	643.45
15Aug1994	0710	388.65	575.95	610.84	617.66
15Aug1994	0720	372.42	551.9	585.33	591.87
15Aug1994	0730	356.19	527.85	559.82	566.08
15Aug1994	0740	339.96	503.8	534.32	540.29
15Aug1994	0750	323.73	479.75	508.81	514.49

15Aug1994	0800	307.5	455.7	483.3	488.7
15Aug1994	0810	292.13	432.91	459.14	464.27
15Aug1994	0820	276.75	410.13	434.97	439.83
15Aug1994	0830	261.37	387.34	410.8	415.39
15Aug1994	0840	246	364.56	386.64	390.96
15Aug1994	0850	230.62	341.77	362.47	366.52
15Aug1994	0900	215.25	318.99	338.31	342.09
15Aug1994	0910	201.58	298.74	316.83	320.37
15Aug1994	0920	187.92	278.48	295.35	298.65
15Aug1994	0930	174.25	258.23	273.87	276.93
15Aug1994	0940	160.58	237.98	252.39	255.21
15Aug1994	0950	146.92	217.72	230.91	233.49
15Aug1994	1000	133.25	197.47	209.43	211.77
15Aug1994	1010	124.71	184.81	196.01	198.2
15Aug1994	1020	116.17	172.15	182.58	184.62
15Aug1994	1030	107.63	159.5	169.16	171.05
15Aug1994	1040	99.08	146.84	155.73	157.47
15Aug1994	1050	90.54	134.18	142.3	143.89
15Aug1994	1100	82	121.52	128.88	130.32
15Aug1994	1110	76.88	113.93	120.83	122.18
15Aug1994	1120	71.75	106.33	112.77	114.03
15Aug1994	1130	66.62	98.73	104.72	105.89
15Aug1994	1140	61.5	91.14	96.66	97.74
15Aug1994	1150	56.37	83.54	88.6	89.59
15Aug1994	1200	51.25	75.95	80.55	81.45

Appendix – B: The routed flood discharges (m^3/s) at different river stations of RS (12086.49), RS (8924.878), RS (4701.743) RS (26.77806) by Froehlich 2008 due to overtopping failure mode.

Date		**At RS= 12086.49**	**At RS= 8924.878**	**At RS= 4701.743**	**At RS= 26.77806**
14Aug1994	1200	733.05	733.05	733.05	733.05
14Aug1994	1210	876.94	742.32	741.89	745.03
14Aug1994	1220	1020.84	759.52	741.06	778.58
14Aug1994	1230	1164.74	824.73	738.26	798.05
14Aug1994	1240	1308.63	960.07	739.31	805.52
14Aug1994	1250	1452.53	1113.81	751.22	804.88
14Aug1994	1300	1596.42	1270.51	791.83	799.04
14Aug1994	1310	1819.05	1422.3	887.9	790.54
14Aug1994	1320	2041.68	1594.03	1029.41	781.5
14Aug1994	1330	2264.31	1814.93	1187.44	773.12

14Aug1994	1340	2486.94	2049.92	1358.13	766.43
14Aug1994	1350	2709.57	2287.39	1556.73	762.8
14Aug1994	1400	2932.2	2521.69	1778.3	764.59
14Aug1994	1410	3258	2754.3	2013.94	776.03
14Aug1994	1420	3583.8	3028.38	2255.34	803.62
14Aug1994	1430	3909.6	3352.22	2496.57	859.53
14Aug1994	1440	4235.4	3680.87	2752.15	953.17
14Aug1994	1450	4561.2	4012.09	3045.28	1105.47
14Aug1994	1500	4887	4344.21	3356.74	1334.4
14Aug1994	1510	5430	4692.12	3676.14	1648.71
14Aug1994	1520	5973	5149.39	4009.57	2025.25
14Aug1994	1530	6516	5692.5	4366.98	2414.79
14Aug1994	1540	7059	6253.29	4778.47	2798.28
14Aug1994	1550	7602	6887.71	5254.55	3177.1
14Aug1994	1600	8145	7573.41	5776.88	3573.69
14Aug1994	1610	8335.05	8014.8	6375.76	4005.84
14Aug1994	1620	8525.1	8250.8	6987.68	4472.06
14Aug1994	1630	8715.15	8446.94	7491.19	4986.82
14Aug1994	1640	8905.2	8639.34	7866.43	5573.9
14Aug1994	1650	9095.25	8830.35	8161.07	6216.2
14Aug1994	1700	9285.3	9021.26	8406.51	6843.28
14Aug1994	1710	9258.15	9196.77	8627.65	7384.81
14Aug1994	1720	9231	9248.65	8833.63	7813.95
14Aug1994	1730	9203.85	9239.1	9003.82	8151.92
14Aug1994	1740	9176.7	9214.3	9113.01	8425.14
14Aug1994	1750	9149.55	9187.26	9166.81	8658.23
14Aug1994	1800	9122.4	9160	9181.45	8855.56
14Aug1994	1810	9013.8	9127.74	9181.74	9002.96
14Aug1994	1820	8905.2	9049.65	9167.23	9097.36
14Aug1994	1830	8796.6	8947.05	9136.38	9148.15
14Aug1994	1840	8688	8839.17	9081.04	9165.8
14Aug1994	1850	8579.4	8731.13	9003.52	9165.62
14Aug1994	1900	8470.8	8622.49	8913.3	9144.58
14Aug1994	1910	8362.2	8514.6	8815.2	9103.93
14Aug1994	1920	8253.6	8406.53	8711.9	9043.46
14Aug1994	1930	8145	8298.28	8607.36	8964.83
14Aug1994	1940	8036.4	8190	8500.69	8875.95
14Aug1994	1950	7927.8	8081.74	8393.51	8781.68
14Aug1994	2000	7819.2	7973.61	8285.53	8683.04
14Aug1994	2010	7642.72	7862.18	8177.39	8581.49
14Aug1994	2020	7466.25	7713.74	8069.06	8476.07
14Aug1994	2030	7289.77	7543.96	7953.38	8369.41

14Aug1994	2040	7113.3	7368.8	7820.79	8262.8
14Aug1994	2050	6936.82	7192.73	7671.26	8156.7
14Aug1994	2100	6760.35	7017.6	7510.85	8046.3
14Aug1994	2110	6597.45	6842.77	7343.78	7924.86
14Aug1994	2120	6434.55	6678.69	7172.88	7791.29
14Aug1994	2130	6271.65	6516.8	7003.86	7648.72
14Aug1994	2140	6108.75	6353.03	6837.71	7497.41
14Aug1994	2150	5945.85	6190.12	6672.99	7338.21
14Aug1994	2200	5782.95	6027.65	6509.1	7177
14Aug1994	2210	5633.63	5866.69	6347.36	7014.99
14Aug1994	2220	5484.3	5712.93	6188.68	6853.73
14Aug1994	2230	5334.98	5564.23	6029.79	6693.58
14Aug1994	2240	5185.65	5416.1	5872.76	6537.03
14Aug1994	2250	5036.33	5268.38	5719.52	6381.11
14Aug1994	2300	4887	5120.03	5569.36	6226.25
14Aug1994	2310	4710.52	4971.47	5420.96	6075.02
14Aug1994	2320	4534.05	4810.74	5271.55	5924.49
14Aug1994	2330	4357.57	4641.9	5122.07	5776.96
14Aug1994	2340	4181.1	4471.52	4968.07	5632.69
14Aug1994	2350	4004.62	4298.86	4808.69	5487.29
14Aug1994	2400	3828.15	4124.83	4644.19	5348.45
15Aug1994	0010	3678.82	3951.49	4475.28	5205.74
15Aug1994	0020	3529.5	3790.07	4306.69	5057.89
15Aug1994	0030	3380.17	3636.03	4140.01	4913.26
15Aug1994	0040	3230.85	3486.21	3975.64	4760.14
15Aug1994	0050	3081.53	3339.3	3814.42	4607.61
15Aug1994	0100	2932.2	3192.49	3661.38	4447.38
15Aug1994	0110	2796.45	3045.66	3508.44	4276.75
15Aug1994	0120	2660.7	2904.42	3358.17	4112.09
15Aug1994	0130	2524.95	2769.9	3208.7	3963.56
15Aug1994	0140	2389.2	2637.25	3061.88	3823.78
15Aug1994	0150	2253.45	2504.47	2922.88	3688.19
15Aug1994	0200	2117.7	2372.24	2790.17	3554.75
15Aug1994	0210	2036.25	2240.87	2658.47	3419.22
15Aug1994	0220	1954.8	2125.38	2529.27	3284.86
15Aug1994	0230	1873.35	2035.33	2399.81	3152.1
15Aug1994	0240	1791.9	1954.1	2273.69	3021.16
15Aug1994	0250	1710.45	1874.09	2162.51	2891.11
15Aug1994	0300	1629	1795.16	2068.52	2770.57
15Aug1994	0310	1566.56	1715.63	1980.8	2651.08
15Aug1994	0320	1504.11	1641.11	1898.72	2537.5
15Aug1994	0330	1441.67	1575.44	1818.96	2426.66

15Aug1994	0340	1379.22	1514.32	1741.71	2319.37
15Aug1994	0350	1316.78	1453.47	1669.16	2216.02
15Aug1994	0400	1254.33	1393.13	1601.85	2118.84
15Aug1994	0410	1221.75	1332.12	1537.55	2028.47
15Aug1994	0420	1189.17	1275.63	1477.25	1942.78
15Aug1994	0430	1156.59	1233.6	1417.76	1866.26
15Aug1994	0440	1124.01	1199.33	1360.52	1794.26
15Aug1994	0450	1091.43	1166.98	1308.09	1728.31
15Aug1994	0500	1058.85	1135.14	1263.35	1669.84
15Aug1994	0510	1018.13	1103.13	1224.17	1614.84
15Aug1994	0520	977.4	1070.32	1188.96	1560.86
15Aug1994	0530	936.68	1033.8	1155.92	1510.04
15Aug1994	0540	895.95	994.49	1123.16	1460.47
15Aug1994	0550	855.22	954.87	1089.8	1413.04
15Aug1994	0600	814.5	915.41	1054.22	1369.18
15Aug1994	0610	785.99	875.79	1017.53	1328.16
15Aug1994	0620	757.48	838.05	980.82	1289.08
15Aug1994	0630	728.98	805.09	943.89	1252.19
15Aug1994	0640	700.47	776.35	906.17	1218.16
15Aug1994	0650	671.96	749.01	870.32	1186.19
15Aug1994	0700	643.45	721.44	836.52	1154.3
15Aug1994	0710	617.66	693.51	811.47	1122.21
15Aug1994	0720	591.87	665.81	781.2	1090.16
15Aug1994	0730	566.08	639.35	754.89	1058.96
15Aug1994	0740	540.29	614.21	731	1027.62
15Aug1994	0750	514.49	589.2	705.94	996.82
15Aug1994	0800	488.7	564.9	679.38	966.49
15Aug1994	0810	464.27	540.72	653.38	938.29
15Aug1994	0820	439.83	516.49	629.83	911.71
15Aug1994	0830	415.39	492.86	605.54	885.73
15Aug1994	0840	390.96	469.3	582.76	860.81
15Aug1994	0850	366.52	445.86	560.54	837.37
15Aug1994	0900	342.09	422.56	538.5	816.08
15Aug1994	0910	320.37	399.55	516.9	796.13
15Aug1994	0920	298.65	376.39	495.33	776.94
15Aug1994	0930	276.93	353.98	470.2	758.51
15Aug1994	0940	255.21	332.55	447.2	740.78
15Aug1994	0950	233.49	312.86	427.09	723.84
15Aug1994	1000	211.77	292.98	409.33	707.54
15Aug1994	1010	198.2	273.34	389.95	690.89
15Aug1994	1020	184.62	253.25	366.88	674.47
15Aug1994	1030	171.05	234.13	352.63	657.3

15Aug1994	1040	157.47	217.84	338.99	639.33
15Aug1994	1050	143.89	206.51	325.25	621.21
15Aug1994	1100	130.32	195.47	312.88	602.99
15Aug1994	1110	122.18	181.36	297.75	584.14
15Aug1994	1120	114.03	169.69	280.85	565.4
15Aug1994	1130	105.89	158.23	266.1	546.12
15Aug1994	1140	97.74	146.44	252.37	527.15
15Aug1994	1150	89.59	136.95	237.84	507.99
15Aug1994	1200	81.45	122.9	222.23	489.33

Appendix – C: The Maximum breach outflow discharges for different methods at the dire dam site due to piping breach scenario.

		Flow (m^3/s)	Flow (m^3/s)	Flow (m^3/s)	Flow (m^3/s)
Date		**Macdonald 1984**	**Von-Thun 1990**	**Froehlich 1995**	**Froehlich 2008**
14Aug1994	1200	432	559.8	602.1	608.85
14Aug1994	1210	516.8	669.69	720.29	728.36
14Aug1994	1220	601.6	779.57	838.48	847.88
14Aug1994	1230	686.4	889.46	956.67	967.39
14Aug1994	1240	771.2	999.35	1074.86	1086.91
14Aug1994	1250	856	1109.23	1193.05	1206.43
14Aug1994	1300	940.8	1219.12	1311.24	1325.94
14Aug1994	1310	1072	1389.13	1494.1	1510.85
14Aug1994	1320	1203.2	1559.15	1676.96	1695.76
14Aug1994	1330	1334.4	1729.16	1859.82	1880.67
14Aug1994	1340	1465.6	1899.17	2042.68	2065.58
14Aug1994	1350	1596.8	2069.19	2225.54	2250.49
14Aug1994	1400	1728	2239.2	2408.4	2435.4
14Aug1994	1410	1920	2488	2676	2706
14Aug1994	1420	2112	2736.8	2943.6	2976.6
14Aug1994	1430	2304	2985.6	3211.2	3247.2
14Aug1994	1440	2496	3234.4	3478.8	3517.8
14Aug1994	1450	2688	3483.2	3746.4	3788.4
14Aug1994	1500	2880	3732	4014	4059
14Aug1994	1510	3200	4146.67	4460	4510
14Aug1994	1520	3520	4561.33	4906	4961
14Aug1994	1530	3840	4976	5352	5412
14Aug1994	1540	4160	5390.67	5798	5863
14Aug1994	1550	4480	5805.33	6244	6314
14Aug1994	1600	4800	6220	6690	6765
14Aug1994	1610	4912	6365.13	6846.1	6922.85
14Aug1994	1620	5024	6510.27	7002.2	7080.7

14Aug1994	1630	5136	6655.4	7158.3	7238.55
14Aug1994	1640	5248	6800.53	7314.4	7396.4
14Aug1994	1650	5360	6945.67	7470.5	7554.25
14Aug1994	1700	5472	7090.8	7626.6	7712.1
14Aug1994	1710	5456	7070.06	7604.3	7689.55
14Aug1994	1720	5440	7049.33	7582	7667
14Aug1994	1730	5424	7028.6	7559.7	7644.45
14Aug1994	1740	5408	7007.87	7537.4	7621.9
14Aug1994	1750	5392	6987.13	7515.1	7599.35
14Aug1994	1800	5376	6966.4	7492.8	7576.8
14Aug1994	1810	5312	6883.47	7403.6	7486.6
14Aug1994	1820	5248	6800.53	7314.4	7396.4
14Aug1994	1830	5184	6717.6	7225.2	7306.2
14Aug1994	1840	5120	6634.67	7136	7216
14Aug1994	1850	5056	6551.73	7046.8	7125.8
14Aug1994	1900	4992	6468.8	6957.6	7035.6
14Aug1994	1910	4928	6385.87	6868.4	6945.4
14Aug1994	1920	4864	6302.93	6779.2	6855.2
14Aug1994	1930	4800	6220	6690	6765
14Aug1994	1940	4736	6137.06	6600.8	6674.8
14Aug1994	1950	4672	6054.13	6511.6	6584.6
14Aug1994	2000	4608	5971.2	6422.4	6494.4
14Aug1994	2010	4504	5836.43	6277.45	6347.82
14Aug1994	2020	4400	5701.67	6132.5	6201.25
14Aug1994	2030	4296	5566.9	5987.55	6054.67
14Aug1994	2040	4192	5432.13	5842.6	5908.1
14Aug1994	2050	4088	5297.37	5697.65	5761.52
14Aug1994	2100	3984	5162.6	5552.7	5614.95
14Aug1994	2110	3888	5038.2	5418.9	5479.65
14Aug1994	2120	3792	4913.8	5285.1	5344.35
14Aug1994	2130	3696	4789.4	5151.3	5209.05
14Aug1994	2140	3600	4665	5017.5	5073.75
14Aug1994	2150	3504	4540.6	4883.7	4938.45
14Aug1994	2200	3408	4416.2	4749.9	4803.15
14Aug1994	2210	3320	4302.17	4627.25	4679.12
14Aug1994	2220	3232	4188.13	4504.6	4555.1
14Aug1994	2230	3144	4074.1	4381.95	4431.07
14Aug1994	2240	3056	3960.07	4259.3	4307.05
14Aug1994	2250	2968	3846.03	4136.65	4183.02
14Aug1994	2300	2880	3732	4014	4059
14Aug1994	2310	2776	3597.23	3869.05	3912.42
14Aug1994	2320	2672	3462.47	3724.1	3765.85

14Aug1994	2330	2568	3327.7	3579.15	3619.27
14Aug1994	2340	2464	3192.93	3434.2	3472.7
14Aug1994	2350	2360	3058.17	3289.25	3326.12
14Aug1994	2400	2256	2923.4	3144.3	3179.55
15Aug1994	0010	2168	2809.37	3021.65	3055.52
15Aug1994	0020	2080	2695.33	2899	2931.5
15Aug1994	0030	1992	2581.3	2776.35	2807.47
15Aug1994	0040	1904	2467.27	2653.7	2683.45
15Aug1994	0050	1816	2353.23	2531.05	2559.43
15Aug1994	0100	1728	2239.2	2408.4	2435.4
15Aug1994	0110	1648	2135.53	2296.9	2322.65
15Aug1994	0120	1568	2031.87	2185.4	2209.9
15Aug1994	0130	1488	1928.2	2073.9	2097.15
15Aug1994	0140	1408	1824.53	1962.4	1984.4
15Aug1994	0150	1328	1720.87	1850.9	1871.65
15Aug1994	0200	1248	1617.2	1739.4	1758.9
15Aug1994	0210	1200	1555	1672.5	1691.25
15Aug1994	0220	1152	1492.8	1605.6	1623.6
15Aug1994	0230	1104	1430.6	1538.7	1555.95
15Aug1994	0240	1056	1368.4	1471.8	1488.3
15Aug1994	0250	1008	1306.2	1404.9	1420.65
15Aug1994	0300	960	1244	1338	1353
15Aug1994	0310	923.2	1196.31	1286.71	1301.14
15Aug1994	0320	886.4	1148.63	1235.42	1249.27
15Aug1994	0330	849.6	1100.94	1184.13	1197.41
15Aug1994	0340	812.8	1053.25	1132.84	1145.54
15Aug1994	0350	776	1005.57	1081.55	1093.68
15Aug1994	0400	739.2	957.88	1030.26	1041.81
15Aug1994	0410	720	933	1003.5	1014.75
15Aug1994	0420	700.8	908.12	976.74	987.69
15Aug1994	0430	681.6	883.24	949.98	960.63
15Aug1994	0440	662.4	858.36	923.22	933.57
15Aug1994	0450	643.2	833.48	896.46	906.51
15Aug1994	0500	624	808.6	869.7	879.45
15Aug1994	0510	600	777.5	836.25	845.62
15Aug1994	0520	576	746.4	802.8	811.8
15Aug1994	0530	552	715.3	769.35	777.97
15Aug1994	0540	528	684.2	735.9	744.15
15Aug1994	0550	504	653.1	702.45	710.32
15Aug1994	0600	480	622	669	676.5
15Aug1994	0610	463.2	600.23	645.58	652.82
15Aug1994	0620	446.4	578.46	622.17	629.14

15Aug1994	0630	429.6	556.69	598.75	605.47
15Aug1994	0640	412.8	534.92	575.34	581.79
15Aug1994	0650	396	513.15	551.92	558.11
15Aug1994	0700	379.2	491.38	528.51	534.43
15Aug1994	0710	364	471.68	507.32	513.01
15Aug1994	0720	348.8	451.99	486.14	491.59
15Aug1994	0730	333.6	432.29	464.95	470.17
15Aug1994	0740	318.4	412.59	443.77	448.74
15Aug1994	0750	303.2	392.9	422.58	427.32
15Aug1994	0800	288	373.2	401.4	405.9
15Aug1994	0810	273.6	354.54	381.33	385.6
15Aug1994	0820	259.2	335.88	361.26	365.31
15Aug1994	0830	244.8	317.22	341.19	345.01
15Aug1994	0840	230.4	298.56	321.12	324.72
15Aug1994	0850	216	279.9	301.05	304.42
15Aug1994	0900	201.6	261.24	280.98	284.13
15Aug1994	0910	188.8	244.65	263.14	266.09
15Aug1994	0920	176	228.07	245.3	248.05
15Aug1994	0930	163.2	211.48	227.46	230.01
15Aug1994	0940	150.4	194.89	209.62	211.97
15Aug1994	0950	137.6	178.31	191.78	193.93
15Aug1994	1000	124.8	161.72	173.94	175.89
15Aug1994	1010	116.8	151.35	162.79	164.62
15Aug1994	1020	108.8	140.99	151.64	153.34
15Aug1994	1030	100.8	130.62	140.49	142.07
15Aug1994	1040	92.8	120.25	129.34	130.79
15Aug1994	1050	84.8	109.89	118.19	119.51
15Aug1994	1100	76.8	99.52	107.04	108.24
15Aug1994	1110	72	93.3	100.35	101.48
15Aug1994	1120	67.2	87.08	93.66	94.71
15Aug1994	1130	62.4	80.86	86.97	87.94
15Aug1994	1140	57.6	74.64	80.28	81.18
15Aug1994	1150	52.8	68.42	73.59	74.41
15Aug1994	1200	48	62.2	66.9	67.65

Appendix – D: The routed flood discharges (m^3/s) at different river stations of RS (12086.49), RS (8924.878), RS (4701.743) RS (26.77806) by Froehlich 2008 due to piping failure mode.

		At RS= 12086.49	**At RS= 8924.878**	**At RS= 4701.743**	**At RS= 26.77806**
Date					
14Aug1994	1200	608.85	608.85	608.85	608.85
14Aug1994	1210	728.36	615.75	619.29	616.63
14Aug1994	1220	847.88	630.44	621.95	641.64

14Aug1994	1230	967.39	673.05	621.5	658.33
14Aug1994	1240	1086.91	775.97	620.04	668.02
14Aug1994	1250	1206.43	908.12	623.46	673.15
14Aug1994	1300	1325.94	1038.38	640.87	674.45
14Aug1994	1310	1510.85	1167.69	693.91	673.09
14Aug1994	1320	1695.76	1307.21	795.48	669.88
14Aug1994	1330	1880.67	1481.3	936.48	665.85
14Aug1994	1340	2065.58	1679.23	1085.89	661.61
14Aug1994	1350	2250.49	1877.77	1241.44	657.81
14Aug1994	1400	2435.4	2073.78	1426.01	655.44
14Aug1994	1410	2706	2269.4	1628.41	656.03
14Aug1994	1420	2976.6	2495.78	1833.3	661.69
14Aug1994	1430	3247.2	2785.99	2037.47	676.31
14Aug1994	1440	3517.8	3133.93	2255.74	707.59
14Aug1994	1450	3788.4	3484.51	2506.82	767.16
14Aug1994	1500	4059	3732.05	2804.16	872.81
14Aug1994	1510	4510	3906.16	3133.71	1043.01
14Aug1994	1520	4961	4233.61	3422.59	1296.79
14Aug1994	1530	5412	4681.22	3672.02	1637.34
14Aug1994	1540	5863	5153.53	3958.57	2040.99
14Aug1994	1550	6314	5619.32	4328.27	2455.67
14Aug1994	1600	6765	6084.14	4749.71	2850.27
14Aug1994	1610	6922.85	6525.45	5198.05	3219.12
14Aug1994	1620	7080.7	6818.5	5649.17	3589.1
14Aug1994	1630	7238.55	7002.33	6079.9	3993.9
14Aug1994	1640	7396.4	7164.84	6441.58	4435.93
14Aug1994	1650	7554.25	7323.94	6721.83	4908.71
14Aug1994	1700	7712.1	7482.26	6947.51	5398.53
14Aug1994	1710	7689.55	7631.79	7141.85	5869.54
14Aug1994	1720	7667	7681.21	7318.17	6281.14
14Aug1994	1730	7644.45	7674.85	7466.36	6616.21
14Aug1994	1740	7621.9	7654.23	7562.6	6885.37
14Aug1994	1750	7599.35	7632.06	7610.07	7106.63
14Aug1994	1800	7576.8	7609.54	7626.23	7289.79
14Aug1994	1810	7486.6	7583.88	7626.11	7427.59
14Aug1994	1820	7396.4	7522.05	7615.53	7523.23
14Aug1994	1830	7306.2	7437.13	7592.53	7581.26
14Aug1994	1840	7216	7347.34	7548.47	7607.99
14Aug1994	1850	7125.8	7257.48	7485.91	7611.54
14Aug1994	1900	7035.6	7167.52	7410.75	7603.06
14Aug1994	1910	6945.4	7077.79	7328.99	7576.06
14Aug1994	1920	6855.2	6987.97	7243.72	7531.3

14Aug1994	1930	6765	6897.79	7156.87	7473.17
14Aug1994	1940	6674.8	6807.97	7069.63	7403.68
14Aug1994	1950	6584.6	6719.6	6980.09	7324.37
14Aug1994	2000	6494.4	6630.61	6891.16	7241.4
14Aug1994	2010	6347.82	6538.6	6802.73	7158.52
14Aug1994	2020	6201.25	6417.07	6713.63	7072.62
14Aug1994	2030	6054.67	6275.06	6618.61	6986.27
14Aug1994	2040	5908.1	6129.19	6510.34	6899.32
14Aug1994	2050	5761.52	5983.42	6387.33	6810.15
14Aug1994	2100	5614.95	5838.19	6256.53	6719.73
14Aug1994	2110	5479.65	5693.58	6120.97	6623.35
14Aug1994	2120	5344.35	5554.54	5979.95	6518.9
14Aug1994	2130	5209.05	5419.37	5837.76	6403.44
14Aug1994	2140	5073.75	5285.23	5697.35	6278.99
14Aug1994	2150	4938.45	5150.35	5559.92	6150.92
14Aug1994	2200	4803.15	5016.37	5424.49	6019.22
14Aug1994	2210	4679.12	4882.54	5288.08	5883.68
14Aug1994	2220	4555.1	4755.27	5153.77	5750.48
14Aug1994	2230	4431.07	4632.64	5020.37	5618.7
14Aug1994	2240	4307.05	4511.62	4891.58	5485.23
14Aug1994	2250	4183.02	4390.09	4764.59	5358.59
14Aug1994	2300	4059	4266.95	4641.35	5231.77
14Aug1994	2310	3912.42	4143.71	4517.55	5101.39
14Aug1994	2320	3765.85	4011.03	4396.21	4978.38
14Aug1994	2330	3619.27	3870.27	4271.45	4858.44
14Aug1994	2340	3472.7	3725.29	4148.09	4735.56
14Aug1994	2350	3326.12	3577.35	4016.77	4618.26
14Aug1994	2400	3179.55	3431.52	3880.23	4502.52
15Aug1994	0010	3055.52	3288.03	3737.69	4377.76
15Aug1994	0020	2931.5	3152.69	3594.11	4244.3
15Aug1994	0030	2807.47	3027.12	3449.17	4112.24
15Aug1994	0040	2683.45	2904.84	3308.28	3989.33
15Aug1994	0050	2559.43	2783.39	3172.65	3871.02
15Aug1994	0100	2435.4	2662.05	3042.46	3749.29
15Aug1994	0110	2322.65	2540.63	2919.14	3626.48
15Aug1994	0120	2209.9	2423.18	2799.83	3500.48
15Aug1994	0130	2097.15	2311.05	2680.56	3374.2
15Aug1994	0140	1984.4	2200.94	2563.3	3249.08
15Aug1994	0150	1871.65	2091.61	2449.97	3127.91
15Aug1994	0200	1758.9	1982.56	2335.35	3008.23
15Aug1994	0210	1691.25	1873.25	2223.43	2889.61
15Aug1994	0220	1623.6	1775.28	2115.61	2780.32

15Aug1994	0230	1555.95	1698.51	2009.34	2672.16
15Aug1994	0240	1488.3	1631.23	1906.73	2567.7
15Aug1994	0250	1420.65	1564.94	1813.6	2465.83
15Aug1994	0300	1353	1500	1732.06	2362.3
15Aug1994	0310	1301.14	1434.2	1658.83	2259.77
15Aug1994	0320	1249.27	1371.65	1590.15	2156.74
15Aug1994	0330	1197.41	1315.82	1523.49	2057.61
15Aug1994	0340	1145.54	1263.75	1460.57	1961.88
15Aug1994	0350	1093.68	1212.79	1400.21	1875.79
15Aug1994	0400	1041.81	1162.43	1344.75	1796.37
15Aug1994	0410	1014.75	1112.12	1292.79	1725.24
15Aug1994	0420	987.69	1064.81	1242.45	1662.93
15Aug1994	0430	960.63	1028.85	1192.94	1605.25
15Aug1994	0440	933.57	999.78	1143.92	1549.74
15Aug1994	0450	906.51	972.58	1097.66	1497.61
15Aug1994	0500	879.45	946.02	1056.65	1446.71
15Aug1994	0510	845.62	919.55	1022.42	1398.52
15Aug1994	0520	811.8	892.23	992.67	1352.53
15Aug1994	0530	777.97	862.38	965.77	1307.78
15Aug1994	0540	744.15	830.97	939.51	1263.93
15Aug1994	0550	710.32	798.58	912.37	1222.82
15Aug1994	0600	676.5	766.72	884.98	1184.44
15Aug1994	0610	652.82	734.71	856.04	1146.99
15Aug1994	0620	629.14	702.44	827.7	1110.75
15Aug1994	0630	605.47	673.52	802.33	1077.37
15Aug1994	0640	581.79	648.64	770.35	1046.33
15Aug1994	0650	558.11	625.55	742.82	1016.56
15Aug1994	0700	534.43	602.7	716.57	988.64
15Aug1994	0710	513.01	579.68	689.03	961.81
15Aug1994	0720	491.59	557.63	663.35	937.13
15Aug1994	0730	470.17	535.94	640.21	913.51
15Aug1994	0740	448.74	515.05	617.63	890.06
15Aug1994	0750	427.32	494.82	595.48	866.92
15Aug1994	0800	405.9	474.34	574.81	844.53
15Aug1994	0810	385.6	453.78	554.86	823.72
15Aug1994	0820	365.31	433.19	535.19	803.86
15Aug1994	0830	345.01	412.99	516.1	784.86
15Aug1994	0840	324.72	393.22	497.23	766.46
15Aug1994	0850	304.42	373.73	475.27	748.68
15Aug1994	0900	284.13	354.57	454.52	731.67
15Aug1994	0910	266.09	335.25	435.74	715.62
15Aug1994	0920	248.05	317.17	418.65	699.67

15Aug1994	0930	230.01	298.84	406.39	683.6
15Aug1994	0940	211.97	281.31	384.36	667.66
15Aug1994	0950	193.93	264.11	365.77	651.01
15Aug1994	1000	175.89	246.97	352.91	633.88
15Aug1994	1010	164.62	230.6	340.62	616.9
15Aug1994	1020	153.34	215.11	328.04	599.68
15Aug1994	1030	142.07	203.67	316.41	582.03
15Aug1994	1040	130.79	191.03	304.77	564.43
15Aug1994	1050	119.51	176.07	288.7	546.43
15Aug1994	1100	108.24	166.1	273.57	528.75
15Aug1994	1110	101.48	153.35	259.71	510.96
15Aug1994	1120	94.71	148.71	246.35	493.22
15Aug1994	1130	87.94	119.97	230.37	477.91
15Aug1994	1140	81.18	144.69	218.45	461.95
15Aug1994	1150	74.41	129.69	209.65	445.48
15Aug1994	1200	67.65	95.96	202.23	428.88